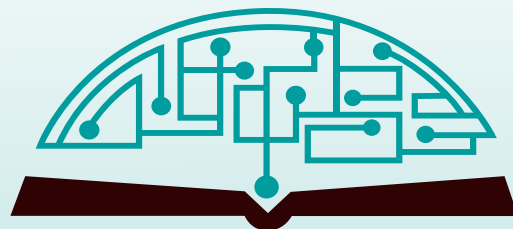


# IJHSR

International  
Journal of  
High School  
Research



September 2020 | Volume 2 | Issue 3

[ijhighschoolresearch.org](http://ijhighschoolresearch.org)

ISSN (Print version) 2642-1046

ISSN (Online version) 2642-1054



# GENIUS OLYMPIAD

*"Let's build a better future together"*



[www.geniusolympiad.org](http://www.geniusolympiad.org)

International Environment Project Fair For Grades 9-12



June 7-12 | Rochester, New York  
Application Deadline: March 1, 2021

@GeniusOlympiad



# Table of Contents

September 2020 | Volume 2 | Issue 3

- 01 | Exploring a Human-Machine Interaction Method  
*Jie Li*
- 07 | What Is the Effect of a Mixed Culture of *Pseudomonas fluorescens* and *Anabaena* on the Degradation of Polyvinyl Chloride?  
*Ojas Kalia*
- 13 | The Optimization of Lead Absorption in Contaminated Water Through Anhydro Galacturonic Acids in Various Citrus Peels  
*Amy Wang, Viveka Chinnasamy, Shreya Tripathi*
- 16 | Miscanthus sinensis (Silver Grass) Fiber as a Component of an Eco-friendly Sorbent Bag for Oil Spill Clean-up  
*Micklare Angelo C. Zepeda, Elarcie Balsomo*
- 21 | Evaluation of the Antioxidant and Anticancer Activity of *Scutellaria barbata*, *Hedyotis diffusa*, and *Celastrus hindsii*  
*Nguyen Viet Quang Nam, Nguyen Cao Hai Vy, Nguyen Minh Trung*
- 26 | Analysis of the Arcade Creek Shows Lower Dissolved Oxygen Levels When Compared with the American River  
*Gabriela A. Rossetti*
- 32 | The Use of Bactericidal Ultraviolet Radiation in the Eradication of *Escherichia coli* K12  
*Benjamin Carranti*
- 35 | Developing Pesticide Resistance to Acetylcholinesterase Inhibitors in *D. pulex*  
*Jordan Harrow*
- 40 | Development of Gel-based Multiplex RT-PCR for Detection of ER/PR/HER2-Positive Breast Cancer Diagnosis  
*Suh Kyung Yoon, Woo Rin Lee*
- 46 | Effects of Milk, Cheese, and Strawberry Counteracting Tooth Discoloration Induced by Coffee or Red Wine  
*Selina Yuri Kim*

*Editorial  
Board*International  
Journal of  
High School  
Research**■ CHIEF EDITOR****Dr. Richard Beal**

Director of International Programs and Accreditation, Terra Science and Education

**■ EXECUTIVE PRODUCER****Dr. Fehmi Damkaci**

President, Terra Science and Education

**Asli Kinsizer**

Graphic and Layout Designer

**■ COPY EDITORS****Emily Olds**

Intern, Terra Science and Education

**Erin Williams**

Intern, Terra Science and Education

**Mary Eileen Wood**

STEM Engagement Coordinator, Terra Science and Education

**■ ISSUE REVIEWERS****Dr. Fasheng Zhou**, School of Physics and Electronic Engineering, Guangzhou University**Dr. Gretchen K. Bielmyer-Fraser**, Environmental Toxicology, Jacksonville University**Dr. Sanguine Byun**, Yonsei University, Seoul, South Korea**Jeff Ahn**, Valor Global Foundation, Portland, Oregon**Dr. Sarina Ergas**, University of South Florida**Dr. Promila Pathak**, Department of Botany, Panjab University**Debbie Nipar**, AP Research**Martice Vasquez**, Environmental Scientist, Central Valley Water Quality Control Board, California**Noor Siddiqui**, Dallas International School, Texas**Ruie Lorenz Reyes**, Eulogio "Amang" Rodriguez Institute of Science and Technology, Manila, Philippines**Ronie Banan**, Catalina Foothills High School, Tuscon, Arizona**Dr. George Andrew S. Inglis**, Anderson Lab



## Exploring a Human-Machine Interaction Method

Jie Li

HFI, the Affiliated High School of South China Normal University, Guangzhou, China

lij.jack2018@gdhfi.com

**ABSTRACT:** Human-machine interaction (HMI) technology directly affects the experience and efficiency of computer users. Graphical interface first allowed us to operate machines with the ease of point-and-click and touchscreens removed the mouse altogether. Now, a new revolution begins as we imagine operating computers with just our heads. We intend to use the user's head as a mouse, with point-and-nod instead of point-and-click. This new technology can solve shortcomings of both mice and touchscreens. To construct a "head mouse," an earphone is embedded with a 3-axis angular velocity sensor that follows and measures the head's angular velocities in three-dimensional space. The theoretical analysis and tested data indicate that the moving direction and nod/shake of head movements can be identified through the polarity and value of the angular velocity of the three-axes. As a result, pointing is done by detecting and identifying the direction of head movements and clicking is done by identifying a nod motion. By using the head mouse, a more convenient HMI can be realized

**KEYWORDS:** Head Mouse; Pointing; Clicking; Head Movement Detection; Human-Machine Interface; Bluetooth Earphone; Human Interface Device; Gyroscopes.

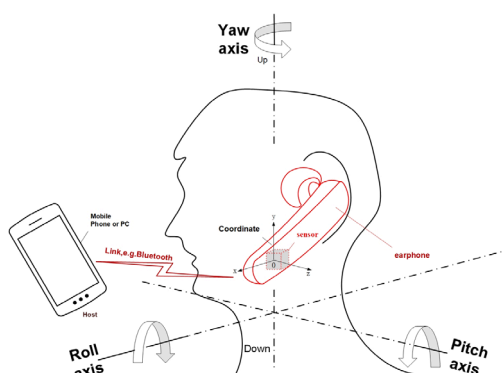


Figure 1: Conception of the head mouse, a human-machine interaction apparatus, and illustrates the mounting position of the angular velocity sensor in the earphone, the coordinate system used, and the direction of rotation of the head movement in 3D space.

## INTRODUCTION

### Background

Human-machine interaction (HMI) technology directly affects the experience and efficiency of users. Every advancement in HMI technology changes the IT industry. The graphical interface known for its implementation in Windows® and Macintosh® in the computer age allowed us to operate a computer with a mouse.<sup>1</sup> However, a flat surface is required for mice, thus making it difficult to apply this technology to small electronic products. Nowadays, mobile phones use touchscreens and move-and-touch rather than a mouse and point-and-click. As electronic devices become smaller, the touchscreen also becomes smaller. With this, many users find it difficult to press a specific key on their phone's small, virtual QWERTY keyboard. In some instances, even a touchscreen can be inconvenient, especially for those who are drivers, fire-

fighters, or disabled. Wearing gloves also renders touchscreens unusable. The question of whether we can find a more convenient and natural input method becomes important.

### HYPOTHESIS

To solve the issues discussed above, this project intends to use a user's head as a "mouse" with point-and-nod instead of the traditional point-and-click method. To detect the head movement, we initially wanted to use facial recognition technology as it is very popular. We assumed that a technology so mature would easily recognize head movements. However, facial recognition technology based on optical photography has low recognition rate in low light and results in high power consumption. Although Apple, Inc. used an infrared camera to solve the problem of low light recognition rate, it still has the power consumption problem. Therefore, facial recognition was deemed unsuitable for HMI.

Optical emitters and photo detectors or time of flight (TOF) sensors are also used to track the head or eyeball movement. These methods use infrared light or lasers to emit and reflect in the eyeball, which is not good for human eyes.

The most ideal technology for HMI is motion sensors through the installation of sensors in an earphone that follows head movement. Compared with eyeglasses or other wearable devices, an earphone is preferred because it not only tracks the movement of the head in the direction of the eye's sight but also reduces the foreign body sensation and avoids the situation in which individuals who already wear glasses must wear an extra pair of glasses.

By studying the characteristics of head motion while browsing a screen and utilizing the look-and-nod operation (assuming that the person is sitting or standing, the body is immobile and only the head moves), it is found that the head cannot move freely due to neck limitations. The head

movement is not a translation, a uniform movement without rotation,<sup>2</sup> but rather it rotates around the neck. Therefore, the rotation sensor (also called an angular velocity sensor or 3-axis gyroscope) is used to detect the head motion as shown in Figure 1.

### Goal

This research aims to find an HMI method that enables user interaction with an electronic device by turning the user's head to provide the mouse's point-and-click functionality.

Turning your head will cause the cursor to move with the distance of the cursor movement being proportional to the amplitude of rotation, nodding to click, and shaking your head to "escape" or backspace.

### Conception

A Bluetooth earphone was selected as a carrier for following head movements and a 3D rotation sensor (3-Axis Digital Micro Electro Mechanical Systems Angular Velocity Sensor) was added to the earphone to detect and sense head movement following the eye movement, including its direction, displacement, and the nodding/shaking head action.

As long as we find a way to recognize the head movement direction, movement displacement, nodding and shaking head action, the actions can be used as a mouse.

The remaining project parts are the standard human interface device (HID) processes, such as like encoding the head motion recognition outputs and mapping to corresponding mouse axis code and left or right button code.<sup>3</sup> For example, the left and right movement of the head and the displacement are mapped to the x-axis code of the standard mouse device:  $\pm d$ , which is used to report the displacement of the cursor along the x-axis, where  $d$  means displacement,  $+$  means right movement, and  $-$  means left movement. Up and down head movement and the displacement are mapped to the y-axis code of the standard mouse device:  $\pm d$ , which is used to report the displacement of the cursor along the y-axis, where  $d$  means displacement,  $+$  represents upward movement, and  $-$  represents downward moving. Nodding is mapped to the mouse's LEFT buttons, and then transmitted to the mapped axis codes packed by the standard HID protocols service to the host to be controlled via wireless or wired connectivity. The host responds to the motion events and dispatches the mapped axis codes to corresponding APP to control the cursor and complete the point-and-click. The host may be any electronic device including a cell phone, PC, or iPad.

The 3D sensor identifies different movement directions (up/down/left/right) via the rotation sensor. The sensor is mounted in a position that its y-axis is parallel to the head's y-axis and the z-axis is parallel to the pitch axis of the user's head rotation. The x-axis is parallel to the roll axis of the user's head to detect and recognize the head rotation. This allows for the motional characteristic that the head rotates around the z-axis when moving up and down and rotates around the y-axis when moving left and right.

The rotation sensor is a digital 3-axis angular velocity sensor similar to the ST<sup>®</sup> L3GD20H<sup>4</sup>, BOSCH<sup>®</sup> BMG250<sup>5</sup>, and NXP<sup>®</sup> FXAS21002C<sup>6</sup> models. The sensor used is 3mm x 3mm x 1 mm and has very low power consumption, which is different from the traditional analog angular velocity sensors that output analog signals. The digital sensor can directly output the angular velocity value.

The angular velocity sensor reports the angular velocity along three coordinate axes with positive and negative signs; a positive value indicates rotation counterclockwise and a negative value indicates rotation clockwise. The direction of the angular velocity is obtained by the righthand-thread rule.

Additionally, the angular velocity sensor has a built-in high-pass filter and a low-pass filter. This makes it easy to delete the DC component of the measured angular rate and removes some noise interference.

The angular velocity sensor usually provides an interrupt function; detecting that the angular velocity value is greater or less than the set threshold will trigger the interruption and handle the event by microprocessor. The interrupt register can also define a detection time where once the time is reached and the threshold is exceeded, an interrupt is triggered. A practical movement and wake-up interrupt are provided for power management; the earphone goes into power-saving mode when not moving and only enters the normal working mode when it is rotated.<sup>4</sup>

### Summary

Based on the above conception of a head mouse, we analyzed the head movement characteristics of the point-and-nod operation and performed an experimental verification. The tested data indicated that the moving direction and nodding/shaking of one's head can be identified by detecting the polarity and value of the 3-axis angular velocity and the moving distance can be obtained by integrating the measured angular velocity. Thus, a more natural and convenient human-machine interaction method can be realized because where you are watching is where the cursor will point.

### Characteristics & Advantages

Compared with other HMI methods, the present method has the following advantages:

- The operation is natural (for example, where you are watching is where the cursor will point) because it does not occupy surface space when used and frees your hands to do other things.
- The head movement is the rotation around the neck and the rotation angle does not exceed  $\pm 180$  degrees. Therefore, an angular velocity sensor that measures rotational motion is more suitable than an accelerometer that detects linear motion.<sup>2</sup>
- Compared with head gesture recognition based on optics (such as camera, optical emitters and photo transistors), head point-and-nod recognition based on an angular velocity sensor has the advantages of small size, low power consumption, and low cost.

- With wireless remote operation capabilities, it is no longer necessary to sit at a table and move the mouse or wave a laser pointer as well as reserve surface space for mouse movement. The head mouse can be used in free 3D space to achieve convenience of operation.

- Instead of eyeglasses or other wearable devices, an earphone can not only track the movement of the head in the direction of the eye's sight, but also reduce the foreign body sensation and avoid having to ask people to wear multiple glasses simultaneously.

## RESULTS AND DISCUSSION

Based on the head mouse conception, we analyzed and tested the head movement characteristics of the point-and-nod operation. There were six cases to analyze and test.

The following is brief instructions for the experiment: the evaluation board (EVB) supplied by the sensor vendor is strapped onto the Bluetooth earphone and the earphone is worn on the head to simulate the head mouse device assumed in this research. The EVB is connected to the PC via a USB cable. The software tool attached to the EVB can be used to test real-time angular velocity and can automatically draw the angular velocity versus time curve. The evaluation kits (EVB+PC software tool) were used to test data under the following cases.

### Case 1: Turn head from right to left

When the head turns left, it rotates around the y axis and there is no rotation around the pitch and roll axes. Therefore, the characteristic of the head turning left should be that the angular velocity on the y-axis is positive (indicating rotating in counterclockwise direction), and the measured angular velocity on the x- and z-axis is zero. The test results for case 1 is shown in Figure 2. The experimental results are mostly consistent with the theoretical analysis.

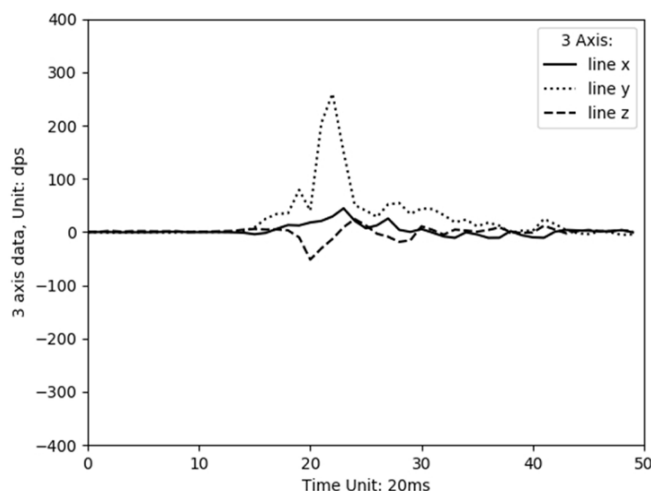


Figure 2: The measured angular velocity versus time curve of the triaxial in case of turning the head left.

### Case 2: Turn head right (from left to right)

When the head turns right, it rotates around the yaw axis, while there is no rotation around pitch and roll axes. The characteristic of head turning right should be that the angular velocity of the y-axis is negative (indicating rotating in clockwise direction) and the angular velocity of the x- and z-axis is zero. The actual test results for case 2 is shown in Figure 3. It shows that the experimental results are mostly consistent with the theoretical analysis.

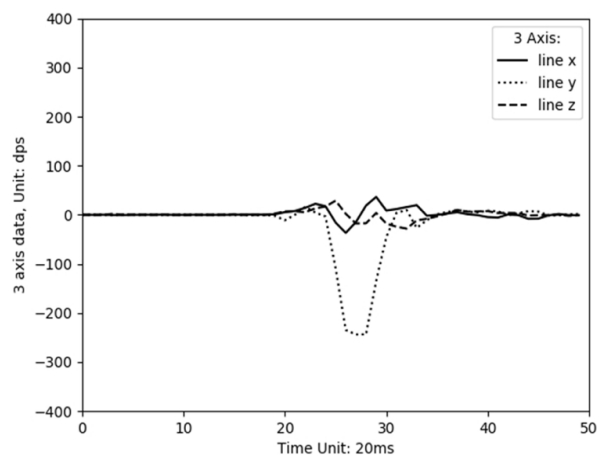


Figure 3: The measured angular velocity versus time curve of the triaxial in case of turning the head right.

### Case 3: Turn head up

When the head turns up, it rotates around the pitch axis and there is no rotation around yaw or roll axes. The characteristic of the head should be that the angular velocity of the z-axis is negative (indicating rotating in clockwise direction) and the angular velocity of the x- and y-axis is zero. The actual test results for case 3 is shown in Figure 4, which show that the experimental results are mostly consistent with the theoretical analysis.

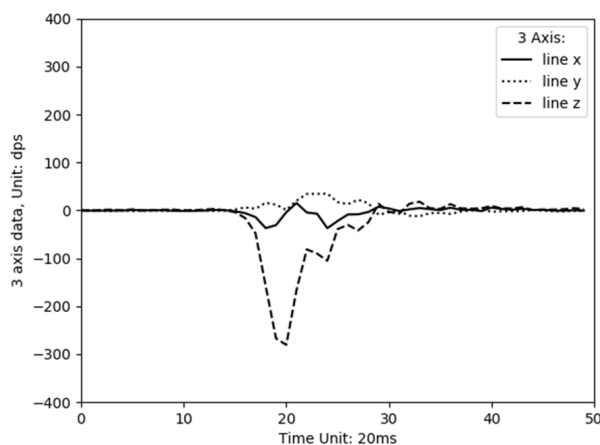


Figure 4: The measured angular velocity versus time curve of the triaxial in case of turning the head up.

#### Case 4: Turn head down

When the head turns down, it rotates around the pitch axis while there is no rotation around the yaw or roll axes. The characteristic of head down should be that the measured angular velocity of the z-axis is positive (indicating counterclockwise rotation) and the measured angular velocity of the x- and y-axis is zero. The actual test result for case 4 is shown in Figure 5. We can see that the experimental results are mostly consistent with the theoretical analysis.

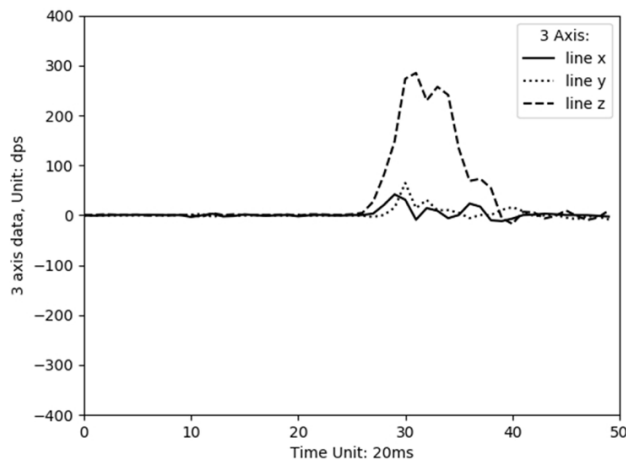


Figure 5: The measured angular velocity versus time curve of the triaxial in case of turning the head down.

#### Case 5: Nodding head action

When the head is nodding (moving quickly up and down), it rotates around the pitch axis while there is no rotation around yaw or roll axes. The characteristic of the nodding action should be that the angular velocity of the z-axis alternates between positive and negative and the angular velocity of the x- and y-axis is zero. The actual test result for case 5 is shown in Figure 6. The experimental results are mostly consistent with the theoretical analysis.

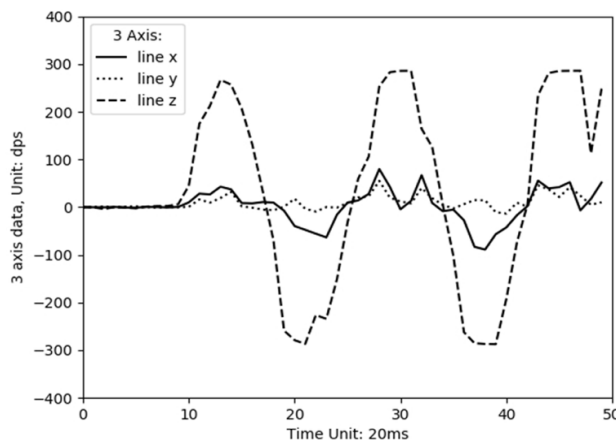


Figure 6: The measured angular velocity versus time curve of the triaxial in the case of nodding head.

#### Case 6: Shaking head action

When the head shakes (moving quickly left and right), it rotates around the yaw axis while there is no rotation around the pitch or roll axes. The characteristic of the shaking action should be that the angular velocity of the y-axis alternates between positive and negative and the measured angular velocity of the x- and z-axes is zero. The actual test result for case 6 is shown in Figure 7. We can see the experimental results are mostly consistent with the theoretical analysis.

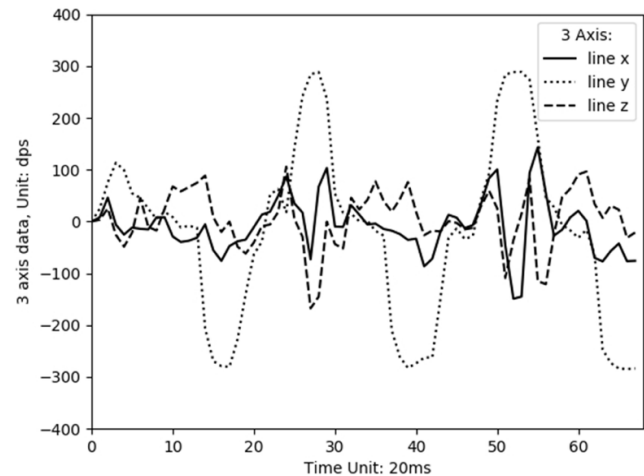


Figure 7: The measured angular velocity versus time curve of the triaxial in case of shaking head.

## DISCUSSION

We found the results were slightly different from our expectations. For example, when the head turns left, theoretical analysis shows the measured angular velocity of the x- and z-axes should be zero. However, it was not zero but had a certain amount of change. There are two reasons for this. One is that when the head turns left, it is difficult to ensure that the head is only translated (moved horizontally, a movement without rotation) because there may be up and down movements. Another reason is that it is difficult to guarantee the rotation sensor is mounted in a position such that the x-, y-, and z-axes are parallel to the roll, yaw, and pitch axes of the head, respectively. Using the experimental data, however, when compared with the large change in the y-axis angular velocity, the angular velocity of the x-axis and z-axis changes very little, which is easily distinguishable. By setting a certain threshold we can filter out these effects.

The angle information is obtained by integrating the angular velocity. Although the angular velocity sensor has a built-in high-pass filter and low-pass filter for removing noise interference, slight deviations in the angular velocity signal causes a cumulative error after the integral calculation. This error will gradually increase with time. To eliminate the cumulative error of the gyroscope, it can be calibrated through the angle information obtained by another acceleration sensor. For this project, the gyroscope angular velocity sensor in the 6-axis inertial measurement unit (3-axis digital accelerometer and 3-axis digital gyroscope 2-in-1 component) is used to identify the head's rotation angle and an acceleration sensor is used to



calibrate. The joint implementation ensures the stable recognition of the head's rotation angle.

### Summary

According to the above theoretical analysis and experimental data, we can develop a recognition method of the head point-and-click.

For movement left, if the measured y-axis angular velocity in a certain duration exceeds a certain threshold value, then the polarity is positive. If this is true and the angular velocity of the x- and z-axis change is small, then the head is considered to be turned left. This is expressed as:

$$A_y > 0 \ \& \ A_y > \text{threshold} \ \& \ A_x < |\text{threshold}_{\min}| \ \& \ A_z < |\text{threshold}_{\min}| \quad (\text{where } A_x, A_y, \text{ and } A_z \text{ represent the angular velocity of x-, y-, and z-axes, respectively})$$

For movement right, if the measured y-axis angular velocity in a certain duration exceeds a certain threshold value, then polarity is negative. If this is true and the angular velocity of the x- and z-axis change is small, then the head is considered to be turned right. This is expressed as:

$$A_y < 0 \ \& \ A_y > |\text{threshold}| \ \& \ A_x < |\text{threshold}_{\min}| \ \& \ A_z < |\text{threshold}_{\min}| \quad (\text{where } A_x, A_y, \text{ and } A_z \text{ represent the angular velocity of x-, y-, and z-axes, respectively})$$

For movement up, if the measured angular velocity of the z-axis in a certain duration exceeds a certain threshold value, then polarity is negative. If this is true and the change in angular velocity of the x- and y-axis is small, then the movement of the head up is considered to have occurred. This is written as the following expression:

$$A_z < 0 \ \& \ A_z > |\text{threshold}| \ \& \ A_x < |\text{threshold}_{\min}| \ \& \ A_y < |\text{threshold}_{\min}| \quad (\text{where } A_x, A_y, \text{ and } A_z \text{ represent the angular velocity of x-, y-, and z-axes, respectively})$$

For movement down, if the measured angular velocity of the z-axis in a certain duration exceeds a certain threshold value, then polarity is positive. If this is true and the angular velocity of the x- and y-axis changes little, then the head is considered to be down. This is written as the following expression:

$$A_z > 0 \ \& \ A_z > |\text{threshold}| \ \& \ A_x < |\text{threshold}_{\min}| \ \& \ A_y < |\text{threshold}_{\min}| \quad (\text{where } A_x, A_y, \text{ and } A_z \text{ represent the angular velocity of x-, y-, and z-axes, respectively})$$

It is also necessary to detect the displacement of the head movement to determine the distance that the cursor will move. Since the head moves with the neck as the axis of rotation (see Figure 1), the distance is the radians of the head's rotation. This is obtained by integrating the measured angular velocity.

The definition of angular velocity is:

$$\therefore A = \frac{d\theta}{dt} \quad (\theta \text{ is radians traversed, } t \text{ is time, } A \text{ is angular velocity, unit is rad/s})$$

$$\therefore \theta = \int A \, dt \quad (t \text{ is the time, } A \text{ is angular velocity, unit is rad/s})$$

The amplitude of rotation( $\theta$ ) is used to determine the cursor movement.

For nodding, if the measured angular velocity of the z-axis in a certain duration exceeds a certain threshold value, then the polarity alternates between positive and negative. If this is true and the angular velocity of the x- and y-axis changes little, then the movement of the nodding is considered to have occurred. This is expressed as:

$$|A_z| > \text{threshold} \ \& \ A_x < |\text{threshold}_{\min}| \ \& \ A_y < |\text{threshold}_{\min}| \quad (\text{where } A_x, A_y, \text{ and } A_z \text{ represent the angular velocity of x-, y-, and z-axes, respectively})$$

For shaking, if the measured angular velocity of the y-axis in a certain duration exceeds a certain threshold value, then the polarity alternates between positive and negative. If this is true and the angular velocity of the x- and z-axis changes little, then the movement of the shaking head is considered to have occurred. It is written as the expression:

$$|A_y| > \text{threshold} \ \& \ A_x < |\text{threshold}_{\min}| \ \& \ A_z < |\text{threshold}_{\min}| \quad (\text{where } A_x, A_y, \text{ and } A_z \text{ represent the angular velocity of x-, y-, and z-axes, respectively})$$

## CONCLUSION

This project found a method to recognize head movement direction, displacement, and nodding/shaking actions. It can be used to construct a "head mouse". Pointing is obtained by detecting and identifying the direction of head movements; clicking is obtained by identifying a nodding motion. This utilizes look-and-nod motions instead of point-and-click motions with a mouse. Through this method, a more natural and convenient human-machine interaction method can be realized, in which the direction you are watching is where the cursor will point.

## METHODS

### Procedures

We purchased demonstration and evaluation kits from the vendor of angular velocity sensors (NXP Semiconductors, ST Microelectronics, and Bosch Sensortec GmbH). The kits include a sensor daughter board and an MCU controller board with a USB port. The kits communicate via USB with a host computer and provides a visualization software tool to support the collection and analysis sensor data through the MCU controller board combo connected to a computer via a USB port. This enables quick visualization of sensor data based on the pre-configured sensor settings in the firmware. The real-time sensor evaluation enables easy changes to critical sensor settings and data logging during sensor demonstrations. The register level interface provides a register map for the sensors thus allowing quick reading and writing of different register bits and enabling detailed sensor evaluation.<sup>7</sup>

The evaluation board (EVB) is strapped to a Bluetooth earphone and is worn with an earphone to simulate the head mouse device assumed in this research. The earphone used in this experiment only serves as a fixed carrier to follow the movement of the head without any electrical connection. The EVB must be mounted in a position such that the y-axis of

the sensor is parallel to the yaw axis of the user's head rotation, the z-axis is parallel to the head's pitch axis, and the x-axis is parallel to the head's roll.

We powered on the EVB and ran the software tool attached to the kits. After initializing the various registers of the sensor, you can measure the angular velocity in real-time. Since it can directly draw the angular velocity versus time curve, we just turn the head in left/right/up/down directions, nod or shake head to simulate the point-and-nod operation and export the angular velocity versus time curve in different test cases.

The experiment needed to control the initialization parameters registers setting such as the following: X/Y/Z axis enable; power mode: normal mode; high Pass filter mode: enable, high pass filter cut off frequency: 16Hz; ODR(Output Data Rates): 60Hz; interrupt: enable.

### ACKNOWLEDGEMENTS

I would like to thank my physics teacher, Jiayun Xu, Dr. Fasheng Zhou, and my father for their guidance and support during my research, as well as my family for their continued support.

### REFERENCES

- (1) Fairfield, C.T.; Susan B; Sacred Heart University R. B. User Friendly: A Short History of the Graphical User Interface. Sacred Heart University Review. 2010,16,1,4.
- (2) Giancoli, D. C.; In Physics for Scientists & Engineers with Modern Physics, 4th ed.; Pearson: Essex, 2014; pp 289-317.
- (3) Google LLC. Input. <http://source.android.com/devices/input/> (accessed March 30, 2020).
- (4) ST Microelectronics. MEMS Motion Sensor: Three-Axis Digital Output Gyroscope. <http://www.st.com/resource/en/datasheet/l3gd20h.pdf> (accessed March 30, 2020).
- (5) Bosch. Gyroscope BMG250. <https://www.bosch-sensortec.com/products/motion-sensors/gyroscopes-bmg250/> (accessed March 30, 2020).
- (6) NXP Semiconductors. 3-Axis Digital Angular Rate Gyroscope. <http://www.nxp.com/docs/en/data-sheet/FXAS21002.pdf> (accessed March 30, 2020).
- (7) NXP Semiconductors. Sensor Toolbox: The Complete Hardware and Software Ecosystem for NXP Sensors. <http://www.nxp.com/docs/en/fact-sheet/SENSETOOLBOXFS.pdf> (accessed March 30, 2020).

### AUTHOR

Jie Li is a senior at International Dep., affiliated High School of South China Normal University, Guangzhou, China. He is particularly interested in solving problems and creating new inventions. Jie Li cultivates his creativity through his avid participation in several science programs.

## What Is the Effect of a Mixed Culture of *Pseudomonas fluorescens* and *Anabaena* on the Degradation of Polyvinyl chloride?

Ojas Kalia

Middleton High School, 16122 Colchester Palms Drive, Tampa, Florida, 33647, United States

ojaskalia@gmail.com

**ABSTRACT:** As our use of plastics continues to increase, the difficulty in degrading these plastics when they reach natural waterways increases as well. The degradation of polyvinyl chloride plastic (PVC) in particular, has posed difficulties for researchers as PVC's even balance of electrical charges complicates the degradation process. The objective of this study was to expose two bacteria - *Pseudomonas fluorescens* and *Anabaena* - to each other to produce an increased supply of energy for a more effective method of degrading PVC. To test this, samples of PVC cloth were massed before and after exposure to these two samples of bacteria to determine if degradation was present or not. After undergoing these trials, the methodology demonstrated that the proposal to expose both bacterium to each other to attempt to degrade PVC was a success, as the degradation rates of this combination of bacteria surpassed previous degradation rates of PVC in the field.

**KEYWORDS:** Bioremediation; environment; Polyvinyl chloride; *Pseudomonas Fluorescens*; *Anabaena*; degradation; Oxygen; Carbon Dioxide.

### INTRODUCTION

Globally, humans produce over 200 million tons of plastic per year.<sup>1,2</sup> Of this, it is estimated that 91% of this plastic isn't recycled.<sup>3,4</sup> Plastics that aren't recycled often end up in landfills, where the chemicals permeate the ground as a result of exposure to UV light from the sun, posing dangers to our air and soil. Additionally, much of this plastic ends up in our waterways: in oceans, lakes, and rivers. It is estimated that almost 8 million metric tons of plastic finds its way to our oceans every year.<sup>5</sup> When these materials enter our water, they disperse harmful chemicals that disrupt the ecosystems within the ocean. Among these plastics, polyvinyl chloride (PVC) has been identified as an extremely hazardous plastic due to the severity of its degradation effects. Upon degradation, it leaches chlorinated organic compounds such as organotin and dimethyltin into the water, which are substances known to be toxic to an organism upon ingestion or exposure.<sup>6</sup>

Polyvinyl chloride is created when the polymerization of initiator compounds and Vinyl Chloride Monomer (VCM) droplets occurs. This starts a chain reaction, which forms the basic monomer of PVC. After water is removed from this structure, polymerization can occur further, and the final product is formed. The even spread of hydrogen and carbon particles throughout common PVC products such as food packaging, water pipes, and medical devices makes it difficult for PVC to be degraded naturally.<sup>7</sup>

Researchers have investigated alternative pathways and conditions that can enhance the degradation of PVC. For example, photodegradation has been linked to the degradation of PVC, as scientists have found that the UV rays emitted by the sun can degrade the polymers in PVC. Certain experiments have even found a link between the degradation of PVC and

increased heat, as thermal degradation studies have shown that PVC mass decreases under temperatures greater than 250 degrees.<sup>8</sup> The field of bioremediation has proved to be one of the most promising. Using bioremediation, scientists have investigated the possibility of using bacteria to break apart the chains within plastic structures. Considering the scale of this problem in oceans, this solution could be one of the most effective and feasible possibilities if properly executed.

Specifically, experiments such as the well-known trials with Anand Chakrabarty's superbug in 1971,<sup>9</sup> have demonstrated the possibility for a bacterial strain that could degrade different forms of plastic by simplifying the structures holding the plastics together. These experiments have advanced the possibility for a solution to the plastics within our oceans using bioremediation. In this instance, this experiment served as a steppingstone for other projects to investigate the effects of bacterium in trying to degrade the plastic that is present within the ocean waters. For example, in 2016, a great advancement within the field was made, as a group of scientists in Japan discovered the specimen *Ideonella sakaiensis* 201-F6 which was capable of degrading plastic using only the structure of plastic as its sole energy source.<sup>10</sup> It utilized an enzyme called PETase, which simplified the structure of the plastic and allowed for the degradation process to occur solely based on the structure of the plastic alone. Just a few months later, scientists improved upon the invention using genetic engineering, making the degradation process more effective.

Yet, even with thousands of experiments analyzing the possibilities of using bacteria to degrade plastic, an underlying problem has halted the possibility for these bacteria to be integrated into an aquatic environment: competition. When these bacteria are tested within a laboratory setting, researchers of-

ten provide a constant supply of substrate within the agar the bacteria are cultured in, such as glucose or peptone to assist in the degradation process, which are not resources that are always available within a natural setting. Bacteria in our oceans meet an unprecedented level of competition from other bacteria. This competition from other bacteria limits their access to resources such as oxygen, an electron acceptor vital to the degradation process, which in turn halts the breaking down of the plastic.

This lack of resources has trumped the possibility of utilizing such bacteria that have evolved to possess characteristics to degrade PVC as these bacteria are not able to break down the plastic without access to these resources. Figure 1 demonstrates this by modeling the release of chloride atoms within bacterial degradation of plastic. This figure demonstrates the limitation of bacterial degradation within the natural environment by illustrating the drop phase, or the phase where release of chloride atoms (an indicator of plastic degradation) becomes stagnant.<sup>11</sup> This phase demonstrates the scenario where a result of a lack of natural resources, such as an energy source or an electron acceptor such as oxygen, stalls the plastic degradation process.

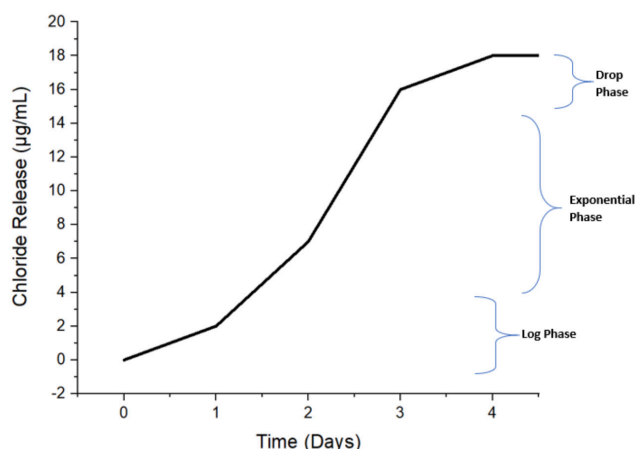


Figure 1. Shows the four phases of plastic degradation first introduced by Asha Yabannavar and Richard Bartha in 1993<sup>12</sup> modeling the limitations of bacterial degradation as a result of a lack of energy within the environment.

In relation, this project aims to modify the relationship that a bacterium has with its surroundings by introducing another specimen of bacteria to continuously supply oxygen, an electron acceptor vital to degradation, so that the bacteria capable of PVC degradation can overcome this drop phase even within the natural environment. *Pseudomonas fluorescens* is a bacterium that has been labeled as capable of degrading PVC plastic. However, without a presence of oxygen, it is not able to complete the process of degradation. *Anabaena* is a cyanobacteria, or a blue-green algae species, that produces oxygen as a byproduct. It requires carbon dioxide (CO<sub>2</sub>) to produce oxygen.

*Pseudomonas fluorescens* produces carbon dioxide as a byproduct of its natural processes. By coupling these bacteria together within a sample, we can effectively create a source of energy between the two that allows the *Pseudomonas fluorescens* bacteria to degrade plastic within our waters without interruption due to competition from surrounding microbial life within the water.

Therefore, we hypothesize for this experiment that if the cyanobacterium *Anabaena* and the soil bacteria *Pseudomonas fluorescens* are exposed to each other through a mixed culture, they will be able to more effectively degrade polyvinyl chloride (PVC) plastic than *Pseudomonas fluorescens* alone.

## RESULTS AND DISCUSSION

In the collection of data, it was found that the total difference in weight was greater in the samples that contained both the *Pseudomonas fluorescens* and the *Anabaena* versus the *Anabaena* alone and the samples that did not contain bacteria. Differences between the mass of the PVC squares within each group (*Pseudomonas fluorescens* and *Anabaena*, *Pseudomonas fluorescens*, and no bacteria present) were present, but an overall trend was consistent between each group. This is demonstrated in Table 1, where the weight of the weight boat, the weight of the plastic before and after exposure, and total differences in weight of the PVC are listed.

Table 1. Demonstrates the weight of the PVC before and after exposure to bacterial strains after exposure to bacterial strains.

Bacterial Strain in Sample	Weight of Polyvinyl Chloride Cloth Squares (in grams)			
	Weight Prior to Exposure with Bacteria	Weight of Weight Boat	Weight After Exposure to Bacteria	Total Difference in Weight
<b><i>Pseudomonas fluorescens</i> and <i>Anabaena</i></b>				
Trial 1	0.0276	2.8042	2.8308	0.0010
Trial 2	0.0301	3.235	3.2624	0.0027
Trial 3	0.0290	2.4674	2.4943	0.0021
Trial 4	0.0414	2.0835	2.1228	0.0031
Trial 5	0.0232	2.5059	2.5286	0.0005
<b><i>Pseudomonas fluorescens</i></b>				
Trial 1	0.0431	2.6809	2.7227	0.0013
Trial 2	0.0301	2.4464	2.4749	0.0016
Trial 3	0.0272	2.6362	2.6622	0.0012
Trial 4	0.0284	2.7500	2.7770	0.0014
Trial 5	0.0272	2.5729	2.5988	0.0015
<b>No Bacteria Present</b>				
Trial 1	0.0302	2.7273	2.7567	0.0009
Trial 2	0.0281	2.9331	2.9596	0.0016
Trial 3	0.0416	2.8712	2.9122	0.0006
Trial 4	0.0283	2.9035	2.9303	0.0015
Trial 5	0.0272	2.7736	2.8001	0.0007

The first column of values demonstrates the weight of PVC prior to any exposure with bacteria. This value is then followed by the weight of the weight boat that the PVC cloth was placed within to mass it after it was exposed to the bacterium. The weight of the boat and the cloth together is also shown. The total difference in the last column shows the difference in the value of the weight of the PVC before and after exposure to bacteria. It demonstrates a change present in all samples. However, the change is much more visible in the sample containing *Pseudomonas fluorescens* and *Anabaena* versus the samples citing only the *Pseudomonas fluorescens* or no bacteria at all. For example, differences such as 0.0031 were



only present when both strains were present. Figure 3 adds to significance of these values by modeling degradation as a percentage of the initial weight.

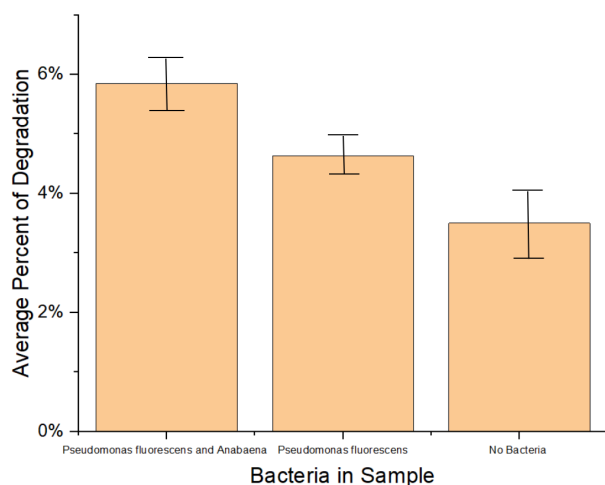


Figure 2. Demonstrates the changes in the mass of the PVC cloth during the experimental trials, calculated as the average of the 5 trials.

To truly acknowledge all possibilities of error within calculations, Figure 2 demonstrates the percent of degradation rather than just the difference in weight. Different weights of PVC could have increased or decreased rates of degradation (as PVC squares with greater surface area are more susceptible to degradation), and so the percentage of the degradation was a necessary addition. This model demonstrates that the percentage of degradation for both strains of bacteria (5.8% average rate of degradation) was constantly greater than the rate of degradation for just one strain of bacteria (4.6% average rate of degradation) and the percentage of degradation for samples without bacteria (3.5%). These differences between percentage of degradation are statistically significant. This was calculated using a two sample T-test where the p-value between a comparison of percentages of degradation between samples of the groups was calculated to be 0.00627, which was lower than the assigned significance level of 0.01. By adding this comparison, the hypothesis is supported further. Figure 3 attempts to test if possible confounding variables, such as the differing weights of the PVC squares used for each sample, could have significantly impacted these values.

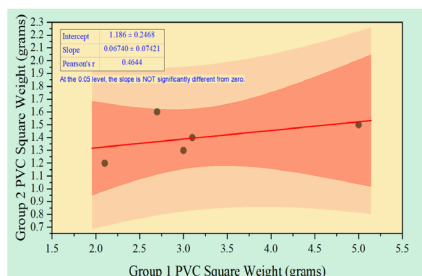


Figure 3. Models the average percent of degradation for different samples by dividing the starting weight of the PVC to the weight after exposure.

Additionally, to ensure the reliability of the results, an analysis to test how uniform the squares of PVC were, was necessary. If the weights of each square were not uniform, then the degradation rates could have been influenced by the different weight of the squares. To ensure this was not the case, a linear regression line analysis was done to demonstrate the uniformity between the weight of the PVC squares. This test aims to better understand if the differences between the weights of the PVC squares are statistically significant or not. If the differences in the weights of the squares are not statistically significant, then it demonstrates that the possibility of the differences between the weight of each PVC square being a confounding variable within the experiment is limited. However, if they are statistically significant, then the differences in the weight of the PVC squares could lead to changes in the percentage of degradation. The result of this analysis was that the differences between the weights of the different groups of PVC squares were not significant, as the differences of the weights yielded a p-value of 0.4464, which was greater than the significance level of 0.01. Therefore, the validity of measuring the difference of weight between the PVC squares remains, as the weights of the cloth itself will not cause a significant change within the results. Lastly, Figure 4 attempts to investigate if differing weights between the weight boats utilized could have significantly changed the results as well.

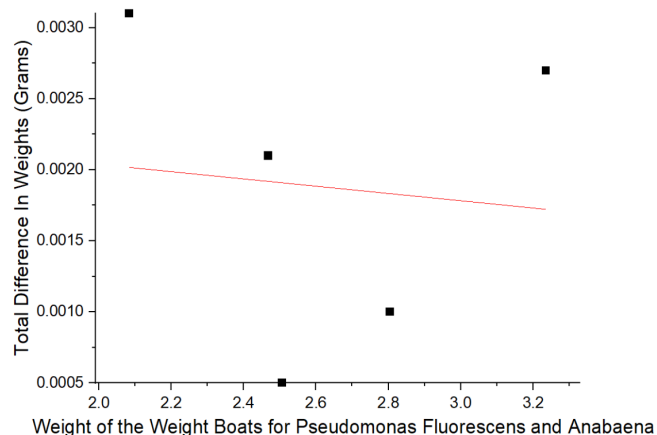


Figure 4. Demonstrates a linear regression analysis between the weight of the weight boats for the samples with *Pseudomonas fluorescens* and *Anabaena* and the total difference in weights (in grams).

A linear regression analysis between the weight of the weight boats and the total difference in weight was also conducted, as a test to see if the differences of the weight of each weight boat had any effect on the resulting difference in weight for the PVC squares. In the end, a value of  $r = -0.16$  demonstrated that such a correlation was not present. Therefore, the weights of the weight boats did not impact the weights of the PVC squares; it was the degradation process itself that resulted in the changes in the plastic.

## DISCUSSION

### *Selection of Weight as a Factor to Measure Degradation*

The mass of the individual PVC squares was utilized as the dependent variable to demonstrate the different rates of degradation for each sample. The weight of each sample should decrease as a result of the degradation of the phthalates that are a part of the industrial plastic structure. This degradation also releases chloride atoms as well, which furthermore supports the idea that the degradation of plastic leads to the loss of weight within each PVC square. Weight has been utilized as a measuring factor within several experiments testing degradation as well.<sup>13</sup> However, an addition of a quantitative way to measure the oxygen present in the tubes, such as the use of Durham Tubes, would provide a great deal of insight into the processes occurring in the test tube themselves. The study of the level of oxygen in the tube would demonstrate the activity of the *Anabaena*, which would produce information that would either better clarify the results in this experiment. Looking towards continuations of this project in the future, such a method will be utilized.

### *A Comparison of the Results of the Mixed Culture and the Pseudomonas fluorescens Strain Alone*

Within the actual results of the experiment, it was evident that the culture that had contained each bacterium was more successful in degrading the PVC than the samples containing just *Pseudomonas fluorescens* alone or no bacteria at all. Within the actual measurements of the weight, an average difference in weight for samples containing both bacterium was 0.00188 milligrams (with a standard deviation of 0.0011 milligrams), the average difference in weight with one bacteria within the sample was 0.0014 milligrams (with a standard deviation of 0.00015 milligrams), and average difference in weight for no bacterial samples was 0.00106 milligrams (with a standard deviation of 0.0029). The differences between all three treatments were significant.

### *Statistical Analysis to Validate Results*

First, to assess the reliability of the conditions set by the methodology of the experiment, significance values were tested between the PVC squares of each group. If the differences in weight between the PVC squares of the groups were statistically significant, then the results of the experiment would be invalidated, as the differences in mass of PVC squares across groups would interfere with the percentage of mass of degradation when compared to the original mass of the PVC square from group to group. The presence of an increased amount of PVC within samples could also lead to an increased level of degradation between certain samples. To ensure that this was not present within the experiment, a paired T-test was created to test the statistical significance of the differences. The null hypothesis stated that the difference of the two groups of PVC squares would equal zero, while the alternate hypothesis stated that the differences between the groups would be greater than zero. However, a p-value of 0.4464, which is greater than the assigned significance level of 0.01, led to the conclusion that

the differences between the squares were not significantly different, and that the trials would not be impacted by the weight of the squares significantly.

Additionally, another paired T-test was created to analyze whether the results of the trials supported the hypothesis or not. The null hypothesis within the test was that the rate of degradation by the *Pseudomonas fluorescens* alone would equal the rate of degradation by the *Pseudomonas fluorescens* and the *Anabaena* together. The alternate hypothesis, therefore, was that the difference in the weight of PVC squares in the groups of both bacteria together minus the *Pseudomonas fluorescens* strain alone would be greater than 0. Since the p-value yielded, where  $p=0.00627$ , is less than the significance level of 0.01, the null hypothesis can be rejected, and the alternate hypothesis can be accepted. This proves that the rate of degradation exemplified by the mixed culture of bacteria was statistically significantly higher than the rate of degradation conducted by the *Pseudomonas fluorescens* strain alone, supporting the original hypothesis of the experiment.

To further show the validity of the methodology, a linear regression analysis between the weight of the weight boats and the outcome of the differences in weight in the samples containing both bacteria was conducted. It could be inferred that if such a correlation existed, then the weight of the weight boats could have influenced the differences in the weight of the PVC squares due to the differing weight boats for each sample changing the mass of the measurements. Yet, within this test, it was shown that a value for  $r=-0.16$  demonstrated that there was no correlation present between the two variables, and therefore, the differences in weight were a result of the degradation itself, not a result of the differing weights of the weight boats.

### *Importance of Results and Future Outlook*

The results of this experiment are important to the issue of plastics ending up in our oceans because they provide evidence for the use of bacterial degradation as a possible solution. Bacterial degradation is integral in trying to rid our waterways of plastics as bacteria can use the structures of these plastic materials as energy and break them down naturally. This could lead to a massive cost reduction in our current efforts and allow us to apply this solution to all waterways, not just a specific area. The underlying problem with an approach involving bacteria has been the lack of energy that these bacteria can acquire when trying to degrade complex structures. This study shows that by coupling two strains of bacteria, we can supply a more plentiful source of oxygen for bacteria capable of degrading plastic. It allows these bacteria to degrade the plastic without nearly as much competition from the environment, which leads to a more efficient process of degradation. These findings could allow us to replicate the success that we have in laboratories with plastic degradation in our aquatic environments as well, which could be a huge step forward for the field of bioremediation.

In a wider context, this study is useful to national governmental agencies such as Environmental Protection Agency (EPA) as the agency has sponsored several different projects

to try to clean up the plastic debris within our oceans.<sup>14</sup> The application of research could potentially change the approach utilized within these projects, as rather than investing in large capture devices – as the EPA currently does for its local projects<sup>15</sup> the agency would be able to apply the projects to a larger scale and still cut costs with the application of these two bacteria. Such a fact would make the results relevant to people on a local scale as these bacteria are both biosafety level (BSL) 1, meaning with proper precaution they can be utilized by people other than just scientists and researchers. Local people could contribute to the project in a much bigger way if these solutions are implemented simply by investing in a possible product that uses the combination of these bacteria to clean up plastic waste within waterways. However, before such ideas are implemented, it is necessary to try to expand the scale of this experimentation. The use of these two bacteria to degrade plastic must be first tried within nature, as several experiments involving bioremediation to degrade plastic often demonstrate promising results within the lab but do not work within nature. It is necessary to scale up the number of samples within the trials as well as the time period that the plastic is exposed to both bacteria to better understand and interpret the results.

### CONCLUSION

Using multivariate methods to analyze the results, a conclusion can be drawn stating that the hypothesis was supported by the experiment. Specifically, the statistical significance between the variables was less than 1% (0.0627% was the exact value), demonstrating that the correlation between the conjugation between both bacterial samples led to increased PVC degradation.

Additionally, beyond just the statistical significance, a substantive significance was shown in this experiment by projecting the data over time. Considering that the difference between both bacteria and just one bacterium was statistically significant in just a span of five days, the difference between the rates of degradation of both bacteria in the sample versus just one bacteria in the sample of the bacteria could continue to increase over time. This data modeled that the correlation between the variables was casual, or that the degradation level of both bacteria was a result of both working together on the PVC sample, not just the result of one bacterium. However, to further prove this, future trials will be conducted with a control group of *Anabaena* as well. This will assist in the understanding of the results within these trials, and better understand the roles that each bacterium plays in the degradation process.

Within this experiment, it was concluded that the combination of both strains of bacteria together could assist each other in overcoming the limitations of plastic degradation caused by competition in the environment. Looking towards the substantive meaning of this finding, one can state that if utilized properly in the future, the combination of both strains of bacteria together in one sample could open new doors for the bioremediation of complex plastics such as polyvinyl chloride.

### Materials and Methods

Fifteen test tubes were required for this experiment, each with test tube caps to ensure that the oxygen produced is

trapped within the tube. 500 ml of liquid agar broth was made and was stored in a 37-degree Celsius freezer to ensure that the agar allowed for the growth of both bacteria. Two strains of bacteria, *Pseudomonas fluorescens* and *Anabaena* were used, each of which was ordered from Carolina Biological. A PVC tablecloth was used because it was made of 100% polyvinyl chloride. An autoclave and a 70% ethanol solution were used to sterilize all substances that were touched by the bacteria. A vortex mixer was used to continuously mix the strains while they were degrading the PVC to ensure that the samples of bacteria interacted with each other. Finally, the experiment was conducted in a Biosafety level 1 laboratory under a laminar hood to prevent any possible airborne contamination.

### Methodology

Using sterilized scissors, the PVC bath cloth was cut into squares of length 1 cm x 1 cm to obtain a total of 15 squares. The PVC cloth squares were then disinfected by rinsing them with ethanol and allowing them to sit for 5 minutes. Then the sheets were labeled by writing the letter “B” on the first five sheets, “O” on the next five, and then “N” on the last five. Each group of five sheets was numbered from 1-5 randomly. Then, the mass of these squares was measured on the analytical balance. After massing, the PVC sheets were placed into an airtight bag using autoclaved forceps.

Next, using a bulb pipette, 13 mL of liquid agar broth was pipetted into each tube. At the end of this procedure, 15 test tubes containing liquid agar broth were present, and the test tube caps were placed on the tubes.

The first five test tubes were labeled with the letter B (which represented the sample for “both strains”) and then a number from 1-5 depending on the order that tube was picked up. The next five were marked with the letter O for “one strain” along with numbering from 1-5 and then the next five.

Next, the inoculating loop was flamed over the Bunsen burner to ensure the removal of the contaminants. The loop was placed within the bacterial vial containing *Pseudomonas fluorescens* and used to scoop a portion of bacteria from the test tube. This process was repeated until all test tubes with the letter “O” contained the *Pseudomonas fluorescens* bacterium.

Then, the metal inoculating loop was flamed once more and used to pick up bacteria from the test tube containing “*Pseudomonas fluorescens*”. This bacterium was added first to the tube labeled “B1”. Next, the loop was flamed once more used to pick up a small portion of bacteria from the “*Anabaena*” vial. The inoculating loop was also added to the test tube labeled B1 and stirred. This process was repeated until all test tubes with the letter B contained both samples of bacterium.

The last five test tubes were not exposed to any bacterial samples since these samples would serve as controls for the experiment.

After, the test tube caps of all fifteen test tubes were removed, and 1 PVC cloth square was added to each tube, depending on the number and letter was labeled as. For example, the square with the labels “B1” was added to the test tube labeled “B1” and so on. All the test tube caps were placed back on after the squares were added, and the test tubes were placed within a



beaker and covered by an autoclaved piece of foil. The beaker was then placed on the vortex machine, and vortexed at a speed of 100 rpm-for 5 days, as demonstrated within Figure 2.

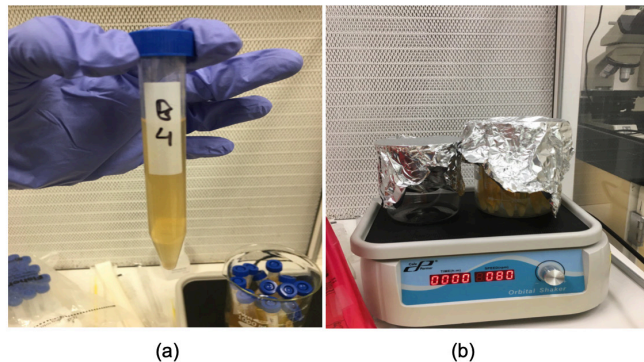


Figure 2. Shows a plastic tube incubated with both strains of bacteria (a) and shows the experimental setup used to vortex the samples (b).

After 120 hours, the test tubes were removed from the beaker covers. Using another pair of autoclaved forceps, all 15 PVC cloth squares were removed from each tube and placed in a 70% ethanol solution. After washing and letting the sheets dry, each sheet was massed.

#### ACKNOWLEDGEMENTS

First and foremost, appreciation is given to Mr. Andre DaSilva who served as a mentor on the proper and safe execution of the experimental trials. Additionally, gratitude is given to Mrs. Patricia Dodson for her generous access to the laboratory facilities at Middleton High School. The formation for the idea for the project and the trials themselves were conducted by the author.

#### REFERENCES

- (1) Yu, Jie, L. Sun, C. Ma, Y. Qiao, H. Yao. "Thermal degradation of PVC: A review." *Waste management* 48 (2016): 300-314.
- (2) Booth, G. H., A. W. Cooper, and J. A. Robb. "Bacterial degradation of plasticized PVC." *Journal of Applied Bacteriology* 31.3 (1968): 305-310.
- (3) "Facts-. About Plastic-. Help - Plastic Oceans Foundation." *Plastic Oceans International*, plasticoceans.org/the-facts/.
- (4) Dufour, Fred. "A Whopping 91% of Plastic Isn't Recycled." *National Geographic*, 20 Dec. 2018, www.nationalgeographic.com/news/2017/07/plastic-produced-recycling-waste-ocean-trash-debris-environment/.
- (5) "Organochlorine Pesticides" Division of Public Health, Delaware Health and Social Services, January 2015, page 1.
- (6) Xu, Y., Q. Wu, Y. Lei, and Q. Zhang. "Natural fiber reinforced poly (vinyl chloride) composites: Effect of fiber type and impact modifier." *Journal of Polymers and the Environment* 16.4 (2008): 250-257.
- (7) Julinova, Marketa, R. Slavik, A. Kalendova, P. Smida, and J. Katrina. "Biodeterioration of plasticized PVC/montmorillonite nanocomposites in aerobic soil environment." *Iranian Polymer Journal* 23.7 (2014): 547-557.
- (8) Ezezika, Obidimma C., and Peter A. Singer. "Genetically engineered oil-eating microbes for bioremediation: prospects and regulatory challenges." *Technology in Society* 32.4 (2010): 331-335.
- (9) Yoshida, Shosuke, K. Hiraga, T. Takehana, I. Taniguchi, H. Yamaji, Y. Maeda, K. Toyohara, K. Miyamoto, Y. Kimura, and K. Oda. "A bacterium that degrades and assimilates poly (ethylene terephthalate)." *Science* 351.6278 (2016): 1196-1199.
- (10) Yabannavar, Asha, and Richard Bartha. "Biodegradability of some food packaging materials in soil." *Soil Biology and Biochemistry* 25.11 (1993): 1469-1475.

(11) Kumar, B. Manoj, Sabike Noobia, and S. Mythri. "Studies on Biodegradation of Plastic Packaging Materials in Soil Bioreactor." *Indian Journal of Advances in Chemical Science* S1 297 (2016): 299.

(12) "Trash-Free Waters Projects." EPA, Environmental Protection Agency, 4 Dec. 2019, www.epa.gov/trash-free-waters/trash-free-waters-projects.

#### AUTHOR

Ojas Kalia is currently a rising senior at Middleton High School in Tampa, Florida. He has participated in his regional science fair since 7th grade and won first in his division twice. This year, he was awarded the Stockholm regional junior water prize because of his research with bioremediation of Polyvinyl chloride. In his free time, he enjoys playing chess, basketball, and tennis.

## The Optimization of Lead Absorption in Contaminated Water Through Anhydro Galacturonic Acids in Various Citrus Peels

Amy Wang, Viveka Chinnasamy, Shreya Tripathi  
Hamilton High School, 3800 S. Arizona Ave., Chandler, AZ, 85248 United States

**ABSTRACT:** Lead poisoning is a severe health condition that impacts around 240 million people annually worldwide, especially in developing nations and regions such as India, Africa, and South America. Furthermore, fruit peel wastes are found in abundance in underdeveloped nations at low costs and have a chemical makeup that may absorb lead in an environmentally friendly way. It was hypothesized that the pectin concentrations in fruit peels would be directly proportional to the lead absorption, therefore causing grapefruit pectin to absorb the most lead, because more pectin signifies greater availability of the chelating agents that allows the polysaccharide to more effectively bind to lead ions. This study tested a sustainable and cost-effective method to create a filtration system that purifies lead contaminated water through the use of anhydro galacturonic acid from various citrus fruits. Anhydro galacturonic acid, the main component of pectin, extracted from citrus peels was tested for lead adsorption using a percent absorption analysis. Each type of pectin was successful in absorbing a significant percent of lead from the initial solution with respect to the control group; however, grapefruit peels had the greatest percent absorbance for lead since they contained the greatest amount of anhydro galacturonic acid, as the hypothesis predicted.

**KEYWORDS:** Filtration; Lead Contamination; Water Purification; Pectin; Citrus Peels; Anhydro Galacturonic Acid.

### INTRODUCTION

Lead poisoning is one of the most severe and common diseases, accounting for nearly 0.6% of global diseases.<sup>1</sup> Lead, a heavy metal found in the earth's crust, is used in many day-to-day products. Widespread use of lead combined with an increase in globalization has resulted in the environmental contamination of lead in large bodies of water, leading to serious health concerns worldwide. The ramifications of lead poisoning have proliferated exponentially through the collective consumption of the food chain, exposing humans to serious health consequences. With respect to the worldwide epidemic of lead contamination, The World Health Organization estimates that 240 million people around the world are overexposed to dangerous lead concentrations. Of those impacted 99% are found in developing nations in Africa, South America, and some parts of India and account for approximately 853,000 deaths annually.<sup>2</sup> Lead toxicity affects all populations, however, young children are more susceptible to its effects and can suffer from permanent adverse effects to their cognitive development.<sup>2</sup> Adults exposed to toxic levels of lead have a higher risk of developing high blood pressure as well as kidney damage.<sup>3</sup> For these reasons, preventing lead exposure is an important issue in the international public health community; however, this proves to be a difficult task as global production of lead is continuously increasing as nations continue to industrialize.

Current solutions to lead contaminated water come in various forms ranging from gravity filters, reverse osmosis systems, faucet mount filters, to distillers. However, it is important to consider that these technologies are not sustainable in rural communities in developing nations. The use of pectin to bind

to lead ions could be a viable form of water filtration in these developing countries, since it is known that pectin has capabilities of binding heavy metal ions. Food products such as some pectin rich fruits and vegetables have been studied for their biosorption capacity, which led to the proposed method of utilizing the pectin in fruit peels to filter lead from water. When considering the environmental sustainability of fruit peels, they are commonly found in underdeveloped nations at low costs and with significant availability. Fruit peels are frequently used in compost or disposed of within these countries, so their utilization as part of our solution would come at no cost. For example, fruit and vegetables make up 39% of food waste in the US.<sup>5</sup> This is why, when considering that the majority of the infected populations are from impoverished communities, sustainable goods such as fruits prove to be promising solutions for lead poisoning. Contaminated water poses a risk to children's development and the health of adults; therefore, it is urgent to find a solution to water pollution. The use of pectin could be the first step to reaching an easily accessible means of filtering lead contaminated water.

The goal of this research project is to create a lead filtration system for environments with lead contaminated water using anhydro galacturonic acid - also known as pectin - found in various citrus fruits. We initially hypothesized that if pectin significantly reduces lead concentration, it can be used as an alternative cost-effective and sustainable filtration system. We also hypothesized that as the pectin concentration of a fruit increases, its ability to absorb lead will also increase due to the heightened amount of chelating agents binding to the metal ions. If pectin from grapefruit, orange, and lemon is placed in a lead solution, it was predicted that the grapefruit pectin would

absorb the most lead because it contains the greatest concentration of anhydro galacturonic acid which is 0.65%.<sup>6</sup> Oranges only contain 0.57% while lemons contain 0.63% pectin.<sup>7</sup>

## RESULTS AND DISCUSSION

To test the hypothesis, nine oranges, nine lemons, and three grapefruits were peeled and placed in separate pots that contained two liters of water. The pots were boiled and filtered to separate the anhydro galacturonic acid from the peel-water system. Dried peels were added to the pectin solution to increase the surface area and porosity to allow for better absorption of the lead. The pectin was then immersed in lead nitrate for 24 hours to allow for absorbance of the lead ions, and the remaining solution left behind was reacted with potassium iodide. The yellow precipitate, lead iodide, was dried and massed. The change in moles of lead indicated the amount of lead absorbed by the pectin within the fruits, and the average percentage of lead absorbed for each fruit pectin was calculated.

When considering the results of the experiment, the orange pectin absorbed approximately 75.52% of the original lead, lemon pectin absorbed approximately 54.36%, and grapefruit absorbed approximately 77.92%. The pectin from the grapefruit absorbed the greatest percentage of lead, while the orange absorbed the least, excluding the control. The control group absorbed approximately 0% of the original amount of lead, as the amount of lead remained the same before and after the reaction took place. The pectin in each fruit successfully removed lead from the lead nitrate solution, implying that using a pectin-based filtrations system, it can be expected to remove approximately 80% of the lead found in contaminated water (Figure 1).

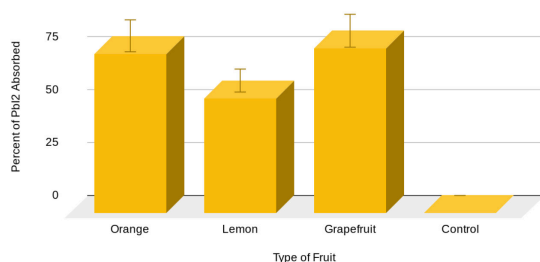


Figure 1. Average percent of PbI<sub>2</sub> absorbed vs type of fruit.

## CONCLUSION

In conclusion, the hypothesis that grapefruit pectin would absorb the most lead was supported by the data: the grapefruit was able to remove about 78% of the lead, more than orange and lemon peels. The higher absorption capacity of the grapefruit is due to a greater concentration of pectin present in grapefruit peels compared to the other citrus fruits that were utilized. As stated in the hypothesis, grapefruit has a 0.65% concentration of the sugar which is greater than the concentrations found in orange and lemon. Even though grapefruit had the greatest absorption, orange absorption was close in percentage due to the overlapping of their error bars. Therefore, the absorption of lead using grapefruit and orange was

not significantly different. Because of this, the experiment contradicted what was hypothesized based on the level of pectin found in orange and lemon peels. The second highest pectin content based on background research was in lemon which absorbed the least amount of lead (excluding the control). There are multiple hypothetical reasons for this occurrence. One of the reasons could lie in the differences in surface area of each fruit. As surface area increases, the adsorption capacity also increases. Orange peels have been found to have a high surface area through the use of Langmuir Isotherm Models and Freundlich models and demonstrate a high capacity for absorbing lead ions.<sup>8</sup> Another reason that orange was effective at absorbing lead ions could lie in the ripeness of the fruit. In this experiment, ripeness was not measured, but this could be a potential factor in the absorption capability of the fruits. As fruit ripens, there is a “softening” process that occurs. In this scenario, “pectin degrading enzymes such as polygalacturonase, pectin methyl esterase, lyase, and rhamnogalacturonan are the most implicated in fruit-tissue softening.”<sup>9</sup> Therefore, ripened fruits contain less pectin due to the higher presence of these enzymes. This indicates that there could have been varying pectin amounts in the fruits, leading to the unexpected higher lead absorption by the orange if the lemons had been riper.

One potential avenue of future research is presented through methylation. The pectin used in the experiment was polymerized to increase the porosity of its surface. The addition of methyl groups from isopropyl alcohol could further increase the ability of the pectin to absorb the lead, as the alcohol contains hydroxyl groups that aid in the chelating agent structure’s binding to the positive lead ions. Additionally, this research can be expanded by improving the pectin polymer system. The pectin polymer system absorbed a small amount of the water from the 0.1M lead solution. To better the system, the project hopes to determine how to increase the amount of water coming out of the filter to retain as much of the original water concentration as possible. This could be achieved by maximizing the amount of dried citrus pith used in the filtration system instead of the zest of the fruit peel.

This experiment demonstrates a sustainable and cost-effective solution to lead contamination in many rural parts of the world. The use of waste products such as peels makes it a sustainable resource, as there are billions of tons of peels generated as waste around the world. The fact that fruit pectin is effective in absorbing lead ions proves that this waste can be useful. Many people around the world struggle to afford high maintenance filtration systems, and they often lack access to any clean water. Contaminated water poses a risk to children’s development and the health of adults; therefore, it is urgent to find a solution to water pollution. The use of pectin is the first step to reaching an easily accessible means of filtering lead contaminated water, especially in underdeveloped countries. Extracting pectin is not a labor-intensive process and requires very little energy to extract. Hopefully, this project can effectively combat metallic ion contamination.



## METHODS

First, we peeled nine small oranges, nine lemons, and three grapefruits, placed them individually in three pots and boiled them with around 2 liters of water each. Once boiling began, we let the pots simmer for 15 minutes and then remove them from the heat. After straining the peels, we preserved the strained liquid in separate containers and baked the dried peels in the oven at 360 degrees for 1 hour. After leaving the baked peels outside to sun dry for 1 week, we blended them to create three powdery substances which were separately stored. In order to prepare the anhydro galacturonic acid solution, we mixed 1 teaspoon of each fruit juice solution with 1 tablespoon of rubbing alcohol. If the alcohol solution formed a solid jellylike mass that could be picked up with a fork, we confirmed that pectin had been created for all three fruits. Next, we labeled 12 250ml beakers (4 per fruit) and transferred 50ml of each pectin solution in the graduated cylinder to the labeled beakers. We then used an electronic balance to measure out 11.25g of each fruit peel and then added that to the respective 250ml beakers while mixing thoroughly with a stirring rod. Each of these pectin solutions were left overnight in a fume hood. Moving on to the next phase of the experiment, we obtained a new batch of 12 150ml beakers, labeled each with the fruit and trial number, placed funnels on top of each, and covered each with a filter paper. Next, we transferred each pectin peel mixture to the filter papers on the respective funnels and created our necessary solutions. In order to create a 0.1M  $\text{Pb}(\text{NO}_3)_2$  solution, we added 33.133g (1 mol) of  $\text{Pb}(\text{NO}_3)_2$  to a 1L volumetric flask and filled it with distilled water to the 1000ml mark. We created a 0.25 M KI solution by adding 41.5025g (1 mol) of KI to a 1L volumetric flask, and filled it with distilled water to the 1000ml mark. Next, we added 50ml of  $\text{Pb}(\text{NO}_3)_2$  to each pectin mixture using the funnel filter paper system, and left the  $\text{Pb}(\text{NO}_3)_2$  infused solution overnight. The next day, we added 50ml of KI to each solution using the funnel/filter paper system and left the KI infused solution overnight (leaves a yellow solution). Before beginning the next experimental phase, we obtained 4 new 150ml beakers for the control group and added 50ml of KI and 50ml of  $\text{Pb}(\text{NO}_3)_2$  to each beaker, labelling the beakers for each of 4 control trials. We also threw away the pectin/peel mixture that remains on the filter paper, and transferred the yellow solution in each beaker to 16 precleaned 250ml beakers using a new funnel/filter paper system until all of the aqueous  $\text{KNO}_3$  came out clear in the beaker, leaving behind  $\text{PbI}_2$  precipitate in the filters. We made sure to record the weight of the filter papers beforehand. Finally, we discarded the  $\text{KNO}_3$  in the beakers and placed the 16 funnel/filter systems that contain the  $\text{PbI}_2$  residue into their respective 16 watch glasses labelled with fruit and trial number. These watch glasses were put in the oven for 10 hours until the  $\text{PbI}_2$  precipitate dried and then we massed out the dried solid in each filter paper in grams using the electronic balance. Moving on to the calculations, we subtracted the mass of the boat and filter paper from the overall resulting mass of each trial. After, we converted each mass to moles of  $\text{PbI}_2$ , which is equivalent to the moles of lead, since there is 1 mole of Pb for

every mole of  $\text{PbI}_2$ . Next, we subtracted this molar amount for each trial from the initial molar amount of Pb in each beaker, which was 0.005 moles, giving the amount of lead absorbed by the pectin in moles. We converted the moles of lead absorbed for each trial into grams and found the percent absorption by dividing the previously found grams of lead absorbed. Finally, we obtained the average percent of lead absorbed for each fruit and created the graph shown in Figure 1

## REFERENCES

- (1) "Lead Poisoning." Lead Poisoning | National Health Portal of India, [www.nhp.gov.in/disease/non-communicable-disease/lead-poisoning](http://www.nhp.gov.in/disease/non-communicable-disease/lead-poisoning).
- (2) Gottesfeld, Perry. "The Environmental and Health Impacts of Lead Battery Recycling." OCCUPATIONAL KNOWLEDGE INTERNATIONAL, 2016, [wedocs.unep.org/bitstream/handle/20.500.11822/13943/1\\_ECOW-AS%20lead%20background%202016.pdf](http://wedocs.unep.org/bitstream/handle/20.500.11822/13943/1_ECOW-AS%20lead%20background%202016.pdf).
- (3) Lessa, Emanuele F., AL. Medina, AS. Ribeiro, AR. Fajardo. "Removal of Multi-Metals from Water Using Reusable Pectin/Cellulose Microfibers Composite Beads." Arabian Journal of Chemistry, Elsevier, 27 July 2017, [www.sciencedirect.com/science/article/pii/S1878535217301417](http://www.sciencedirect.com/science/article/pii/S1878535217301417).
- (4) "Which Water Filters Are Best for Removing Lead?" The Safe Healthy Home, 14 Dec. 2019, [thesafehealthyhome.com/best-lead-removal-water-filters/](http://thesafehealthyhome.com/best-lead-removal-water-filters/).
- (5) FreshPlaza, "Fruit and Vegetables Make up 39% of Food Waste in the US," 21 Nov. 2017, [www.freshplaza.com/article/2185243/fruit-and-vegetables-make-up-39-of-food-waste-in-the-us/](http://www.freshplaza.com/article/2185243/fruit-and-vegetables-make-up-39-of-food-waste-in-the-us/).
- (6) Braddock, Robert J. Handbook of Citrus By-Products and Processing Technology. John Wiley & Sons, 1999.
- (7) Ross, J K, C. English, and CA. Perlmutter. "Dietary Fiber Constituents of Selected Fruits and Vegetables." Journal of the American Dietetic Association, U.S. National Library of Medicine, Sept. 1985, [www.ncbi.nlm.nih.gov/pubmed/2993399](http://www.ncbi.nlm.nih.gov/pubmed/2993399).
- (8) "Efficacy of Adsorption of Cu (II), Pb (II) and Cd (II) Ions onto Acid Activated Watermelon Peels Biomass from Water." International Journal of Science and Research (IJSR), vol.5, no. 8, 2016, pp. 671–679., doi:10.21275/art2016929.
- (9) Prasanna, V, TN. Prabha, and RN. Tharanathan. "Fruit Ripening Phenomena--an Overview." Critical Reviews in Food Science and Nutrition, U.S. National Library of Medicine, 2007, [www.ncbi.nlm.nih.gov/pubmed/17364693](http://www.ncbi.nlm.nih.gov/pubmed/17364693).

## *Miscanthus sinensis* (Silver Grass) Fiber as a Component of an Eco-friendly Sorbent Bag for Oil Spill Clean-up

Micklare Angelo C. Zepeda, Elarcie Balsomo

Senior High School (SHS) in San Nicholas III, San Nicolas III, Bacoar City, Cavite, 4102, Philippines

balsomoelarcie@yahoo.com

**ABSTRACT:** Oil spills are one of the most serious global, environmental problems; however, synthetic sorbents used to manage oil spills have significant environmental drawbacks due to low biodegradability. This study was conducted to determine the potential of *Miscanthus sinensis* (silver grass) as a component of an eco-friendly sorbent bag for oil spill clean-up. Randomized complete block design, a standard in agricultural experiments, was used in the study. *Miscanthus sinensis* fibers were sorted into different sizes (595  $\mu\text{m}$ , 841  $\mu\text{m}$ , and 2000  $\mu\text{m}$ ), and sorbent bags were prepared. Scanning electron microscope (SEM) was used to characterize morphology, and samples were subjected to dry and oil layer systems to measure diesel and kerosene oil sorption capacities. *Miscanthus sinensis* fiber was found to be stable and porous, exhibiting a unique bamboo-shaped structure which was sunken in the middle and protruding on both sides. No significant differences between diesel and kerosene sorption capacities were observed among the sorbent bags with *Miscanthus sinensis* fibers in dry and oil layer systems. Evaluating fiber size and sorption capacities in dry and oil layer systems, the highest diesel and kerosene oil sorption capacities were exhibited by the five hundred ninety-five micrometer *Miscanthus sinensis* fibers, followed by 841  $\mu\text{m}$  and 2000  $\mu\text{m}$  *Miscanthus sinensis* fibers. These results demonstrate the possibility of using *Miscanthus sinensis* as a component of eco-friendly sorbent bags. Additional research should be conducted to determine the sorption capacities of sorbent bags with *Miscanthus sinensis* on the other types of oil.

**KEYWORDS:** Oil spill; Sorbent bag; *Miscanthus sinensis*; Fiber; Sorption capacity.

### INTRODUCTION

Demand for oil has increased over recent decades with oil serving as one of the most important sources of energy for modern society. Oil is used to create synthetic polymers and chemicals, and used to run vehicles, industrial plantations, and factories worldwide.<sup>1</sup>

Nevertheless, recent events have demonstrated that oil storage, transportation from production to consumers, and consumption entail risks of accidental oil spills in natural waterways and bodies of water.<sup>2</sup> The greatest contributing factors include tanker disaster, wars, equipment breakdown, natural disasters and routine operations during the transportation phase.<sup>3</sup> Data shows that oil spills in the last decade resulted in 24,000 tons of oil being leaked from tankers worldwide per annum.<sup>3</sup> In Korea in 2007, an oil spill was recorded where the tanker spilled 11,000 tons of oil.<sup>4</sup> In the Philippines in 2006, 500,000 L of oil leaked into the southern coastal region of Guimaras that produced damage estimated at 352 million pesos.<sup>5</sup> These oil spills resulted in pollution with detrimental effects on marine ecosystems and human health.<sup>6</sup>

The public is conscious of the environmental problems caused by oil spills. Several studies have recently been carried out to evaluate the use of booms and skimmers, oil pumping, *in-situ* burning, bioremediation, chemical dispersant and solidifier agents,<sup>3</sup> and synthetic sorbents like polypropylene and polyurethane foams.<sup>7</sup> Despite the superior sorption qualities of synthetic sorbents, they have low biodegradability. As a result, several researchers have investigated the use of organic materials as alternative sorbents to remediate oil spills with

a number of studies showing the importance of plant fibers as alternative sorbent materials.<sup>8,9</sup> Abejero et al. (2013),<sup>10</sup> determined that natural kapok fibers packed in nylon nets have potential to be used as a sorbent for oil spills. With a limited amount of research dealing with oil spill management using natural fibers found in the Philippines, the authors of this paper wanted to address the challenge of exploiting local plants as possible sources of natural fibers for oil spill sorption.

Given this challenge, the research authors conducted a study that investigated the potential of *Miscanthus sinensis* (silver grass) fiber as an eco-friendly component of sorbent bags for oil spill clean-up. *Miscanthus sinensis* is a coarse perennial, herbaceous plant introduced to the Philippines during the early 20<sup>th</sup> century.<sup>11</sup> It contains cellulose, pentosans, extractives, ash and Klason lignin.<sup>12</sup> The research authors wanted to investigate and share a more practical and economical way to manage oil spills and to help the community by promoting green innovation to control oil spills using *Miscanthus sinensis*, a randomly distributed and not-widely-used weed in the Philippines. *Miscanthus sinensis* may provide considerable benefits as a natural plant with few side-effects and potentially no significant difference in sorption capacity compared to commercially used synthetic sorbents with negative impact on the environment as well as on non-target organisms.

The main objective of the study was to determine the potential of *Miscanthus sinensis* in an eco-friendly sorbent bag for oil spills. Specifically, the study determined the diesel and kerosene oil sorption capacities of different sizes (595  $\mu\text{m}$ , 841  $\mu\text{m}$ , and 2000  $\mu\text{m}$ ) of *Miscanthus sinensis* fibers in dry and oil



layer systems. The authors also sought to determine the level of significance of the differences among the sorption capacities of all control and treatment samples used in each system.

## RESULTS AND DISCUSSION

Morphological characterization analysis of *Miscanthus sinensis* (silver grass) fiber under scanning electron microscope (SEM) is shown in Figure 1. The study was limited to a magnification of 30  $\mu\text{m}$  of the *Miscanthus sinensis*.

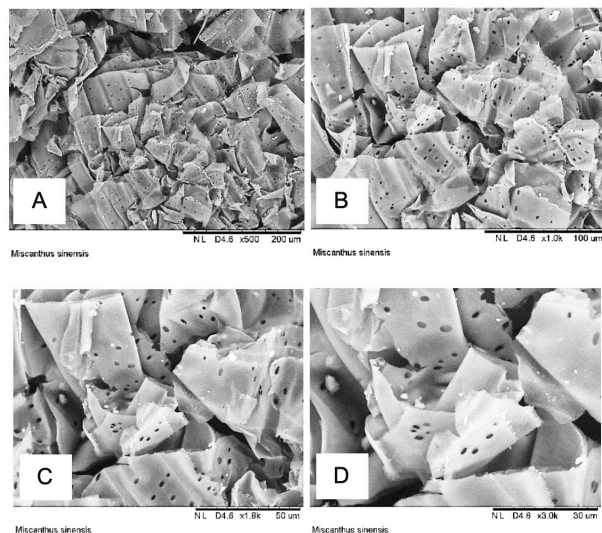


Figure 1. (A–D) Scanning electron microscope (SEM) images of *Miscanthus sinensis* (silver grass) fiber.

Table 1. Diesel oil sorption capacity of sorbent bags in dry systems.

Sorption Capacity (g/g)			
595 $\mu\text{m}$	841 $\mu\text{m}$	2000 $\mu\text{m}$	Polypropylene
3.91	3.29	2.00	4.14

Polypropylene also exhibited the highest diesel oil sorption capacity in oil layer system with 1.83 g/g, followed by 595  $\mu\text{m}$  and 841  $\mu\text{m}$  *Miscanthus sinensis* fibers with 1.33 g/g and 0.83 g/g, respectively. The least sorption capacity was found with 2000  $\mu\text{m}$  *Miscanthus sinensis* fibers absorbing 0.27 g/g as shown in Table 2.

Table 2. Diesel oil sorption capacity of sorbent bags in oil layer systems.

Sorption Capacity (g/g)			
595 $\mu\text{m}$	841 $\mu\text{m}$	2000 $\mu\text{m}$	Polypropylene
1.33	0.83	0.27	1.83

Meanwhile, in the kerosene oil dry system, as shown in Table 3, results obtained showed that polypropylene had the highest sorption capacity with 4.48 g/g, followed by 595  $\mu\text{m}$ , and 841  $\mu\text{m}$  *Miscanthus sinensis* with 3.33 g/g and 2.81 g/g, respectively. Two thousand micrometer *Miscanthus sinensis* fibers was identified to have the least sorption capacity with 2.33 g/g

Table 3. Kerosene oil sorption capacity of sorbent bags in a dry system.

Sorption Capacity (g/g)			
595 $\mu\text{m}$	841 $\mu\text{m}$	2000 $\mu\text{m}$	Polypropylene
3.33	2.81	2.33	4.48

Polypropylene also registered the highest kerosene oil sorption capacity in the oil layer system with 1.33 g/g. It was followed by 595  $\mu\text{m}$  and 841  $\mu\text{m}$  *Miscanthus sinensis* fibers with 1.00 g/g and 0.83, respectively. The least sorption capacity was found in sorbent bag with 2000  $\mu\text{m}$  fibers with 0.43 g/g. The results of kerosene oil sorption capacity of sorbent bags in oil layer system are shown in Table 4.

Table 4. Kerosene oil sorption capacity of sorbent bags in oil layer systems.

Sorption Capacity (g/g)			
595 $\mu\text{m}$	841 $\mu\text{m}$	2000 $\mu\text{m}$	Polypropylene
1.00	0.83	0.43	1.33

Bioactive components such as cellulose and lignocellulose have high potential for oil sorption. *Miscanthus sinensis* contains cellulose, one of the favorable components of an organic sorbent.<sup>12</sup> The sorption capacity of organic sorbents is attributed to its natural fiber that is mainly composed of cellulose. Through capillary action, these hollow tubular structures cause the oil to be adsorbed.<sup>10</sup> Furthermore, greater sorption capacities with smaller sizes of *Miscanthus sinensis* fiber was observed which corresponds to the improvement of sorption capacity when the particles size decrease due to increasing surface area.<sup>13</sup>

The significant variations in the oil sorption capacities among sorbent bags in each system were investigated using two-way Analysis of Variance (ANOVA). The results of the ANOVA indicate that significant differences between the diesel and kerosene oil sorption capacities of sorbent bags used was observed in both dry and oil layer systems. The results of two-way ANOVA are shown in Tables 5 and 6.

Table 5. Difference between the diesel and kerosene oil sorption capacities of *Miscanthus sinensis* (silver grass) fibers and standard sorbent agent used in dry systems using two-way ANOVA.

Source of Variation	SS	Df	Ms	F	P	F crit	Remarks
Total	20.19	23	-	-	-	-	-
Between Oils	0.05	1	0.05	0.21	0.66	4.49	NOT SIGNIFICANT
Among Sorbent Bags	13	3	4.33	16.56	3.66E-05	3.24	SIGNIFICANT
Oils x Sorbent Bags	2.94	3	0.98	3.75	0.03	3.24	SIGNIFICANT

Table 6. Difference between the diesel and kerosene oil sorption capacities of *Miscanthus sinensis* (silver grass) fibers and standard sorbent agent used in oil layer systems using two-way ANOVA.

Source of Variation	SS	Df	Ms	F	P	F crit	Remarks
Total	20.19	23	-	-	-	-	-
Between Oils	0.002	1	0.002	0.004	0.95	4.49	NOT SIGNIFICANT
Among Sorbent Bags	5.87	3	1.96	3.84	0.03	3.24	SIGNIFICANT
Oils x Sorbent Bags	1.12	3	0.37	0.73	0.55	3.24	NOT SIGNIFICANT

Since there are significant differences among the oil sorption capacities of sorbent bags in dry and oil layer systems, Tukey's HSD was employed to determine which among the sorbent bags had significant variations.

Table 7. Tukey's HSD test for the oil sorption capacities of sorbent bags A, B, C and D in dry systems.

Sorbent Bags	q <sub>s</sub>	q'	Remarks
A vs B	7.14	4.49	SIGNIFICANT
A vs C	4.74		SIGNIFICANT
A vs D	4.05		NOT SIGNIFICANT
B vs C	2.40		NOT SIGNIFICANT
B vs D	11.19		SIGNIFICANT
C vs D	8.79		SIGNIFICANT

#### Legend

- A - 595  $\mu\text{m}$  *Miscanthus sinensis* (silver grass) fibers
- B - 841  $\mu\text{m}$  *Miscanthus sinensis* (silver grass) fibers
- C - 2000  $\mu\text{m}$  *Miscanthus sinensis* (silver grass) fibers
- D - polypropylene

As indicated in Table 7, there was no significant difference between the diesel and kerosene oil sorption capacities of sorbent bags with 595  $\mu\text{m}$  *Miscanthus sinensis* fibers and polypropylene, and between 841  $\mu\text{m}$  and 2000  $\mu\text{m}$  *Miscanthus sinensis* fibers. Nevertheless, results showed that there was a significant difference between the diesel and kerosene oil sorption capacities of 595  $\mu\text{m}$  and 841  $\mu\text{m}$  *Miscanthus sinensis* fibers; 595  $\mu\text{m}$  and 2000  $\mu\text{m}$  *Miscanthus sinensis* fibers; 841  $\mu\text{m}$  *Miscanthus sinensis* fibers and polypropylene and; 2000  $\mu\text{m}$  *Miscanthus sinensis* fibers and polypropylene.

Table 8. Tukey's HSD test for the oil sorption capacities of sorbent bags A, B, C and D in oil layer systems.

Sorbent Bags	q <sub>s</sub>	q'	Remarks
A vs B	2.67	4.49	NOT SIGNIFICANT
A vs C	3.45		NOT SIGNIFICANT
A vs D	1.75		NOT SIGNIFICANT
B vs C	0.78		NOT SIGNIFICANT
B vs D	4.42		NOT SIGNIFICANT
C vs D	5.20		SIGNIFICANT

#### Legend

- A - 595  $\mu\text{m}$  *Miscanthus sinensis* (silver grass) fibers
- B - 841  $\mu\text{m}$  *Miscanthus sinensis* (silver grass) fibers
- C - 2000  $\mu\text{m}$  *Miscanthus sinensis* (silver grass) fibers
- D - polypropylene

As shown in Table 8, there was no significant difference between the diesel and kerosene oil sorption capacities of 595  $\mu\text{m}$  and 841  $\mu\text{m}$  *Miscanthus sinensis* fibers; 595  $\mu\text{m}$  and 2000  $\mu\text{m}$  *Miscanthus sinensis* fibers; 595  $\mu\text{m}$  *Miscanthus sinensis* fibers and polypropylene; 841  $\mu\text{m}$  and 2000  $\mu\text{m}$  *Miscanthus sinensis* fibers and; 841  $\mu\text{m}$  *Miscanthus sinensis* fibers and polypropylene. Nevertheless, results showed that there was a significant difference between the diesel and kerosene oil sorption capacities of 2000  $\mu\text{m}$  *Miscanthus sinensis* fibers and polypropylene.

#### CONCLUSION

Based from the results of the study, *Miscanthus sinensis* fibers can be used as eco-friendly sorbent bag for oil spill clean-up. It was noted that the smaller size of *Miscanthus sinensis* fiber was more effective in diesel and kerosene sorption in dry and oil layer systems. It was found that in diesel and kerosene sorption capacities in dry systems, 841  $\mu\text{m}$  *Miscanthus sinensis* fiber is as good as 2000  $\mu\text{m}$  *Miscanthus sinensis* fiber. It was also found that in diesel and kerosene sorption in oil layer systems, 549  $\mu\text{m}$  *Miscanthus sinensis* fiber is as good as 841  $\mu\text{m}$  and 2000  $\mu\text{m}$  *Miscanthus sinensis* fiber.

The sorption capacities of *Miscanthus sinensis* fibers are attributed to its porous characteristics and its cellulose composition, good properties of an organic sorbent. The findings of the study have demonstrated the possibility of using *Miscanthus sinensis* fibers as a component of eco-friendly sorbent bags for use in oil spill remediation.

#### METHODS

**A. Collection of *Miscanthus sinensis* (silver grass).** Three kilos of *Miscanthus sinensis* (silver grass) were collected from a vacant lot at Baran-gay Molino, Bacoar City. The collected leaves were placed in a plastic bag and prepared for laboratory use.

**B. Preparation of *Miscanthus sinensis* (silver grass) fibers.** Collected *Miscanthus sinensis* (silver grass) fibers were washed thoroughly using tap water to remove all debris, cut using scissors, and dried in an oven at 80°C for three hours. After drying, fibers were crushed using an electric blender and sieved into different sizes using 595  $\mu\text{m}$ , 841  $\mu\text{m}$ , 2000  $\mu\text{m}$  sieves.

**C. Morphological characterization analysis.** Morphological structure of *Miscanthus sinensis* (silver grass) was analyzed by scanning electron microscope (Hitachi TM3000) with magnifications

of 200 µm, 100 µm, 50 µm and 30 µm at the University of Santo Tomas, Manila. The samples were mounted onto round, stainless steel holders using double-sided, conductive adhesive tape.

**D. Purchasing of materials and setting up of containers.** Three liters of Petron diesel (density 0.86 g/cm<sup>3</sup>) and kerosene oil (density 0.81 g/cm<sup>3</sup>) were collected from Brgy. Gawaran, a mechanical shop in Bacoar City.<sup>14</sup> A one-meter nylon net was purchased in the market at Antonio S. Arnaiz Ave., Pasay City. The net was measured using a ruler, and thirty-six 6.5 cm x 12 cm x 1 cm nylon net bags were sewed. Forty-eight 250 mL beakers were set up to determine the oil sorption capacity of sorbent bags in each system.

**E. Preparation of sorbent bag with *Miscanthus sinensis* (silver grass) fibers.** Seven grams of different-sized (595 µm, 541 µm, 2000 µm), natural fibers from *Miscanthus sinensis* (silver grass) were weighed using a digital balance. Fibers were packed in nylon net bags with three replicates each per test. Polypropylene (The Liquidator), purchased in the market at Dona Soledad Ave., Parañaque City, was used as the positive control for the study.

**F. Diesel oil sorption capacity of sorbent bags with *Miscanthus sinensis* (silver grass) fibers.**

**a. Dry system.** Fifty milliliters of diesel oil were poured into a 250 mL beaker. Each sorbent bag was soaked in the container for 60 min. After the sorption time, the bag was lifted out and hung over the beaker for 15 minutes to allow unabsorbed diesel oil to separate.

**b. Oil layer system.** One hundred milliliters of artificial sea water (3.5% NaCl), prepared by dissolving 35 g NaCl in 1000 mL of distilled water, and 10 mL of diesel oil were poured in a 250 mL beaker. Each packed sorbent bag was soaked in the beaker for 60 min. After the sorption time, the bags were lifted out and hung over the beaker for 15 min to allow unabsorbed diesel oil to separate. Bags were then placed in a beaker filled with 50 mL n-hexane where the absorbed oil was dissolved, and the water sank to the bottom of graduated cylinder due to its higher density.

**G. Kerosene oil sorption capacity of sorbent bags with *Miscanthus sinensis* (silver grass) fibers**

**a. Dry system.** Fifty milliliters of kerosene oil were poured into a 250 mL beaker. Each sorbent bag was soaked in the container for 60 min. After the sorption time, it was lifted out and was hung over the beaker for 15 min to allow unabsorbed kerosene oil to separate.

**b. Oil layer system.** One hundred milliliters of artificial sea water (3.5% NaCl), prepared by dissolving 35 g NaCl in 1000 mL of distilled water, and 10 mL of kerosene oil were poured in a 250 mL beaker. Each packed sorbent bag was soaked in the beaker for 60 min. After the sorption time, it was lifted out and was hung over the beaker for 15 min to allow unabsorbed kerosene oil to separate. Bags were then placed in a beaker filled with 50 mL n-hexane where the absorbed oil was dissolved,

and the water sank to the bottom of graduated cylinder due to its higher density.

**H. Monitoring of the set-up and recording of the data.** A digital balance was used to measure the mass of samples before sorption and the mass of oil containing samples (after dripping). The quantity of water absorbed by the sample (after dripping) was also measured using a beaker.

**I. Statistical Analysis.** The diesel and kerosene oil sorption capacities of sorbent bags in dry and oil layer systems were calculated according to the equations adapted from Dong, et al. (2015).<sup>7</sup>

where  $m_f$  is the sample mass before sorption (g),  $m_{f15}$  is the mass of the oil containing sample after 15 min of dripping (g), and  $m_{w15}$  is the mass of the water absorbed by the sample after 15 min of dripping.

Data were statistically analyzed using Two-way Analysis of Variance (ANOVA). Two-way ANOVA was used to determine the statistical significance among the sizes of *Miscanthus sinensis* (silver grass) fibers. Tukey's HSD test was used to determine the post-statistical difference between sorbent bags used in the study.

#### Equation 1. Sorption Capacity in Dry System

$$\text{Oil sorption capacity} = \frac{m_{f15} - m_f}{m_f}$$

#### Equation 2. Sorption Capacity in Oil Layer System

$$\text{Oil sorption capacity} = \frac{m_{f15} - m_f - m_{w15}}{m_{w15}}$$

#### ACKNOWLEDGEMENTS

The researchers would like to thank the Analytical Services Laboratory Department – Research Center for the Natural and Applied Sciences of the University of Santo Tomas, Manila, for allowing them to conduct morphological characterization of samples. The researchers would like to acknowledge June Lisangan for assistance in using the scanning electron microscope. They would also like to thank Dr. Helen A. Gutierrez and Adorando R. Darwin for guidance and encouragement. This work was supported by the Faculty and Staff of SHS in San Nicholas III, Bacoar City.

#### REFERENCES

- (1) Denizceylan, S.; Burakkaracik, S. Evaluation of Butyl Rubber as Sorbent Material for the Removal of Oil and Polycyclic Aromatic Hydrocarbons from Seawater. *Environmental Science Technology Journal* 2009, 43 (10), 3486–3852.
- (2) Chang, S. E.; Stone, J.; Demes, K.; Piscitelli, M. Consequences of Oil Spills: A Review and Framework for Informing Planning. *Ecology and Society* 2014, 19 (2), 26.
- (3) Aliyu, U. M.; Muhammad, I. M. Oil Removal from Crude Oil Polluted Water Using Banana Peel as Sorbent in a Packed Column. *Journal of Natural Sciences Research* 2015, 5 (2), 157–162
- (4) Oil Tanker Spill Statistics 2015; Impact PR and Design Limited: Canterbury, United Kingdom, 2016.
- (5) Padilla, J. E. Analysis of Coastal and Marine Resources: A Contribution to the Philippine Country Environmental Analysis; Coastal and Marine Sector, Bureau of Fisheries and Aquatic Resources, 2008.
- (6) Ober, H. K. pdf, 2018.

(7) Asadpour, R.; Sapari, N. B.; Tuan, Z. Z.; Jusoh, H.; Riahi, A.; Uka, O. K. Application of Sorbent Materials in Oil Spill Management: A Review. *Caspian Journal of Applied Sciences Research* 2013, 2 (2), 46–58.

(8) Hussein, M.; Amer, A.; El-Maghraby, A.; Taha, N. A., Availability of Barley Straw Application on Oil Spill Clean Up., *International Journal for Environmental Science and Technology* 2009, 6 (1), 123–130.

(9) Shamsudin, R.; Abdullah, H. Properties of Oil Sorbent Material Produced from Kenaf Fiber. *International Journal of Environmental Science and Development* 2015, 6 (7), 551–554

(10) Abejero, A. L.; Alcantara, A. J.; Trinidad, L. C.; Flavier, M. Kapok Fiber Packed in Nylon Net as Sorbent for Diesel Oil Spill and Its Ex-Situ Bioremediation. *Journal of Environmental Science and Management* 2013, 16 (1), 72–83.

(11) Centre for Agriculture and Biosciences Int. “*Miscanthus sinensis*,” July 16, 2008. <https://www.cabi.org/isc/datasheet/34269>.

(12) Gismatulina, Y.; Budaeva, V. Comparative Analysis of Chemical Composition of *Miscanthus* Var. *Soranovskii*. *BIO Web of Conferences* 2018, 11 (17), 1–2.

(13) Behnood, R.; Anvaripour, B.; Fard, N. J.; Farasati, M. Application of Natural Sorbents in Crude Oil Adsorption. *Iranian Journal of Oil and Gas Science and Technology* 2014, 2 (4), 1–11.

(14) Dong, T.; Xu, G.; Wang, F. Adsorption and Adhesiveness of Kapok Fiber to Different Oils. *National Center for Biotechnology Information* 2015, 296, 101–111.

## AUTHORS

Micklare Angelo C. Zepeda is an ICT senior high school student at SHS in San Nicholas III, Bacoar City. As a student researcher, he has represented the school in different regional to national-level science fairs. He plan to study computer engineering in college.

Elarcie Balsomo is a Special Science Teacher I at SHS in San Nicholas III, Bacoar City. He graduated Cum Laude with a BS degree in Biology for Teachers under DOST-SEI RA 10612. He is currently taking an Integrated Science MASEd under a Gokongwei Brothers Foundation TeachSTEM scholarship in the Philippines.



## Evaluation of the Antioxidant and Anticancer Activity of *Scutellaria barbata*, *Hedyotis diffusa*, and *Celastrus hindsii*

Nguyen Viet Quang Nam, Nguyen Cao Hai Vy, Nguyen Minh Trung  
Wellspring Saigon International Bilingual School, 92 Nguyen Huu Canh, Ho Chi Minh, 700000, Vietnam  
trungsinh.gd@gmail.com

**ABSTRACT:** *Scutellaria barbata*, *Hedyotis diffusa*, and *Celastrus hindsii* (SHC) each contain abundant medicinal properties and have been used by the Vietnamese for decades as traditional medicines. Nonetheless, there is no scientific research to prove the efficacy these usages. The purpose of this research project is to examine the chemical composition and biological activity of the three medicinal plants. Chemical composition analysis utilizing GC/MS determined 48 chemical compounds in extracts of the plants. Furthermore, a DPPH radical scavenging method was applied to examine the antioxidant activity of SHC extract which was found to have an  $IC_{50}$  value of  $311.90 \pm 20.89$   $\mu$ g/ml. Monks method verifies in vitro viral toxicity and yielded the following results: breast cancer cell line MCF7 was  $77.16 \pm 1.46\%$ ; liver cancer cell line HepG2 was  $54.36 \pm 1.32\%$ ; and lastly, lung cancer cell line NCI H460 resulted in  $27.76 \pm 1.50\%$ . The extracts did not affect fibroblast cell line,  $-24.27 \pm 1.40\%$ .

**KEYWORDS:** Antioxidant; GC/MS; DPPH; Anticancer; Medical; *Hedyotis diffusa*; *Scutellaria barbata*; *Celastrus hindsii*

### INTRODUCTION

#### Purpose statement

Oxidative stress is an imbalance attributed to the increase in the concentration of reactive oxygen species (ROS) in cells and the body's oxidative resistance system. Studies showed incurable diseases such as Atherosclerosis, Glycosuria, and many types of cancer are all related to oxidative stress.<sup>1,2</sup>

Cancer is a group of diseases involving abnormal cell growth with the potential to invade or spread to other parts of the body.<sup>3</sup> According to the World Health Organization (W.H.O), in 2018 approximately 9.6 million deaths were caused by cancer worldwide. Of this amount, 2.09 million cases of lung cancer, followed by 2 million cases of breast cancer and over 782,000 cases of liver cancer led to mortality.<sup>4</sup> Further investigations of oxidative and cancer resistance are required for improved cancer outcomes through a transdisciplinary approach involving biochemistry, biomedical, and health sciences.

Vietnam has diverse vegetation with many medicinal herbs such as *Scutellaria barbata*, *Hedyotis diffusa*, and *Celastrus hindsii* (SHC), all of which contain valuable medical properties and are utilized by the Vietnamese in the belief that they can heal diseases. *Hedyotis diffusa* is a type of herb in the *Rubiaceae* family, found primarily in the tropics of Asia and typically grows on moist meadows and farmland. Visually, it has a flat body, scabrous and symmetrical leaves, flowers in pairs with white corollas. The plant is commonly used in treating *Hepatitis*, *Urethritis*, and *Appendicitis*.<sup>5-6</sup> *Scutellaria Barbara* of the *Labiatae* family is often seen at the edge of rice-fields and moist meadows. This herb has a straight body, alternate leaves, rough petiole, purple-blue corollas, and flat brown nuts. It is a medicinal plant used for curing Hepatitis and Enterocolitis.<sup>8,9</sup> *Celastrus hindsii* from the *Celastraceae* family grows primarily in China and Thailand. In Vietnam, *Celastrus hindsii* originates in Hoa Binh and Lao Cai forests. It has delicate green leaves, black sap, white flowers grow on top of the limbs, yel-

low-orange nuts when ripe. For traditional medication, these three herbs are used for anti-inflammation.<sup>10,11</sup> In addition, they possess the potential for promoting oxidative activity and cancer treatment. However, there is no scientific proof of the efficacy of the usages of these folk remedies.

Thus, we launched our research with the hope of developing a foundation in the methods for supporting cancer treatments. Further, we hope the results will be an important factor in the application of health and biomedicine.

#### Theory

We made an extract from three medicinal herbs *Hedyotis diffusa*, *Scutellaria barbata*, and *Celastrus hindsii* using methanol solvent. We proceeded to examine the chemical compositions and compound mass percentages through GC/MS, followed by a free radical scavenging DPPH method which determines antioxidant activity. The in vitro cell toxicity test method was implemented to scrutinize the effect of the extract on cancer cells as well as common wild type - fibroblast cells.

#### The novelty of the research

This is the first research project to examine methanolic extracts from the medicinal herbs *Hedyotis diffusa*, *Scutellaria barbata*, and *Celastrus hindsii*. The combination of these three herbs has been used as a medicine by Vietnamese people for years; however, our research furthers this traditional medicine application and develops new methods for cancer treatments. The SHC extract is scrutinized to record chemical composition and substance concentration as well as tested for antioxidant activity and cancer cell inhibition.

### RESULTS AND DISCUSSION

#### Methanolic extraction of SHC

By using immersion and rotary evaporation method, the weight obtained for the extract was 7.7 grams per 100 grams of dry specimen. SHC extract was acquired with the mass percentages shown in Table 1.



Table 3. Percentage DPPH free radical scavenging of methanolic extract of SHC.

T (µg/mL)	Trial 1	Trial 2	Trial 3	$Q_{avg}$ of methanolic extract
500.0	91.17	91.78	91.76	<b>91.57 ± 0.35</b>
250.0	78.80	77.67	78.28	<b>78.25 ± 0.57</b>
125.0	47.96	49.45	47.32	<b>48.24 ± 1.09</b>
62.5	21.74	30.06	27.84	<b>26.55 ± 4.31</b>
31.25	10.33	18.40	15.48	<b>14.74 ± 4.09</b>

The increase in concentration from 31.25 - 500 µg/mL resulted in a proportional DPPH free radical scavenging percentage growth. It can be concluded that the antioxidant activity of SHC extract is in direct proportion to the increase of concentration (see Table 3). With the highest concentration at 500 µg/mL, the percentage of DPPH free radical scavenging activity of SHC methanolic extract reached the highest value at 91.57%. We implemented the results above to construct a linear regression equation:  $y = 20.536x - 9.738$  ( $R^2 = 0.97964$ ). Utilizing the results above, we constructed a linear regression equation and the value of IC<sub>50</sub> was calculated after three experiments as shown in Table 4.

Table 4. The IC<sub>50</sub> value of the methanol extract of SHC.

	Trial 1	Trial 2	Trial 3	Average + Standard deviation
<b>IC<sub>50</sub> value</b>	126.60	112.30	118.80	<b>119.23 ± 7.16</b>

After three trials to determine the IC<sub>50</sub> value, the results yielded the following: 126.60 from the first trial, 112.30, and 118.80 respectively for the second and third trials. The numerical data were aggregated to calculate an average value of 119.23 and a standard deviation of 7.16. The IC<sub>50</sub> value of SHC extract holds antioxidant activity and DPPH free radical scavenging capacity is compared to other herbal extractions as detailed in Table 5.

Table 5. Comparison table of IC<sub>50</sub> values of the methanolic extracts.

	Trial 1	Trial 2	Trial 3	Average + Standard deviation
<b>IC<sub>50</sub> value</b>	126.60	112.30	118.80	<b>119.23 ± 7.16</b>

The four methanolic extract samples chosen were *Streptocaulon juvenas* (349.35), *Solanum hainanense* (1,734), *Imperata cylindrica* (313.76), and *Sophora japonica* (185.2), all of which had high antioxidant and anticancer activity. The selected samples also featured a wide range of capabilities to be implemented in the medical field and are highly regarded as potential medical products.

As observed from Table 5, it is noticeable that the IC<sub>50</sub> value of SHC extract is lower than the values of other herbal extractions such as *Streptocaulon juvenas*, *Solanum hainanense*, *Imperata cylindrica*, and *Sophora japonica*. This shows the highly effective antioxidant activity and free radical inhibition of the SHC extract which was examined in this research.

#### Evaluating Monks method of the methanolic extract

We proceeded to scrutinize cancer cell toxicity activity by utilizing Monks method on three cancer cell lines: breast

cancer cell (MCF-7), lung cancer cell (NCI H460) and liver cancer cell (Hep G2), while simultaneously examining a wild type cell line - fibroblast cell to evaluate the effect SHC extract has on this wild type cell of connective tissue. Cancer cell toxicity at the concentration of 100 µg/mL is detailed in Table 6.

Table 6. Percentage of cytotoxic cancer resistance of methanolic extract of SHC determined by Monks method at a 100 µg/mL concentration.

Cell line	Percentage of cytotoxic cancer resistance (%) of methanolic extract			
	Trial 1	Trial 2	Trial 3	Average + Standard deviation
MCF-7	68.87	67.98	66.53	<b>67.79 ± 1.18</b>
Hep G2	45.58	48.62	42.43	<b>45.54 ± 2.53</b>
NCI H460	34.56	35.87	33.32	<b>34.58 ± 1.28</b>
Fibroblast	-25.57	-22.78	-24.45	<b>-24.27 ± 1.40</b>

(Positive values represent intoxication ability, while negative values represent growth ability)

As seen from the results, SHC extract most effectively inhibited the breast cancer cell line MCF7 with 67.79 ± 1.18%, next in line was liver cancer cell line, Hep G2 with 45.54 ± 2.53%, and finally lung cancer cell line NCI H460 with 34.58 ± 1.28%. Besides cancer cell resistance ability, the extraction is completely innocuous to the growth of normal cells with the fibroblast cell developing -24.27 ± 1.40%.

## CONCLUSION

The mass percentage of the methanolic extract is 7.7%.

The chemical composition of the methanolic extract: 48 chemical compounds were examined from SHC extract including 10 main compounds.

The antioxidant activity, detected by DPPH free radical scavenging IC<sub>50</sub> value of SHC methanolic extract was determined to be 119.23 ± 7.16 µg/mL.

SHC methanolic extract most effectively reduced breast cancer cell line MCF7 with 67.79 ± 1.18%, the liver cancer cell line HepG2 with 45.54 ± 2.53%, and finally the lung cancer cell line NCI H460 with 34.58 ± 1.28%. However, the extract was completely innocuous to the growth of a normal cells with the fibroblast cell developing -24.27 ± 1.40%.

According to the results of this research, SHC extract which comprises *Scutellaria barbata*, *Hedyotis diffusa*, and *Celastrus hindsii* holds multiple potentials in treating cancer, possessing high antioxidant ability as well as being a practical application in the field of health science.

## METHODS

### Research material

*Hedyotis diffusa*, *Scutellaria barbata*, *Celastrus hindsii* were harvested in Sa Pa, Lao Cai Province, Vietnam.

Cancer cell lines were provided by American Type Culture Collection-ATCC (US).

Common cell-Fibroblast was provided by the Department of Biotechnology-Faculty of Medicine, National University of Ho Chi Minh City.



### Immersion method

*Scutellaria barbata*, *Hedyotis diffusa*, and *Celastrus hindsii* with a ratio of 2:1:1 in 100 grams were washed and dried inside a drying chamber at 50°C until there was no difference in mass and all water had been drained out of the sample. Next, 100 grams of dry specimen were grinded to a smooth powder to increase diffusion in the solution. Samples were soaked in pure methanol with a concentration of 1:10 (g/mL) for 48 hours. The mixture after the immersion was decanted to obtain leachate.<sup>13</sup>

### Preparation of the extract

To begin, we poured 500 mL of leachate into a 1 L pear-shaped container to avoid overflow. Next, we utilized a rotary evaporator at 50°C, 250 mbar tension in 40-minute duration. The extract was left to dry naturally and preserved in a cool tray in the refrigerator at 4°C for later examination.<sup>13</sup>

### Determination of chemical composition through GC/MS method

Gas chromatography-mass spectroscopy (GC/MS) is a material analysis method that employs gas chromatographs (GC) fitted with mass selective detectors called mass spectrometers (MS). GC/MS analysis is an ideal tool for identifying unknown substances or contaminants that are present in extremely low quantities.

The sample was injected into a gas chromatograph port which was heated to up to 300°C where the material was then volatilized. Gaseous components were separated as they flowed through the column; the column was wound within a special oven which modulates temperatures between -20° to 320°C. Its surface is coated with a material that separates the various chemical compounds in the sample based on size and polarity. The separated components flow directly out of the column and into the MS which has three internal steps:

1. Ionization source – components are blasted with electrons, causing them to break up and turn into positively charged ions.
2. Filter – the ions pass through an electromagnetic field and are filtered based on mass. Analysts set a predetermined range of masses to be allowed to pass through from the ionization source.
3. Detector – counting the number of filtered ions, the information is sent to a computer, and a mass spectrum and distribution of ions of different sizes are generated.

The mass spectrum is used to identify the components by comparing each to extensive reference libraries. To quantify compounds within the analyzed sample, analysts establish a standardized curve of known concentrations of each material.<sup>13</sup>

### DPPH free radical scavenging method

The  $\alpha$ -diphenyl-B-picrylhydrazyl (DPPH) method gives the oxidative activity of a substance or other biological basis by developing free radicals as EtOH saturates. The outcome shows high precision. The method is simple, manageable, and suitable for multiple oxidative activity resistant compounds.

Oxidative resistant compounds neutralize DPPH radicals by allowing hydrogen to absorb wavelengths as the solution pigment fades, resulting in the ability of oxidative activity when the solution switches from purple pink to pale yellow. The lower the OD value the higher the DPPH free radical scavenging activity.<sup>13</sup>

To begin, we poured 5 mL of DPPH (0.8mM, diffused in methanol) into tubes containing the extract at various concentrations, ranging between 0 to 1000 µg/ml. Under no-light condition, we annealed for 30 minutes then analyzed the OD values in which the active resistance depends on the light absorption percentage with a 517 nm wavelength. The positive control sample stands as acid ascorbic (15 µg/mL) and a negative control sample was twice-distilled water. The formula for the percentage of activity is calculated by:

$$\text{Percentage DPPH free radical scavenging} = \frac{(ODc - ODm)}{ODc} \times 100$$

ODm: Optical density (OD) value

ODc: Optical density (OD) of the control sample (-)

For the percentages we obtained, note the IC<sub>50</sub> value (Concentration of reactant which is able with a 50% chance of analyzing a free radical) as the premise for comparison. The lower IC<sub>50</sub> values measured, the greater the oxidative activity.<sup>13</sup>

### Monks tested in vitro cell toxicity method

Monks tested in vitro cell toxicity method provides a high-quality outcome at a low expense. This technique has been authenticated by The National Cancer Institute - NCI which can identify potential compounds that reduce the development of cancer cells.

According to the toxicity status of cells, in order to define compounds that have the possibility to reduce the development of cancer cells by identifying the protein amount based on optical density as the cells are dyed in Sulforhodamine B (SRB). OD values are recorded by the machine. In addition, it contains the SRB quantity that yields a propitious ratio with the proportion attached to protein molecules. As the OD value gain gives a greater number of cells.

Reductant compound (10 µl) was dissolved in DMSO 10% and into wells of 10 µl/ml. Trypsin separated cells, at the same time adjust the suitable density. We poured more cells with a reasonable amount in 190 µl environment to develop for 3 to 5 days. The tray containing cancer cells (180 µl) was used as a comparison for day 0. After 1 hour, we situated the cells in Trichloroacetic acid-TCA.

The cells were soaked in a warm container of CO<sub>2</sub> in order to be fixed into the bottom of the culture well TCA. After 30 minutes, we dyed them in SRB for 1 hour at 37 Celsius. Next, we poured out SRB and then washed it 3 times with acetic acid 5%. We then let it dry at room temperature. We used tris (hydroxymethyl) aminomethane 10 mM and dissolved the leftover SRB. We also dyed the protein molecules and then shook it slightly for 10 minutes.

The ELISA Plate Reader (Bio-Rad) machine was used to examine the outcome of the color content SRB dye under the spectrum observed at 515 nm wavelength. The formula is shown below:



$$\% \text{Alive cells} = \frac{OD(\text{Reductant}) - OD(\text{Day0})}{OD(\text{Negative control}) - OD(\text{Day0})} \times 100$$

$$\% \text{Dead cells} = 100\% - \% \text{Alive cells}$$

This was repeated several times to increase reliability. Ellipticine (Sigma) as a positive control sample and DMSO 10% as the negative control sample were used. We evaluated IC50 values by TableCurve software.<sup>14</sup>

#### ACKNOWLEDGEMENTS

Our most sincere appreciation to M.Sc. Nguyen Minh Trung, who has been conscientiously guiding and helping us from the very beginning of this research project.

We would like to thank teachers at Ho Chi Minh City University of Science, Ho Chi Minh City University of Technology, Medicine - Vietnam National University Ho Chi Minh City, and Ho Chi Minh City Pedagogy University for granting us opportunities to complete this project. Finally, our deepest gratitude to family and friends who have always been supportive and encouraged us to do our best.

#### REFERENCES

- (1) Lazo-de-la-Vega-Monroy, M-L. & Fernández-Mejía, C. (2013), "Oxidative Stress in Diabetes Mellitus and the Role Of Vitamins with Antioxidant Actions", *Oxidative Stress and Chronic Degenerative Diseases - A Role for Antioxidants*, pp. 209 – 232.
- (2) Phan Kim Dinh, Dai Thi Xuan Trang "Study on the antioxidant and anti-cancer activities in HepG2 cells of *Ixora duffii*", *Can Tho University, Science and Technology development journal: Natural Science*, vol 1, issue 6, 2017.
- (3) World Healthcare Organization, Cancer Overview.
- (4) World Healthcare Organization, Cancer fact sheets, 12 September 2018.
- (5) Tao C., Taylor C.M. Rubiaceae. In: Wu Z.Y., Raven P.H., Hong D.Y., editors. *Flora of China*. Volume 19. Science Press; Beijing, China: Missouri Botanical Garden Press; St. Louis, MO, USA: 2011. pp. 147–174.
- (6) Willd.Li M, Wong YL, Jiang LL, Wong KL, Wong YT, Lau CB, Shaw PC Food Chem, Application of novel loop-mediated isothermal amplification (LAMP) for rapid authentication of the herbal tea ingredient *Hedyotis diffusa*. 2013 Dec 1; 141(3):2522-5.
- (7) Lee HZ, Bau DT, Kuo CL, Tsai RY, Chen YC, Chang YHAm J Chin Med, "Clarification of the phenotypic characteristics and anti-tumor activity of *Hedyotis diffusa*", 2011; 39(1):201-13.
- (8) T.S. Wang, S.Q.Wang, D.L. Xiao, J Med Plants Res "A review of phytochemistry and antitumor of a valuable medicinal species: *Scutellaria barbata*", 6 (2012), pp. 4259-4275.
- (9) D. Don, Prodr. Fl., "Scutellaria barbata", Nepal. 109, 1825.
- (10) Tram, L.N, "Separation process of rosmarinic acid and their derivatives from *Celastrus hindsii* benth leaves", *VJST* 2016, 54, 380–387.
- (11) Nguyen Trong Nghia, "What is *Celastrus hindsii*? How to identify and it is medically used", 2019.
- (12) National Center for Biotechnology Information, (2018, Sep 2), Pubchem, [Online].
- (13) Nguyen Thi Hang, Nguyen Thi Thanh Tam, Mai Huu Phuong, (2016) "DPPH free radical scavenging and reducing power properties of *Boerhavia diffusa* in Can Gio, Ho Chi Minh City", *Science magazine of The University of Pedagogy of Ho Chi Minh City*, No. 12(90), 2016.
- (14) Pham Thanh Loan, Tran Huy Thai, Phan Van Kiem, Hoang Lê Tuan Anh, Chau Van Minh, Do Th Thao, Tran Thi Suu, "Biological active of *Dalbergia oliveri* Gamble ex Prain Compounds", *Biology magazine*, 35(4): 439-444, 2013.
- (15) Dai Thi Xuan Trang, Lam Hong Bao Ngoc, and Vo Thi Tu Anh (2015) "Studies on antibacterial and antioxidant activities of methanolic extract from *Streptocaulon juvenas* MERR.", *Department of Natural Science, Can Tho University*.
- (16) Le Quynh Loan, Nguyen Luong Hieu Hoa, Le Van Minh, Phung Bao Chi, Nguyen Hoang Dung "Depigmenting effect of *Sophora japonica* L.

in B16F10 Melanoma cells", *Science Technology and Agribusiness Magazine* 17 (1) (2018):14-20.

(17) National Center for Biotechnology Information, (2018, Sep 2), Pubchem, [Online].

#### AUTHORS

Nguyen Viet Quang Nam is an eleventh grader currently studying at Wellspring Saigon International Bilingual School. Nam has a strong passion for science and physics, and he desires to pursue the field of Mechanical Engineering. He is striving to get accepted by the top technological universities in the United States.

Nguyen Cao Hai Vy currently studies at Wellspring Saigon International Bilingual Schools as a tenth-grader. She shows impressive performances in Biology and Chemistry with the ambition of becoming a veterinarian. Moreover, she attempts to get approved and receive a scholarship by the top biological college of the United States.

Nguyen Minh Trung is a supervisor and carries out the project with Nguyen Viet Quang Nam and Nguyen Cao Hai Vy. The author, Nguyen Quang Viet Nam, is a biology and scientific research teacher at Gia Dinh School and Wellspring Saigon International Bilingual Schools.

## Analysis of the Arcade Creek Shows Lower Dissolved Oxygen Levels When Compared with the American River

Gabriela A. Rossetti

Mira Loma High School, 4000 Edison Ave, Sacramento, CA, 95821, United States

gabiaam2@gmail.com

**ABSTRACT:** This paper outlines the differences in dissolved oxygen between the Arcade Creek and the American River located in California's Sacramento Valley as well as the plausibility that the Arcade Creek needs more attention to preserve its local ecosystem based on these results. A comparison was made using data collected over the span of several years by multiple stations along both water bodies. Such stations are analyzed individually to account for error and evaluated together to provide a basis of comparison. Results show the American River has higher dissolved oxygen concentrations than the Arcade Creek. Prior research indicates the American River as being in good condition and so the Arcade Creek, having a lower dissolved oxygen content, is in need of environmental improvement. The results call for further investigation of the Arcade Creek the impacts urban development and roadside pollution have on its dissolved oxygen levels and the implications this has upon the local ecosystem reliant on the Arcade Creek.

**KEYWORDS:** Environment; Sacramento; Arcade Creek; American River; Dissolved Oxygen.

### INTRODUCTION

This project aims to determine if there are disparities in dissolved oxygen levels between the Arcade Creek and the American River. The significance of any disparity can be attributed to the overall health of the two water bodies present in the Sacramento Valley, mostly focused on the Arcade Creek as it is closer to urban development. Thus, the possible effects of urban development and roadside pollution can be discussed and further investigated.

#### *Concerning the importance of dissolved oxygen*

In bodies of water, up to ten molecules of oxygen are dissolved in one million water molecules, varying depending on the state of the water body. This oxygen, entering via small streams or groundwater discharge, is needed by organisms to survive in aquatic environments. Thus, fast-flowing water tends to have a higher amount of dissolved oxygen than stagnant bodies. Fast-flowing water increases the diffusion of atmospheric oxygen into larger bodies of water.<sup>1,2</sup> Low-flow conditions prevent oxygenation and can cause critically low oxygen levels when coupled with high temperatures.<sup>2</sup> Another issue is the consumption of oxygen as organic matter decays. The build-up of excessive organic decay can cause eutrophic conditions and a lack of oxygen in the water. Seasonal and daily fluctuations also occur; colder temperatures correlate to higher dissolved oxygen levels and why bodies of water in late winter and early spring have the highest levels of dissolved oxygen. Low levels of dissolved oxygen present lethal hazards to all aquatic life in a body of water.<sup>1</sup> The oxygen content is considered dangerous around 5 mg/L with 2mg/L being critically low.<sup>1,3</sup> While too little dissolved oxygen is problematic for aquatic life, too much dissolved oxygen also presents issues. High levels of dissolved oxygen result from an excess of

photosynthesizing plants and cause harmful algal blooms. This can be caused by excessive fertilizer and/or sewage runoff and results in cultural eutrophication.<sup>4</sup>

Other California bodies of water that have low dissolved oxygen levels include the Santa Margarita River and San Joaquin River. Both exhibit eutrophic conditions and illustrate the dangers organisms face with low dissolved oxygen levels.<sup>5,6</sup> Pollution is a leading cause of eutrophication.

#### *The Arcade Creek*

The Arcade Creek, flowing from Orangevale to the Sacramento River via the Natomas East Main Drainage Canal, spans approximately 16.2 miles and covers a basin area of almost 30 miles. The portion tested in this study runs from Auburn Blvd to Haggin Oaks, stations A through G. The creek is mostly bordered by valley and blue interior oaks. Native vegetation often persists in open areas, providing habitats for organisms, but this is slowly diminishing with recent border development.<sup>7</sup> The Arcade Creek has a mean flow rate of 0.2 cubic meters per second.<sup>9</sup>



Figure 1. The map with the Arcade Creek Sites 8,14,15,16,17,18,19. The names (from left to right): Site A, Site B, Site D, Site G, Site E, and Site F.

### The American River

The American River consists of three forks originating from the Sierra Nevada Mountains. This project studied the South Fork which covers approximately 90 miles, a total of 850 square miles, and originates in the High Sierras in the El Dorado National Forest before entering the Folsom Reservoir and flowing to the Sacramento River. The portion investigated covered stations from the mouth of the Folsom Reservoir up to the Nimbus Dam where the Sacramento Water Pollution Control Lab is located. The American River is considered to be highly oxygenated and relatively healthy. However, erosion from land usage is presenting an increasing problem of sediment addition into the water.<sup>10</sup> The American River has a flow rate of 112.1 cubic meters per second.<sup>11</sup>

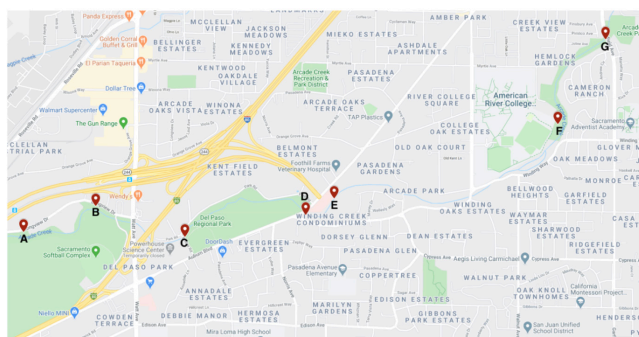


Figure 2. The map of the American River Stations. The names from left to right: Nimbus (N), Nimbus Flat Right (NFR), Nimbus Flat Left (NFL), Nimbus Flat Middle (NFM), Lake Natoma Willow Creek (WC), Lake Natoma Middle (NM), Lake Natoma Right (NR), Lake Natoma Left (NL), and American River at Rainbow Bridge (RB)

### RESULTS AND DISCUSSION

The levels of dissolved oxygen for the Arcade Creek and the American River are shown in Figures 13 and 14. All stations between Arcade Creek and American River show an increase in dissolved oxygen as the year progressed from the beginning winter months to the spring months. Most stations along the Arcade Creek displayed a slight decrease in dissolved oxygen after the spring months. The American River saw a decrease in dissolved oxygen after the summer months.

From January to May, the range of dissolved oxygen along the Arcade Creek was 6-13 mg/L with an outlier at 14 mg/L and the American River had dissolved oxygen concentrations between 10-13.5 mg/L. There was a decrease of dissolved oxygen in June as the Arcade Creek had a concentration range of 5-10 mg/L and the American River's levels ranged between 8-11 mg/L. From September until December, the Arcade Creek had concentrations between 6-10 mg/L with some fluctuations lower than 6 mg/L while the American River had concentrations between 7-12 mg/L.

Seasonal trends are also noted; there were lower dissolved oxygen concentrations during the summer and higher concentrations during the winter and spring for both bodies of water.

The graphs detailing the individual stations display larger error bars for the Arcade Creek Stations (Figures 2-9) than the American River Stations (Figures 11 and 12). This is because the Arcade Creek data was collected using less sophisticated instruments than the American River's data. All data for each body of water was then combined into one graph, Figures 10 and 13.

#### Arcade Creek Stations

The Arcade Creek graphs illustrate monthly averages taken from 2008-2019 and display the seasonal fluctuations of dissolved oxygen levels as temperatures rise and fall.

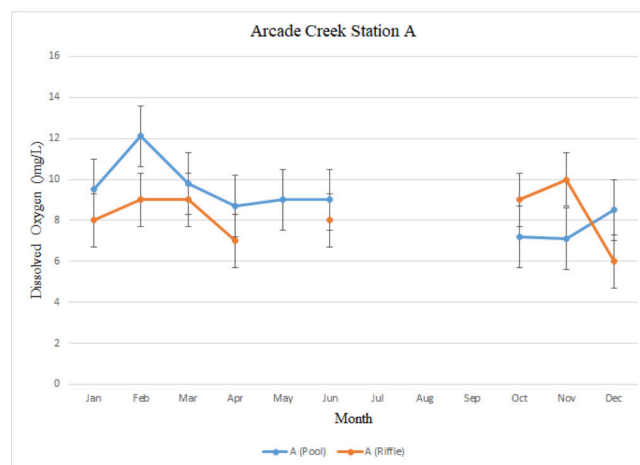


Figure 3. Arcade Creek Station A

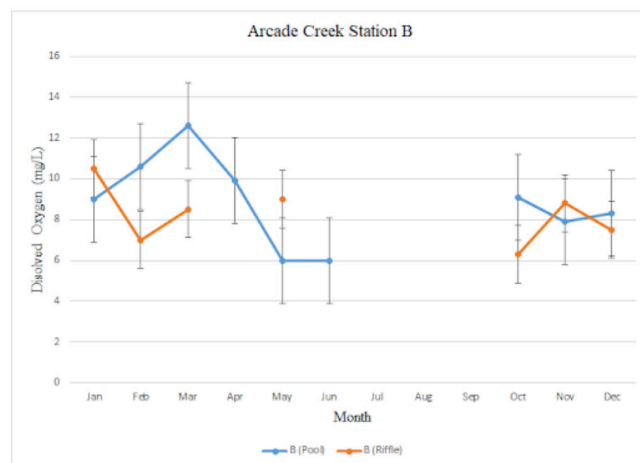


Figure 4. Arcade Creek Station B

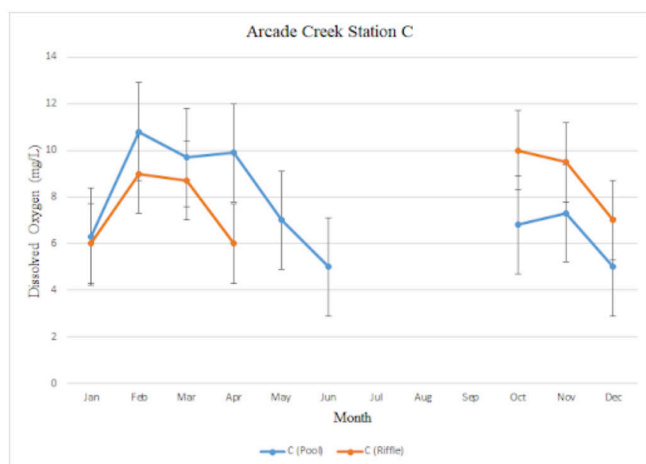


Figure 5. Arcade Creek Station C

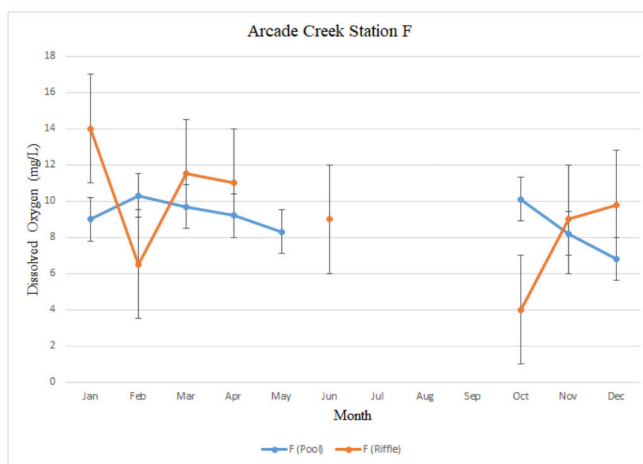


Figure 8. Arcade Creek Station F

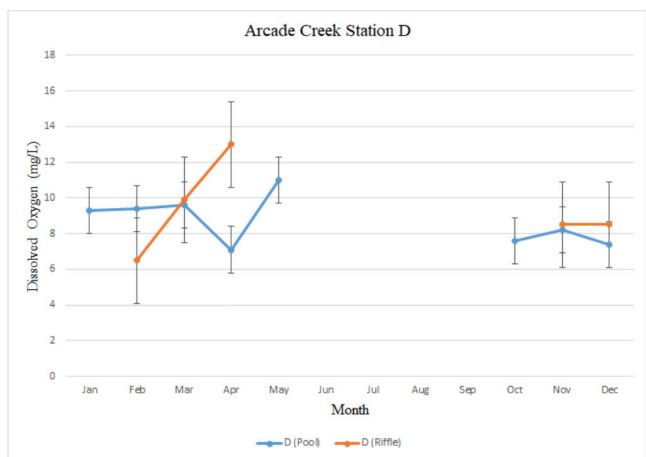


Figure 6. Arcade Creek Station D

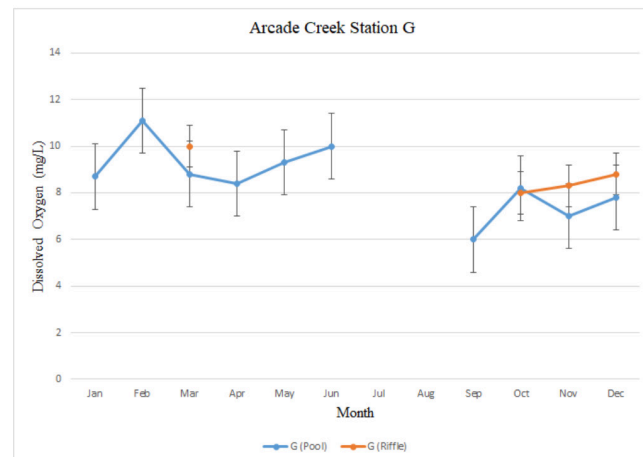


Figure 9. Arcade Creek Station G

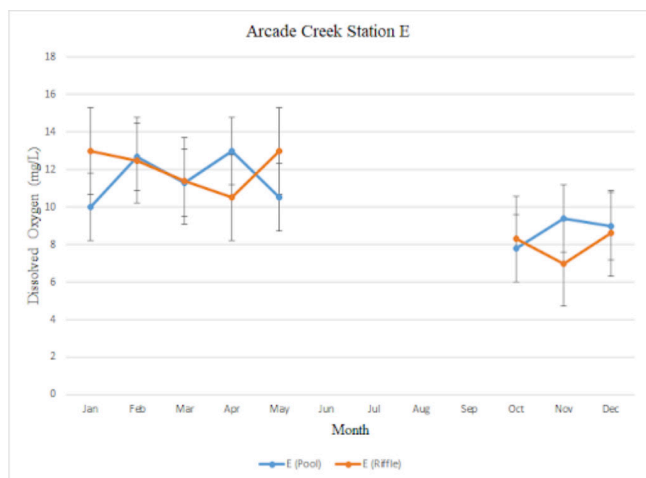


Figure 7. Arcade Creek Station E

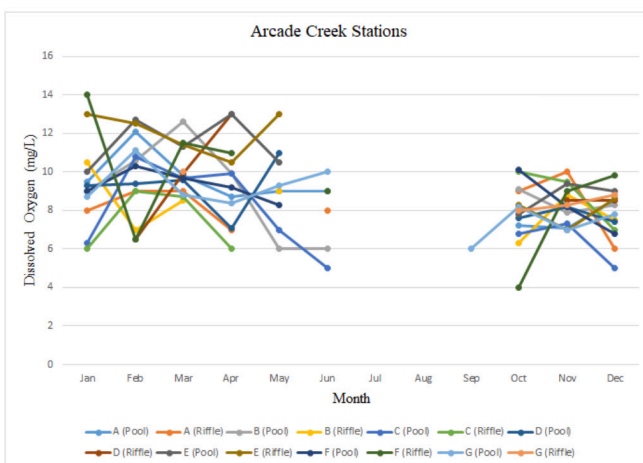


Figure 10. The Arcade Creek Stations

### American River Stations

The American River graphs illustrate monthly averages taken from 2003-2015 and display the seasonal fluctuations of dissolved oxygen levels as temperatures rise and fall.



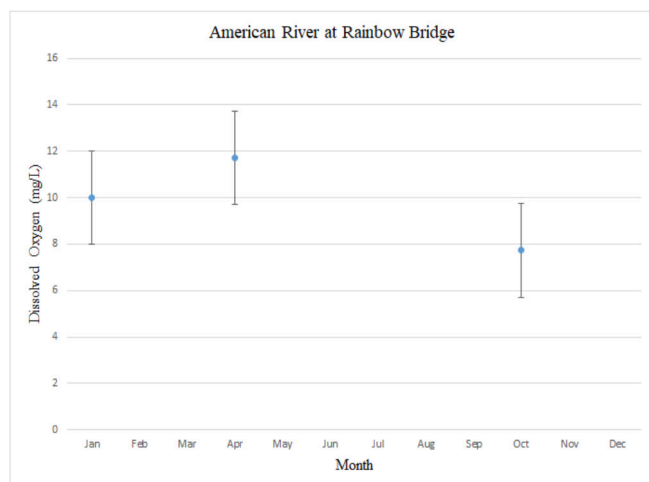


Figure 11. The Rainbow Bridge Station. There was limited data so finding the trend is difficult.

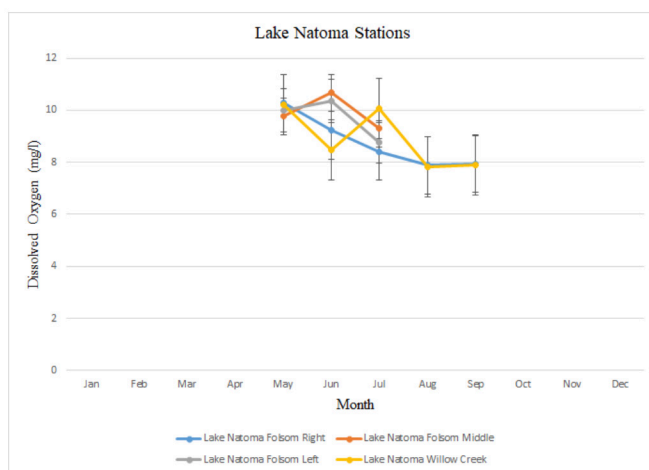


Figure 12. The Lake Natoma Stations

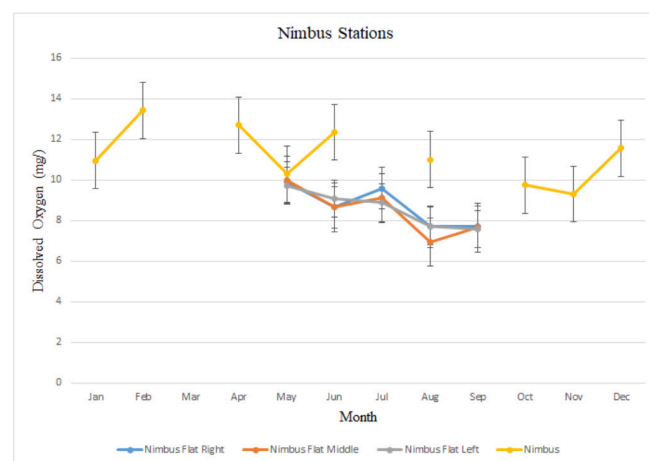


Figure 13. The Nimbus Stations

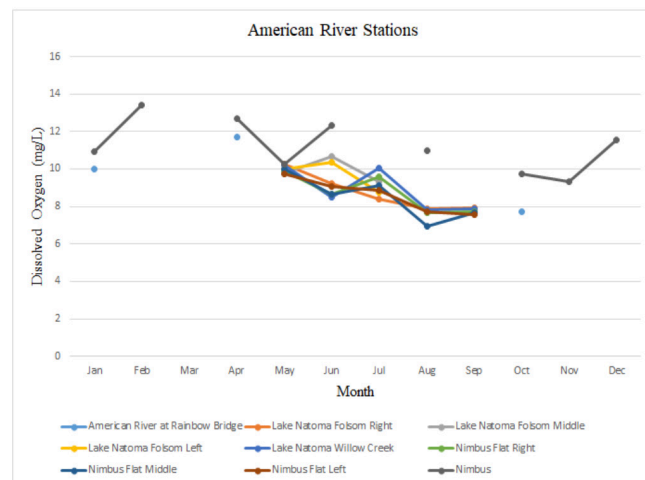


Figure 14: All the American River Stations

The Arcade Creek's dissolved oxygen range is lower than the American River. Despite the different years covered by each data set, the results are consistent for each year when the averages were taken. Therefore, extrapolated data for both bodies of water remains consistent with the trends of the shared years, 2008-2015. Considering this, as well as the American River's previously mentioned healthy status, the Arcade Creek is less healthy because of its lower dissolved oxygen levels. The Arcade Creek is dangerously close to the fatal oxygen level of 5mg/L when looking at the monthly averages and lowest levels shown in Figure 13. Additionally, while the Arcade Creek saw an increase in oxygen levels during the summer, the American River's oxygen levels remained higher during these months, shown in Figures 13 and 14.

These results warrant concern for the inhabitants of the Arcade Creek. The Arcade Creek is relatively small and has a low flow rate. So, while the Arcade Creek shows decreased flow during the warmer months, the implications of run-off and pollution is still concerning due to the creek's proximity to urban development. There is less concern for the American River because it has forests and natural vegetation as a barrier from urban development.

The use of multiple stations along the two bodies of water is to both illustrate a diversity in data samples and avoid grouping the large lengths of water into one average dissolved oxygen concentration value. This aggregation would omit possible fluctuations in different parts, possibly due to shade coverage and vegetation or proximity to urban development. Figures 2-10 take into account pools and riffles, as standing water has a lower dissolved oxygen level. Monthly averages were taken to illustrate yearly and seasonal trends.

Concerning the American River, data was taken along stations from the start of Folsom Lake up until the Nimbus Dam to account for fluctuations in dissolved oxygen between standing water and water release that occurs past the Nimbus Dam.

Looking at both graphs summarizing individual station results for both bodies of water (Figures 10 and 14), the data is

difficult compare due to a decreased overlap in months when data was taken. This because student volunteers were not present during the summer months at Arcade Creek. There is overlap in other months before and after the summer and some overlap in the early and late summer months, which allowed for relatively accurate analysis. Further data collection in the summer months for the Arcade Creek would provide a more accurate representation of the health of each body of water.

The main uncertainty arises from the data taken from the Arcade Creek, as the procedures were less sophisticated compared to the lab procedures for the American River. Additionally, the Arcade Creek data was taken from volunteer high school students as opposed to professionals. This is correlated with the more drastic error bars noticed for the Arcade Creek Stations than with the American River Stations.

Another issue was the time each sample was collected each day. Daily temperature changes can cause fluctuating dissolved oxygen levels. The peak dissolved oxygen level is 4:00 pm. The Arcade Creek data was collected sometime between 3:30 and 4:30 daily. The American River had a higher data collection time range, between 7:00 am to 4:30 pm, and so further experimentation is needed to ensure accuracy. However, despite that the American River data was not always collected at its peak time, it still had higher averages than the Arcade Creek whose data collection was closer to its oxygen peak. This implies the disparities in dissolved oxygen between the bodies of water may be more drastic since the American River is likely to have an increased concentration range when measured at 4:00 pm. Thus, the health of the Arcade Creek can be regarded as even worse since the American River is the healthy standard.

## CONCLUSION

The overall significance of this paper illustrates a need for closer attention to the Arcade Creek, such as possible testing for how large a part urban development and roadside pollution plays in the creek's health, in addition to testing during the summer months to gauge the overall yearly and seasonal health of the water body. Furthermore, lower levels of dissolved oxygen are harmful to organisms in the creek and can lead to possible death, especially since levels are near the dangerous amount of 5mg/L. This, in turn, can have a drastic effect on the overall ecosystem of the Arcade Creek area.

## METHODS

### Procedures

There were two methods were used for data collection, one used by students and one used by the Sacramento Water Pollution Control Lab. Both methods are listed and discussed.

#### *Arcade Creek Dissolved Oxygen Collection (student handbook)*

The Water Chemistry Analysis Handbook outlines using HACH kits to conduct this research.<sup>12</sup> Data collection was done Monday through Wednesday every month while school was in session from September to May. Collections were made at Stations A through G around 4:00 pm. First, water samples

are collected in the largest glass DO bottle. The kits use the Winkler method, so students pour DO reagents #1 (Manganous Sulfate Powder Pillow) and #2 (Alkaline Iodide-Azide Powder Pillow) into the bottle then seal the cap and shake the bottle until orange-brown floc precipitate clearly forms. The students set the bottle on a flat surface and wait approximately two minutes so the floc can settle. Using nail clippers to open the pillow packet containing DO reagent #3 (Sulfamic Acid Powder Pillows), the student pours it into the bottle to form a yellow solution. The solution is poured into the measuring tube and the rectangular mixing bottle is placed over the top of the tube. The students invert the tube and the rectangular mixing bottle so that the solution pours down into the bottle before adding sodium thiosulfate solution dropwise into the bottle. The bottle is swirled between drops and the students count the number of drops until the solution is clear. This value is recorded.

#### *American River Dissolved Oxygen Collection*

Collections were made at the Rainbow Bridge, Lake Natoma, and Nimbus Stations. The times these results were taken varied by day depending on when collection was able to be taken. A hand-held portable meter is used for this collection, such as a YSI Pro2030, following Standard Method 24500-O G-2001 approved by the Environmental Protection Agency.<sup>13</sup> Methods of sampling are highly dependent on the sampled source and method of analysis. Surface water samples are collected in narrow-mouth glass-stoppered BOD 300-mL bottles, ensuring the sample is not in contact with air or agitated because this causes a change in its gaseous content. Also, avoid entraining or dissolving atmospheric oxygen. In sampling from a line under pressure, attach a glass or rubber tube to the tap and extend to bottom of bottle. Let bottle overflow two or three times its volume and replace stopper so that no air bubbles are entrained. A Kemmerer-type sampler is used for samples collected from depths greater than 2 m. Bleed the sample from bottom of the sampler through a tube extending to bottom of a 300-mL BOD bottle. Fill bottle and allow to overflow for approximately 10 seconds to prevent turbulence and formation of bubbles while filling. Record sample temperature to nearest degree Celsius.

#### *Sample Calculations*

Calculating monthly averages:

December monthly average for Nimbus station:

$$(11.00 + 13.00 + 14.50 + 6.30 + 13.00 + 13.00 + 10.60 + 13.40 + 12.00 + 8.80) / 10 = 11.56$$

Standard deviation calculated by Excel

## ACKNOWLEDGEMENTS

I would like to thank the Sacramento Water Pollution Control Lab scientists and the Mira Loma High School student volunteers for their help in data collection.

## REFERENCES

- (1) Dissolved oxygen and water, [https://www.usgs.gov/special-topic/water-science-school/science/dissolved-oxygen-and-water?qt-science\\_center\\_objects=0#qt-science\\_center\\_objects](https://www.usgs.gov/special-topic/water-science-school/science/dissolved-oxygen-and-water?qt-science_center_objects=0#qt-science_center_objects).

- (2) Stream flow. (2008, January 17). Water on the web. <https://www.wa-terontheweb.org/under/waterquality/flow.html>
- (3) Lennotech. (n.d.). Why oxygen dissolved in water is important. [https://www.lennotech.com/why\\_the\\_oxygen\\_dissolved\\_is\\_important.htm](https://www.lennotech.com/why_the_oxygen_dissolved_is_important.htm)
- (4) DeBrosse, S. (Ed.). (1995). Water quality. NASA, <https://www.grc.nasa.gov/WWW/k-12/fenlewis/Waterquality.html>
- (5) Southern California Coastal Water Research Project. (n.d.). Eutrophication. <https://www.sccwrp.org/about/research-areas/eutrophication/>
- (6) Stringfellow, W., Herr, J., Litton, G., Brunell, M., Borglin, S., Hanlon, J., Chen, C., Graham, J., Burks, R., Dahlgren, R., Kendall, C., Brown, R., & Quinn, N. (2009). Investigation of river eutrophication as part of a low dissolved oxygen maximum daily load implementation. *Water Science & Technology*, 59(1), 9-14. <https://www.doi.org/10.2166/wst.2009.739>
- (7) patucker]. (2011, July 7). Arcade Creek history. Sacramento Area Creeks Council. <https://www.saccreeks.org/know-your-creeks/arcade-creek-history/>
- (8) Arcade Creek Project. (2010, December 17). Site A [Video]. Vimeo, <https://www.vimeo.com/17912829>
- (9) U.S. Geological Survey. (n.d.). USGS 11447360 Arcade c nr del Paso Heights CA. [https://www.waterdata.usgs.gov/nwis/uv?site\\_no=11447360](https://www.waterdata.usgs.gov/nwis/uv?site_no=11447360)
- (10) Sacramento River Watershed Program. (n.d.). Upper American River watershed. <http://www.sacriver.org/aboutwatershed/roadmap/watersheds/american/upper-american-river-watershed>
- (11) U.S. Geological Survey. (n.d.). USGS 11446500 American r a Fair Oaks CA. [https://www.waterdata.usgs.gov/ca/nwis/uv?site\\_no=11446500](https://www.waterdata.usgs.gov/ca/nwis/uv?site_no=11446500)
- (12) Wong, J., Liu, G., & Frydendal, N. (Eds.). (2019). Water chemistry analysis handbook. <https://docs.google.com/document/d/1u-EL5yERAcy-tre3011e7j5pf2ESfETyAUDkbpYK9NM/edit>
- (13) 4500-O<sub>2</sub> oxygen (dissolved). Inorganic Nonmetals. [http://www.edgeanalytical.com/wp-content/uploads/Inorganic\\_SM4500-O.pdf](http://www.edgeanalytical.com/wp-content/uploads/Inorganic_SM4500-O.pdf)
- (14) Arcade Creek Project. (2010, December 17). Site B [Video]. Vimeo, <https://www.vimeo.com/17912798>
- (15) Arcade Creek Project. (2010, December 17). Site C [Video]. Vimeo, <https://www.vimeo.com/17912634>
- (16) Arcade Creek Project. (2010, December 17). Site D [Video]. Vimeo, <https://www.vimeo.com/17912593>
- (17) Arcade Creek Project. (2010, December 17). Site E [Video]. Vimeo, <https://www.vimeo.com/17912461>
- (18) Arcade Creek Project. (2010, December 17). Site F [Video]. Vimeo, <https://www.vimeo.com/17912436>
- (19) Arcade Creek Project. (2010, December 17). Site G [Video]. Vimeo, <https://www.vimeo.com/17912403>

#### AUTHOR

Gabriela Rossetti is a senior at Mira Loma High School in Sacramento, CA and plans to major in astrophysics.

## The Use of Bactericidal Ultraviolet Radiation in the Eradication of *Escherichia coli* K12

Benjamin Carranti  
Marcellus High School

**ABSTRACT:** For half a century, ultraviolet (UV) radiation has been a common method of sterilization in fields such as food manufacturing, water sterilization, and hospital surface disinfection. To further explore UV radiation's effectiveness as a germicidal agent, my research focused on the irradiation of *Escherichia coli* (*E. coli*). A two-stage study was conducted where the effects of irradiation before and after incubation of the bacteria were measured to test the sterilization efficiency of UV radiation. The non-shiga toxin producing K12 *E. coli* strain was used instead of the more dangerous O156:H7 strain—however, they have similar structural dexterities and reproductive patterns. Based on these trials, the results were inconclusive despite showing consistent decrease in colony sizes because the differences in size were not statistically significant. In the most successful trial (Trial 2; irradiation pre-incubation), the maximum difference in survival was about 40% lower in the experimental group than the control. The problems with data validity were partially due to limitations in available equipment and methods in a high school environment.

### INTRODUCTION

*Escherichia coli* (*E. coli*) is a relatively harmless strain of bacteria found in the colon of many warm-blooded organisms. A particular strain, *E. coli* O156:H7, produces a powerful Shiga toxin and can cause diarrhea, abdominal pains, and kidney failure if ingested. The bacteria strain exists in raw or undercooked foods. It is prevalent in raw beef due to the bacteria's natural cultivation on cattle farms.<sup>1</sup> Prolonged exposure to ultraviolet (UV) radiation at a wavelength of 254 nanometers (nm) kills foodborne pathogens such as *E. coli* without affecting the quality of the meat.<sup>2</sup> This is due to DNA mutations that occur when UV light is absorbed by deoxyribose molecules of prokaryotic bacteria and viruses.<sup>2</sup> UV radiation has been a part of food sterilization for over 50 years; grocers treat produce, beverages, and cheeses with UV light throughout the production process.<sup>3</sup> However, many people are skeptical about the effects of UV radiation on food quality (organic food legally cannot be irradiated) as well as the cost of such radiation treatments.

Radiation is a popular means of disinfecting water, food contact surfaces, medical instruments and surfaces, and ensuring sterile processing of popular grocery items such as cider, juice, produce, cheeses, and egg products.<sup>4</sup> Despite this, many people find the concept of food radiation sterilization unsettling. Radiation's negative connotation hinders the use of radiation in the food production process. Although UV irradiation is a proven method of prolonging shelf life and ensuring consumer safety, skeptics of radiation as well as high costs and federal regulations affects companies from implementing irradiation treatments.

### RESULTS AND DISCUSSION

We evaluated the effectiveness of UV-C irradiation on cultures of *E. coli* grown in nutrient-rich agar under several environmental conditions to simulate the different stages of the farm-to-table process. We tested the effects of UV irradiation pre- and post-incubation of the bacteria. Due to limitations in material availability, the tests were limited to the non-Shiga

toxin-producing K-12 strain of *E. coli* in an *in vitro* experiment as opposed to the preferred method of culturing the ground beef O156:H7 strain. Our research was also limited to hand-held UVC-3 3-watt DC surface sterilizers as opposed to industrial grade sterilizers that perform at 40 watts.<sup>5</sup>

The radiation's destructive effects are shown by the decrease in colony density relative to the control which continued to increase in size. However, given that an estimated area was being compared to another estimated area, there is no statistical test to compare our data and therefore no statistical significance in our data. In future studies, this will be fixed via more trials and larger sample sizes.

The samples were incubated at 37°C and had an approximate area decrease of 9.74% while the control area increased by 6.4%. At 23°C, there was about 14.26% decrease in area while the control increased by 3.37%. There was no growth in the petri dishes incubated at 5°C. Although 5°C is within the temperature range where *E. coli* can survive, the colder temperature slows the bacterial metabolic processes and inhibits reproduction. The refrigeration temperature was adjusted accordingly to 10°C beginning in trial 2.



Table 1: Results from Trial 1 (Bottom half is control)

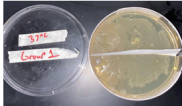
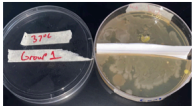
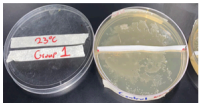
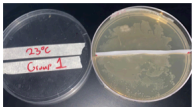
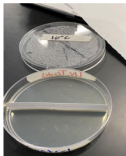
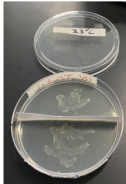
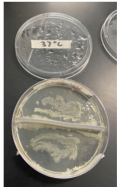
<p>Day 1 - 37°C Post- 72-hour incubation period prior to irradiation</p> <p>Average Control Radius: 3.0cm Average UV Radius: 4.0cm</p> <p>Initial Estimated Area: Control: 14.14 cm<sup>2</sup> UV: 25.13 cm<sup>2</sup></p> 	<p>Day 5 - 37°C After 10 irradiation sessions</p> <p>Average Control Radius: 3.1cm Average UV Radius: 3.8cm</p> <p>Final Estimated Area: Control: 15.10 cm<sup>2</sup> → +6.4% UV: 22.68cm<sup>2</sup> → -9.74%</p> 
<p>Day 1 - 23 °C Post- 72-hour incubation period prior to irradiation</p> <p>Average Control Radius: 2.9cm Average UV Radius: 2.7cm</p> <p>Initial Estimated Area: Control: 13.21 cm<sup>2</sup> UV: 11.45 cm<sup>2</sup></p> 	<p>Day 5 - 23 °C After 10 irradiation sessions</p> <p>Average Control Radius: 2.95cm Average UV Radius: 2.5cm</p> <p>Final Estimated Area: Control: 13.67cm<sup>2</sup> → +3.37% UV: 9.82cm<sup>2</sup> → -14.26%</p> 
<p>Day 1 - 5°C Post- 72-hour incubation period prior to irradiation</p> <p><b>NO GROWTH</b></p>	<p>Day 5 - 5°C After 10 irradiation sessions</p> <p><b>NO GROWTH</b></p>

Table 2: Results from Trial 2 (Bottom half is control)

<p>(10°C)</p> <p>No Growth</p> 	
<p>(23°C)</p> <p>Average Control Radius: 1.8cm Estimated Area: 10.18 cm<sup>2</sup> Average UV Radius: 1.4 cm Estimated Area: 6.16 cm<sup>2</sup> Difference: 39.49%</p> 	
<p>(37°C)</p> <p>Average Control Radius: 2.1cm Estimated Area: 13.85 cm<sup>2</sup> Average UV Radius: 2.0cm Estimated Area: 12.57 cm<sup>2</sup> Difference: 9.24%</p> 	

Trial 1: Mean % Change in Area vs. Group

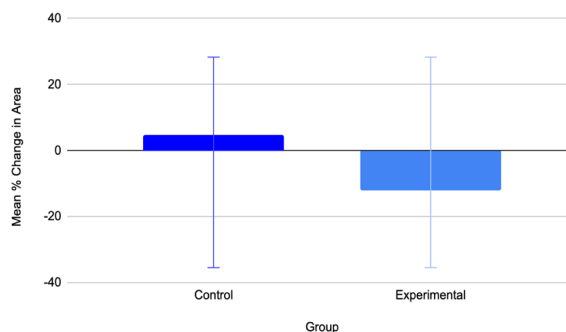


Figure 1. The graph portrays the resulting mean percent changes of the control and experimental groups of the first trial. The graph shows clearly that there is no statistical difference between the two means as the standard error bars of both overlap. These results led to a conclusion of no statistical significance.

Trial 2: Mean Area After Incubation vs. Group

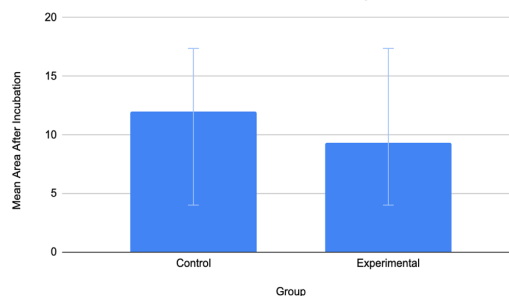


Figure 2. The graph for the results of trial two represents the mean areas of the control and experimental groups following the irradiations sessions and incubation. The graph does show a small difference in mean area between the two groups, but due to the small sample size the standard error bars overlap proving no statistical significance.

During the first trial, UV radiation was relatively ineffective against *E. coli* colonies when irradiated post-incubation. Despite the difference in percent change between the control and experimental groups, a t-test showed the results were not statistically significant. Given the large standard deviations visible in the bar chart as overlapping error bars (the control was 2.1425 and the experimental was 3.1961), there is not enough evidence to support a statistically significant difference. Although the experiment showed a clear difference between the control and variable groups, the percent change is not large enough to consider UV light effective in the destruction of already existing colonies. This is likely due to UV light being germicidal. UV radiation damages bacterial DNA, which prevents the bacteria from replicating and effectively neutralizes it; when a pre-existing colony is irradiated a mac-

roscopic observation will show little decrease in density, but further reproduction will not occur.

It was found during the second trial that UV radiation has an obvious effect on the reproductive efficiency of the *E. coli*. However, the results were far from the 99% difference between the control and experimental treatments advertised on the lamp packaging. A t-test showed large standard deviations (Control: 2.5951 and Experimental: 4.5326) that overlap as error bars. These large standard deviations are a thought to be a result of the inability to collect more data; one Petri dish for each temperature within the control and experimental groups is not enough to show statistically significant results.

It was found that the refrigerated sample, even at 10°C, prevented reproduction. The sample incubated at 37°C produced only a 9.24% difference between the control and irradiated side, while the room temperature sample experienced a difference of 39.49%. These differences are reasonable given that *E. coli* is more likely to thrive in an environment similar to that of the human colon.

The second trial focused on using radiation to prevent the reproduction and colonization of *E. coli* rather than destroying existing colonies. The test was set up with three dishes divided in half with cardstock and exposed to the bacteria. One side of each dish acted as the control and the other was exposed to UV radiation in the same manner as the previous trials. For this trial, there was one 30-second irradiation session followed by 48 hours of incubation.

## CONCLUSION

The poor results were likely due to a lack of resources. Cross-contamination between the control and UV exposed side of the Petri dish is also likely which allowed for increased reproduction in the irradiated side; the control and experimental groups were in the same Petri dish and the partition was not airtight. In the future, more trials would be conducted to provide statistically significant results. Additionally, the control and independent variables would be separated into different dishes to avoid cross-contamination. Larger UV lamps with a wavelength closer to 264 nm would be used because it is likely that higher UV-C wavelengths are more effective.

This research will continue to look into the effectiveness of UV radiation as a germicidal agent. Further experimentation can include using UV radiation against bacterial accumulation on students' cell phones as well as UV radiation on ground beef samples.

## METHODS

Tests on the effectiveness of UV radiation in the eradication of *E. coli* consisted of two 3-part trials. For the first trial, three Petri-dishes of *E. coli* were cultivated at the following temperatures: 38°C (roughly the temperature of human intestines), 24°C (room temperature), 5°C (temperature of the average home refrigerator), and 1°C (temperature of a standard meat cooler). The three dishes were divided in half via a piece of cardstock inserted into the nutrient agar; one side of each dish served as the control while the other side was treated with a 30-second dose of 254 nm UV-C radiation twice a day and

then incubated for 24 hours.<sup>6</sup> This process was repeated for five days. UV-C light was administered via a portable UV-C light wand composed of a 3W DC lamp. Since we did not have the tools to measure the pre-treatment colony density and post-treatment colony density, our findings were only visual observations and estimated calculations from measurements of the colonies' radii. Area estimates were done by measuring the four radii from the center to the furthest extent of the colony in four directions. These measurements were averaged, and a circular area was calculated from this number.

The second trial focused on using irradiation to prevent the reproduction and colonization of *E. coli* rather than destroying existing colonies. The test was set up with three dishes divided in half with cardstock and exposed to the bacteria. One side of each dish acted as the control and the other was exposed to UV radiation in the same manner as the previous trial. In this trial, there was one 30-second irradiation session followed by 48 hours of incubation.

The intent of these trials was to confirm UV radiation's sterilization abilities and explore using UV radiation to destroy bacterial colonies. In the future, we hope to further explore the applications of UV sterilization.

## Equipment

This research used 12 sterile Petri dishes, Carolina® Nutrient-rich agar, Caroline® K-12 non-Shiga toxin-producing *E. coli*, and a portable Socean-UV Germicidal UVC 3W DC lamp.

## ACKNOWLEDGEMENTS

I would like to thank my physics teacher, Jiayun Xu, Dr. Fasheng Zhou, and my father for their guidance and support during my research, as well as my family for their continued support.

## REFERENCES

- (1) CNN Editorial Research. E. Coli Outbreaks Fast Facts. [www.cnn.com/2013/06/28/health/e-coli-outbreaks-fast-facts/index.html](http://www.cnn.com/2013/06/28/health/e-coli-outbreaks-fast-facts/index.html)
- (2) Zimmer, J. L.; Slawson, R. M. Potential Repair of Escherichia coli DNA following Exposure to UV Radiation from Both Medium- and Low-Pressure UV Sources Used in Drinking Water Treatment. *Appl. Environ. Microbiol.* 2002, 68 (7), 3293-3299.
- (3) Lewis, S. Is UV Light Safe For Pathogen Reduction In Food Processing? <https://www.foodonline.com/doc/is-uv-light-safe-for-pathogen-reduction-in-food-processing-0001>.
- (4) Genetic Engineering & Biotechnology News. UV Light That Is Safe for Humans but Bad for Bacteria and Viruses. <https://www.genengnews.com/topics/translational-medicine/uv-light-that-is-safe-for-humans-but-bad-for-bacteria-and-viruses/>.
- (5) Viqua. UV Water Treatment. <https://viqua.com/water-treatment/uv-water-treatment/>.
- (6) Conner-Kerr, T. A.; Sullivan, P. K.; Gaillard, J.; Franklin, M. E.; Jones, R. M. The Effects of Ultraviolet Radiation on Antibiotic-Resistant Bacteria In Vitro. *Ostomy Wound Manage.* 1988, 44 (10), 50-56.

## Developing Pesticide Resistance to Acetylcholinesterase Inhibitors in *D. pulex*

Jordan Harrow

Episcopal School of Jacksonville, 4455 Atlantic Blvd, Jacksonville, FL, 32207, United States of America

harrowjo01@esj.org

**ABSTRACT:** As pesticide use has increased in agriculture, the substantial effects on nontarget organisms have grown. This investigation worked to mitigate the effects of pesticide run-off on non-target organisms by generating pesticide resistance in *Daphnia pulex*. *D. pulex* is a species of zooplankton present in most freshwater environments and is an essential component of freshwater ecosystems. *D. pulex* can naturally develop pesticide resistance and can act as a buffer to pesticide effects on aquatic organisms in higher trophic levels. Resistance was created in the lab through gradual exposure of *D. pulex* to the Lethal Concentration for 50% of the organisms (LC50) of the pesticide, malathion, an acetylcholinesterase inhibitor, over 54 days, for approximately six generations. Mortality rates after exposure of *D. pulex* to the Lethal Concentration for 75% of the organisms (LC75) of malathion were compared between previously exposed and unexposed individuals. It was hypothesized that previously exposed *D. pulex* would have higher survival rates than sensitive *D. pulex* when exposed to the LC75 of malathion. After exposure to LC75 malathion, results showed that the unexposed *D. pulex* had a higher mortality rate than the previously exposed *D. pulex*. Between the previously exposed *D. pulex* and the sensitive *D. pulex*, there was a difference of 80% mortality. This data suggests that lab-engineered pesticide resistance was generated in *D. pulex*. This process could therefore potentially be repeated on a larger scale to mass-produce resistant *D. pulex* that could be introduced into affected environments and lower mortality rates of non-target freshwater organisms.

**KEYWORDS:** Environmental Science; Freshwater Ecology; Pesticide Resistance; Acetylcholinesterase Inhibitors; *D. pulex*.

### INTRODUCTION

The purpose of this project was to develop lab-engineered pesticide resistance in *D. pulex* to acetylcholinesterase inhibitors, specifically malathion, to protect non-target freshwater organisms from the negative effects of pesticide run-off. Generating pesticide resistant *Daphnia* is beneficial to the environment because pesticide resistant *Daphnia* may act as environmental buffers that protect freshwater organisms from the harmful effects of pesticides.<sup>1</sup> Success of lab-engineered resistance potentially allows for protection of freshwater environments affected by pesticide run-off and decrease in mortality rates of organisms in at-risk environments.<sup>2</sup>

*Daphnia pulex* is a type of small crustacean and a common species of zooplankton. They have a generational period of 5-10 days. They are in the order Cladocera, meaning that the crustaceans have a bivalve shell, four legs, and a pair of antennae.<sup>3</sup> They live in freshwater ecosystems around the world, residing on all continents except for Antarctica and in almost every permanent freshwater body. *D. pulex* are capable of absorbing ions, chemicals, and other environmental particles through chloride-absorbing glands in their shell glands and maxillary glands.<sup>1</sup> This ability, along with their small size, causes heightened sensitivity to various chemicals that enter their environments. Therefore, they serve as reliable indicators of stress to freshwater ecosystems.<sup>4</sup> Because of these factors, *D. pulex* are commonly used in ecotoxicology testing to determine the effects of chemicals on aquatic organisms.<sup>3</sup> *D. pulex* feed on particles ranging from 1  $\mu\text{m}$  up to 50  $\mu\text{m}$ , which general-

ly consists of planktonic algae, yeast, and bacteria.<sup>1</sup> *D. pulex* are an important food source for a variety of organisms and are therefore essential to freshwater ecosystems.<sup>4</sup> Past studies indicate that trophic cascades induced by pesticides are initiated by the effects of pesticides on zooplankton.<sup>5</sup> Certain zooplankton, like *Daphnia*, have been reported to exhibit a resistance to these pesticides which yields the conclusion that resistant *Daphnia* could help buffer freshwater ecosystems from the trophic cascades induced by pesticides.<sup>6</sup>

Organophosphates are the most commonly used insecticides in the world.<sup>7</sup> Organophosphates are also known as acetylcholinesterase (AChE) inhibitors. By inhibiting AChE, organophosphates prevent the breakdown of the neuromuscular transmitter acetylcholine (ACh) resulting in overstimulation of synapses, which leads to continuous muscle contractions, immobility, and eventual death in *D. pulex* and other zooplankton.<sup>8</sup> Many organophosphates have been banned due to their toxicity and negative effects on the environment; however, some organophosphates are still available and widely used for domestic and agricultural use.<sup>9</sup> One common acetylcholinesterase inhibitor used today is malathion. Malathion is used to control a wide variety of insects in agricultural and domestic settings, especially in public health for mosquito control, and it is moderately toxic to aquatic organisms.<sup>10</sup>

*D. pulex* resistance to outdated AChE inhibitors not used in modern agriculture such as chlorpyrifos, aldicarb, and dichlorvos has been reported; therefore, pesticide resistance to these chemicals has become less environmentally significant.

Resistance of *D. pulex* to malathion has been reported in naturally occurring populations when they were exposed to low concentrations for multiple generations.<sup>5</sup> Pesticide resistance in *D. pulex* is beneficial to the environment because it may buffer the effects of pesticides on higher trophic levels.<sup>6</sup> This study focused on creating lab engineered pesticide resistance to the commonly used modern pesticide, malathion.

It was hypothesized that *D. pulex* that are exposed to malathion in lower concentrations of 5 µg/L for 54 days would develop resistance to the AChE inhibitor malathion and demonstrate higher survival rates when exposed to 7.5 µg/L malathion as compared to *D. pulex* that were not previously exposed to malathion.

## RESULTS AND DISCUSSION

The statistical significance of all data was calculated using standard deviation and standard error of the mean formulas.

### Bioassay

The mortality rates of three different cultures of *D. pulex* with six organisms in each jar initially, and after 48 hours, in the presence of 1 µg/L, 3 µg/L, and 5 µg/L malathion were calculated and recorded. In the control group no *D. pulex* died; the 1 µg/L group had a 100% mortality rate; the 3 µg/L group had a 17% mortality rate; and the 5 µg/L group had a 50% mortality rate (Figure 1). The 50% mortality rate of the 5 µg/L solution made 5 µg/L malathion the LC50 for *D. pulex*. The 1 µg/L should have had a <10% mortality rate, and likely had the 100% mortality rate due to contamination when the solution was created.

### Long Term Exposure Period

The amount of *D. pulex* alive in each jar was monitored every 9 days. At the beginning of the 54-day period, 10 *D. pulex* were alive in each jar. The days that the populations were tracked coincided with malathion addition. The average *Daphnia* alive in the four jars in each group was calculated across the 3 trials and recorded. The averages of those calculations were then determined across the 4 jars and placed in a line graph to show the gradual population decline in each experimental group, as shown in Figure 2.

After 54 days in the 100 ml environments, on average over the 3 trials, out of the original 10 *D. pulex* in each jar, 7 *D. pulex* were dead in the malathion addition jars, 7 *D. pulex* were dead in the malathion control jars, and 7 *D. pulex* were dead in the overall control jars. The malathion-exposed *D. pulex* averaged a mortality rate of 70%, the malathion control averaged a mortality rate of 70%, and the overall control averaged a mortality rate of 70%, showing that the *D. pulex* could still survive and only declined in population due to less available resources.

Additionally, the similarities in mortality rates across the 3 different populations shows that *D. pulex* survival was not significantly affected by the presence of 5 µg/L malathion over 54 days, which suggests the development of resistance over the

## Mortality Rates of *D. pulex* After Bioassay

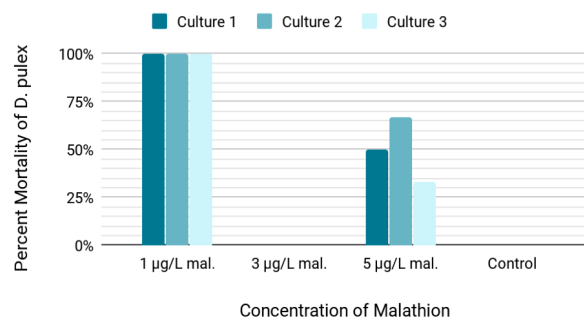


Figure 1: The mortality rates of *D. pulex* 48 hours after the addition of 5 µg/L malathion for each of the 3 cultures are shown in this graph, with 5 µg/L's mortality average of 50% making it the LD50 for *D. pulex*.

## Average Survival of *D. pulex* During 54 Day Exposure Period

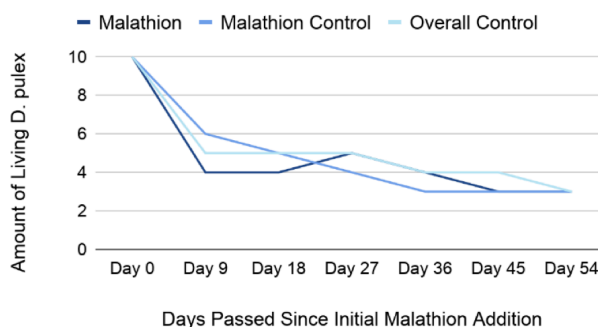


Figure 2: The average survival of the *D. pulex* in each trial over the 4 jars in each experimental and control group is shown in this graph. All 3 groups show a steady decline over the course of the 54 day exposure period, finishing at an overall mortality rate of 70% for all 3 groups of *D. pulex*.

generations of the *D. pulex*. The belief that resistance was developed over many generations is supported by the continued reproduction of the *D. pulex* throughout the exposure period and the survival of the sixth generation *D. pulex* in later resistance testing.

### Resistance Testing

Before the 7.5 µg/L malathion was added, each jar in each trial contained the amount of living *D. pulex* that were present from the exposure period. 48 hours after exposure to a 7.5 µg/L malathion solution, on average 3 *D. pulex* were alive in the previously exposed *D. pulex* jars, 1 *D. pulex* was alive in the unexposed *D. pulex* jars, and 3 *D. pulex* were alive in the control jars. On average, the previously exposed *D. pulex* had a 4% mortality rate, the newly exposed *D. pulex* had an 84% mortality rate, and the control *D. pulex* had a 7% mortality rate, which is broken down by trial in Figure 3 and shown overall in Figure 4. These results showed that the unexposed *D. pulex* had an 80% higher mortality rate than the previously exposed *D. pulex*. Compared to the unexposed *D. pulex*, which is shown to the left and under the conclusion, the previously exposed *D. pulex* had a 3% lower mortality rate and the unexposed *D. pulex* had a 77% higher mortality rate, leading to a difference of 80% as compared to the control between the 2 experimental groups. The standard errors of the mean, 4.5% mortality for the malathion group, 6.6% mortality for the malathion control



group, and 0.7% mortality for the overall control, indicate statistical significance in the differences in mortality percentages between the 2 experimental groups. These values were calculated by using the averages from each jar over the course of 3 trials.

## CONCLUSION

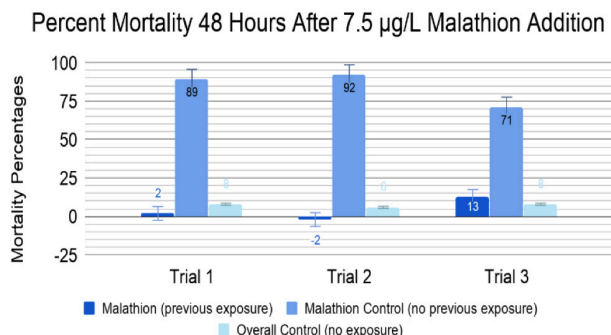


Figure 3: The percent mortalities of *D. pulex* 48 hours after 7.5 µg/L malathion addition are shown and broken down by the averages of trial, with the malathion control group having significantly higher mortality rates according to standard deviation calculations and the error bars shown in the graph.

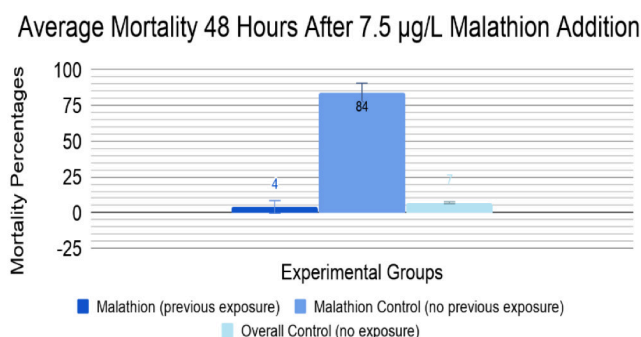


Figure 4: The average percent mortalities of *D. pulex* 48 hours after malathion addition over 3 trials are shown and broken down by experimental group to show the overall comparison between *D. pulex* that were previously exposed to malathion and *D. pulex* that were newly exposed to malathion, as well as the non-exposed *D. pulex* that were kept to monitor environmental conditions.

The research hypothesis was supported because the *D. pulex* previously exposed to 5 µg/L malathion had significantly lower mortality rates as compared to the previously unexposed *D. pulex* when exposed to 7.5 µg/L malathion for 48 hours. The 87% difference in mortality rates between the previously exposed *D. pulex* and the newly exposed *D. pulex* is statistically significant and demonstrates a developed resistance in the malathion experimental groups. The creation of resistance through exposure in the lab shows that pesticide resistance to AChE inhibitor pesticides, organophosphates, can be engineered in a lab environment. This suggests that the process could be repeated on a greater scale to create larger quantities of organophosphate resistant *D. pulex* with potential for introduction to natural environment. Many freshwater environments that are in proximity of the agricultural and domestic settings are exposed to pesticides. Pesticides are applied to plants around homes and

in larger quantities on crops in agricultural settings. When the plants are watered or exposed to rainfall, the residue from the pesticides is washed off and moves into nearby bodies of water, which leads to the exposure of organisms in the local bodies of water to suffer the negative effects of pesticide. Organophosphates in particular are toxic to aquatic organisms, causing population decreases. Lab engineered resistance allows for the potential of mass production of resistant *D. pulex* that could be introduced to freshwater ecosystems. Pesticide resistant *D. pulex* could be introduced to freshwater ecosystems affected by pesticide runoff and act as environmental buffers to protect other organisms from the negative effects of AChE inhibitor pesticides.

In the future, the success of resistant *D. pulex* created in a lab environment as environmental buffers needs to be investigated. Previous research has shown that naturally resistant *D. pulex* successfully protect other freshwater organisms from population endangerment, but no research has been done on the potential for protection by lab resistant *D. pulex*. This could be investigated by creating microcosms with a species of freshwater organism in a higher trophic level and two types of *D. pulex*: sensitive and resistant. The survival of the other freshwater organisms could be monitored in the presence of a high concentration of malathion and compared between those with sensitive and resistant *D. pulex*. Additionally, the survival of these resistant organisms in a natural environment and the heritability of resistance genes needs to be monitored to ensure that organisms with engineered resistance can survive and pass on resistance to their offspring. This future research will further support the environmental applicability of this project.

## METHODS

### Preparation

*D. pulex* were maintained in 100 mL jars of spring water. They were fed every 2 weeks using approximately 1/8 of a pellet in powdered form of *Daphnia* food containing primarily soybean meal, ground yellow corn, fish meal, and brewers dried yeast provided by Carolina Biological.<sup>11</sup> The water was changed in the tanks every 3 weeks by removing and replacing 500 mL of spring water.

The specific type of this pesticide used in this experiment was Spectracide Malathion. Its chemical composition is C<sub>10</sub>H<sub>19</sub>O<sub>6</sub>PS<sub>2</sub>.<sup>10</sup> Malathion was serially diluted by first diluting the pesticide into a 1 mg/L solution that would be used to create other concentrations. This dilution was done by combining 1 mL of 50% malathion solution using a volumetric pipet with 999 mL of spring water in a volumetric flask and sealed with a #4 rubber stopper. The 1 mg/L malathion solution was then used to create 1, 3, and 5 µg/L malathion solutions that were stored in volumetric flasks, shown in Figure 5, and labeled accordingly under a free-standing laboratory fume hood with a motor mounted on the top, front glass protection, and a steel liner.

### Bioassay

*D. pulex* were individually collected from the 2.5 L tanks using a pipet and transferred in groups of 6 into 12 100 mL glass jars filled with spring water. Jars were divided into groups of 3 and labeled as 1 µg/L, 3 µg/L, 5 µg/L, and Control, which is shown in Figure 6. 5 mL of the designated concentration of malathion was added to each jar using a volumetric pipet, shown in Figure 7, and the amount of *D. pulex* alive after 1 hour, 24 hours, and 48 hours was observed and recorded in a data table in the logbook. Traditionally, the chemical solution would have been added to the environments prior to the addition of the organisms; however pesticide solutions were added after integration of the organisms into their new environments to model the addition of pesticides in natural ecosystems after pesticide run-off.



Figure 5: In the bioassay, the jars were kept in 4 rows of 3 and labeled as 1 µg/L malathion, 3 µg/L malathion, 5 µg/L malathion, and control.

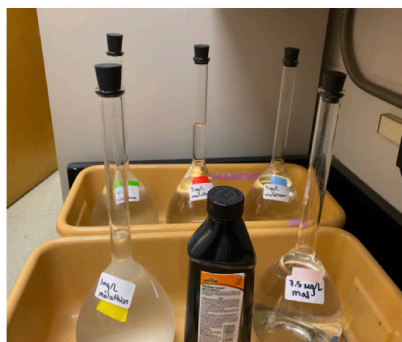


Figure 6: The volumetric flasks and the 50% malathion solution were kept in the chemical closet next to the fume hood and labeled with their concentration and a designated color of glass tape that was recorded in the logbook.

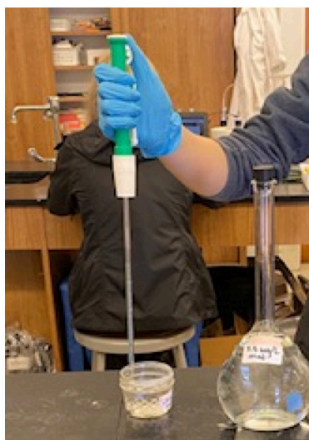


Figure 7: A volumetric pipet was used to extract different concentrations of malathion from the volumetric flasks and to place specific amounts into the jars of *D. pulex*.

The mortality rates from the initial addition to 48 hours were calculated for each jar in each group and the mean was determined. The concentration that kills approximately 50% of organisms in an experimental group (LC<sub>50</sub>) was calculated.

The LC<sub>50</sub> of 5 µg/L malathion was used in later experimentation.

### Long Term Exposure Period

For each of the three trials, 120 *D. pulex* were individually caught from the 2.5 L tanks using a pipet and transferred into 100 mL glass jars. Ten *D. pulex* were added to each jar. 20 mL of water was transferred with the *D. pulex* into each jar, and then 60 mL of spring water was added to each jar. The *D. pulex* were divided into 12 different 100 mL jars in groups of ten with three different experimental groups: malathion, which was exposed long-term to malathion; malathion control, which was later exposed to malathion; and overall control, which was used to monitor environmental conditions of the microcosms. Each jar was labeled with its designated experimental group and a number one through four to designate the jar number within each group, which is shown in Figure 8. Additionally, a designated colored mark was put on each label to distinguish between Trials 1, 2, and 3 and recorded in the logbook's color code.

Initially, 5 mL of 5 µg/L malathion was added to each of the four malathion jars in each trial to achieve a nominal concentration of 0.25 µg/L. Mathematical calculations were completed to determine that, in order to maintain a nominal concentration of 0.25 µg/L, 20 mL of spring water had to be removed and replaced with 19 mL of spring water and 1 mL of 0.25 µg/L malathion. Every 9 days, the water was changed, and 1 mL malathion was added using a volumetric pipet to maintain the nominal concentration. This repeated addition was performed to ensure continual exposure to malathion because the stability of malathion in aquatic environments is largely unknown beyond its harmful effects on aquatic organisms in its presence.<sup>13</sup> Repeated addition of malathion also simulates natural conditions of repeated exposure of ecosystems due to pesticide runoff. The water in malathion control and overall control jars was changed every 18 days, and the water changes were recorded on charts in the logbook along with feedings and malathion additions for each trial. Additionally, the amount of *D. pulex* alive in each jar was counted every 9 days using a magnifying glass, as seen in Figure 9, and recorded in data tables in the logbook. Nine days was the chosen interval because generational time for *D. pulex* is between 5 and 10 days, and 9 days is the longest possible generational period that doesn't allow for the potential of two short generations that would exist in a period of 10 days. The data was then placed into a line graph to track the increases and decreases in surviving *D. pulex* in each of the experimental groups.

### Resistance Testing.

After 54 days passed in each trial, all *D. pulex* were transferred to fresh, uncontaminated spring water for a 1-day rest period before resistance testing. The amount of *D. pulex* in each jar remained the same as the amount in the jars at the end of the 54-day exposure period and varied based on the amount of *D. pulex* that survived the exposure period in each microcosm.

A 7.5 µg/L malathion solution was created by combining the 1 mg/L solution with spring water in a volumetric flask. 7.5 µg/L was chosen because it is the approximated LC<sub>75</sub> for



Figure 8: For each trial, the jars were set up in 3 rows of 4 and labeled in groups for 5 µg/L malathion, malathion control, and overall control with numbers 1–4 within each experimental group.

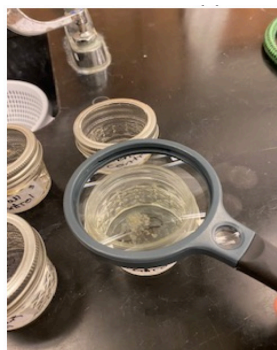


Figure 9: A magnifying glass was used to count the *D. pulex* in each jar and ensure accuracy before data was recorded in data tables in the logbook.

nonresistant *D. pulex* based on the previously completed bioassay. 5 mL of the 7.5 µg/L malathion solution was added to each jar and the water was gently stirred with a volumetric pipet to mix the malathion with the environment and simulate natural water movements. A magnifying glass was then used to count the *D. pulex* alive in each jar immediately after 7.5 µg/L malathion addition, 1 hour after addition, 24 hours after addition, and 48 hours after addition. The values were recorded in a data table in the logbook.

The data was used to calculate the mortality rates of each jar of *D. pulex*. The data was then averaged between the 4 jars in each group and the mortality rates were also averaged to generate average percentages for each experimental group. These final percentages were placed in a bar graph to show the differences in mortality between the previously exposed, unexposed, and control *D. pulex*. After the completion of each trial, the resistant *D. pulex* were placed in a 2.5L tank and labeled as resistant *Daphnia*. The other *D. pulex* and their contaminated environments were placed in the malathion waste jar in the fume hood. Once all trials were finished and the *D. pulex* were moved out of their jars, the malathion mixtures in the volumetric flasks were poured into malathion waste containers, labeled, and dropped off at the chemical waste facility.

#### ACKNOWLEDGEMENTS

I would like to thank my family for the support they provided during my experiment. I would also like to thank my Honors Science Seminar teacher, Mrs. Zeiner. Her advice throughout the experimental process was invaluable from start to finish.

#### REFERENCES

- (1) Ebert, D. Introduction to Daphnia Biology <https://www.ncbi.nlm.nih.gov/books/NBK2042/>. (accessed October 29, 2019)
- (2) Hoeven, N. V. D., Gerritsen, A. A. M. Effects of Chlorpyrifos On Individuals and Populations of Daphnia Pulex In the Laboratory and Field. Environmental Toxicology and Chemistry, 1997, 16(2), 2438–5028
- (3) Jansen, M., Coors, A., Stoks, R., Meester, L. D. Evolutionary ecotoxicology of pesticide resistance: a case study in Daphnia. Ecotoxicology, 2003, 20(3), 543–551.

(4) Miller, C. *Daphnia pulex*. [https://animaldiversity.org/accounts/Daphnia\\_pulex/](https://animaldiversity.org/accounts/Daphnia_pulex/). (accessed October 30, 2019), published 2001.

(5) Bendis, R. J.; Relyea, R. A. Living on the edge: Populations of two zooplankton species living closer to agricultural fields are more resistant to a common insecticide. Environmental Toxicology and Chemistry 2014, 33(12), 2835–2841.

(6) Wetland defense: naturally occurring pesticide resistance in zooplankton populations protects the stability of aquatic communities. Oecologia, 2016, 181(2), 487–498.

(7) Centers for Disease Control and Prevention. Fallon Nevada: FAQs: Organophosphates. [www.cdc.gov/nceh/clusters/fallon/organophosfaq.htm](http://www.cdc.gov/nceh/clusters/fallon/organophosfaq.htm). (accessed October 25, 2019).

(8) Russo, S. Episcopal School of Jacksonville, Jacksonville, FL. Personal communication, October 31, 2019.

(9) National Pesticide Information Center. Malathion. <http://npic.orst.edu/factsheets/malagen.html>. (accessed October 15, 2019), published 2003.

(10) "Spectracide Malathion Insect Spray Concentrate Safety Data Sheet." Malathion SDS. [images.homedepot-static.com/catalog/pdfImages/aa/aa3b-c0ca-9215-469a-893e-5406398c697b.pdf](https://images.homedepot-static.com/catalog/pdfImages/aa/aa3b-c0ca-9215-469a-893e-5406398c697b.pdf). (accessed October 20, 2019), published 21 Dec. 2018

(11) Bottorff, S., Carolina Biological Supply Company, Burlington, NC. Personal Communication, June 09, 2020.

(12) Wolfe, N., Zepp, R., Gordon, J., Baughman, G., Cline, D., Kinetics of Chemical Degradation of Malathion in Water. Environmental Science Technology, 1977, 11(1), 88–93.

(13) Pimentel, D., Burgess, M., Environmental and Economic Costs of the Application of Pesticides Primarily in the United States. Integrated Pest Management, 2008, 47–71.

#### AUTHOR

Jordan Harrow is a junior at Episcopal School of Jacksonville. She is focused on a career in medical research and will pursue a PreMed track in university in 2021. She has spent the past year in environmental research and will continue this research for the rest of high school.



## Development of Gel-based Multiplex RT-PCR for Detection of ER/PR/HER2-Positive Breast Cancer Diagnosis

Suh Kyung Yoon<sup>1</sup>, Woo Rin Lee<sup>2</sup>

1. Hong Kong International School, 1 Red Hill Rd, Tai Tam, Postal Code, Hong Kong

2. Department of Biological Science, University of Suwon, Wau-ri, Bongdam-eup, Hwaseong, Gyeonggi-do, 16419, Republic of Korea

200553@hkis.edu.hk<sup>1</sup>, gosyber@suwon.ac.kr<sup>2</sup>

**ABSTRACT:** Estrogen receptor (ER), progesterone receptor (PR), and human epidermal growth factor receptor 2 (HER2) expression levels play a central role as prognostic and predictive markers in breast cancer specimens. Therefore, detecting ER, PR, and HER2 statuses is essential for determining a correct therapeutic method to treat breast cancer. The most commonly used assays in clinical studies for detecting the expression levels of these genes are immunohistochemistry (IHC) and fluorescence in situ hybridization (FISH). However, IHC and FISH frequently underestimate ER, PR, and HER2 levels. A multiplex quantitative and cost-effective assay using gel-based reverse transcription-polymerase chain reaction (RT-PCR) for the assessment of ER, PR, and HER2 was developed to overcome this problem. Multiplex RT-PCR provided consistent data in four breast cancer cell lines without any cross-amplification of cDNA from other genes indicating that the developed assay was reliable in its specificity. In fact, this multiplex RT-PCR assay proved to be a sensitive and convenient method to rapidly and simultaneously detect the expression levels of ER, PR, HER2, and Pumilio homolog 1 (PUM1). In conclusion, multiplex RT-PCR could be useful for routine diagnosis of ER-, PR-, and HER2-positive breast cancers.

**KEYWORDS:** Biology; Cancer Biology; Breast Cancer; Gene Expression; RT-PCR.

### INTRODUCTION

The advancement and widespread application of genomics, transcriptomics, and proteomics has provided novel understanding of breast cancer's molecular complexity.<sup>1</sup> However, clinical decisions still rely on the assessment of three molecular markers: estrogen receptor (ER), progesterone receptor (PR), and human epidermal growth factor 2 (HER2).<sup>2</sup> Identifying these markers is essential for efficient targeted treatment for different types of breast cancer.<sup>2</sup>

ER is activated by estrogen.<sup>3</sup> There are two types of ER: ER $\alpha$  and ER $\beta$ .<sup>4</sup> Once activated, ER $\alpha$  and ER $\beta$  form dimers and translocate into the nucleus to facilitate the regulation of various genes.<sup>4</sup> Approximately 80% of breast cancer patients display ER-positive breast cancer.<sup>5</sup> ER-positive breast cancer typically responds readily to hormone-targeted therapy.<sup>6</sup> ER-positive cancers are treated with tamoxifen, a drug that blocks hormone receptors and the inhibition of estrogen production.<sup>7</sup>

PR is a receptor that blocks transcription until activated by progesterone.<sup>8</sup> Approximately 65% of breast cancer patients display PR positive breast cancer.<sup>9</sup> While PR may not respond to endocrine therapy directly, its activation may have significant impacts on the ER signaling pathway, thus showing value in determining which tumors may be subject to PR reprogramming of ER.<sup>10</sup>

HER2 is a breast cancer diagnostic marker that aids the therapeutic decisions in the treatment of breast cancer.<sup>11,12</sup> Up to 30% of patients display HER2 positive breast cancer.<sup>13</sup>

HER2 gene amplification in breast cancer cells is linked to a more clinically aggressive response in patients and corresponds to a higher death rate.<sup>14,15</sup> HER2 positive breast cancer is normally treated with trastuzumab, a monoclonal antibody that induces the downregulation and internalization of HER2 as well as upregulates cell cycle inhibitors.<sup>16,17</sup>

Previously, detection of ER, PR, and HER2 in breast cancer cells had been widely done using the immunohistochemistry (IHC) and fluorescence in situ hybridization (FISH) methods.<sup>18,19</sup> However, immunostaining methods like IHC are naturally prone to errors as the results are semi-quantitative and subject to interobserver variability.<sup>20</sup> The specificity of IHC depends on the quality of antibodies because IHC involves the process of selectively identifying antigens in cells of a tissue section.<sup>21</sup> Thus, these methods often lead to false positive/negative results. FISH is often used for diagnostic decisions by determining the ratio of the number of signals from two different chromosomal regions to determine gene amplification.<sup>22</sup> FISH assessments deliver more sensitive and quantitative results but is expensive and time-consuming, thus not appropriate for widespread use.<sup>23</sup> Furthermore, FISH-methods are prone to ambiguous results as standard protocols for sample collection and storage have not been developed.<sup>23</sup>

Detection of receptor DNA or cDNA by PCR meets the criteria of speed and high sensitivity and is used frequently for diagnostic purposes.<sup>24</sup> Gel-based reverse transcription polymerase chain reaction (RT-PCR) assay was reportedly



successful in the diagnosis of African swine fever (ASF).<sup>25</sup> This assay is sensitive and specific for the fast and early diagnosis of ASF. Therefore, RT-PCR could be an alternative method for the detection of ER, PR, and HER2.<sup>26</sup> Furthermore, multiplex PCR allows for simultaneous amplification of multiple target sequences in a single tube using specific primer sets in combination.<sup>24,27</sup> Thus, multiplex PCR favors higher throughput and automation compared to singleplex PCR especially when testing repeated and numerous patient analyses of the same targets.<sup>28</sup> To overcome the problems of two-step real time singleplex RT-PCR, a highly sensitive and specific gel-based multiplex RT-PCR assay was developed in this study by testing ER, PR, and HER2 negative and positive breast cancer cell lines.

## RESULTS

With the molecular classifications of breast cancer, researchers focus on breast cancer cell lines to determine whether the molecular profiles observed in breast cancer patients are reflected in cell line models of the disease.<sup>18</sup> Applications of transcriptional profiling to breast cancer cell lines using various platforms provided the cell lines' characteristics by the expression of estrogen receptor (ER $\beta$ ), progesterone receptor (PR), and human epidermal growth factor receptor 2 (HER2).<sup>29</sup> Four cell lines were selected to observe ER, PR, and HER2 expressions with RT-PCR method (Table 1).

Table 1. Categorization and molecular information of four breast cancer cell lines and the clinical features of tumors where they are derived. AC is "adenocarcinoma" and IDC is "invasive ductal carcinoma."

Cell lines	ER	PR	HER2	Tumor
MCF7	+	+	-	IDC
MDAMB231	-	-	-	AC
MDAMB453	-	-	+	AC
BT474	+	+	+	IDC

A previous study indicated that PUM1 is one of the best housekeeping genes for normalization of gene expression levels in both ER positive and negative subgroups and in normal breast tissue.<sup>30</sup> We designed the primer sets for ER, PR, HER2, and PUM1 at different lengths so they could be differentiated during agarose gel electrophoresis (Table 2).

The PCR reaction is visualized using agarose gel electrophoresis. DNA fragments of the expected size of amplified HER2, ER $\beta$ , PR, and PUM1 form a strong amplified DNA band on the gel by singleplex RT-PCR in all four breast cancer cell lines (Figure 1). Even though PCR conditions were optimized to amplify the target genes, some nonspecific bands were detected. PCR conditions were not perfectly optimized but the primers were sensitive enough to amplify the targeted gene.

Table 2. Sequence information for primers used in RT-PCR.

Gene	Forward Primer	Reverse Primer	Expected Size (bp)	Targeted Exon
HER2	GAAGGTGAAGTGCTTGGATCTGG	TAGCTCATCCCTTGGCAATCTGC	342	Exon 18-20
ER-beta	TCCTCCTACAACCTGCAGTCA	ACTGGCGATGGACCACTAAA	244	Exon 2 only
PR	ATGGAAGGGCAGCACAATA	AGGCGTTGGCTTTCATTGG	224	Exon 2-4
PUM1	TGAGGTGTGCACGATGAAC	CAGATGTGCTTGCCATAGG	187	Exon 21-22

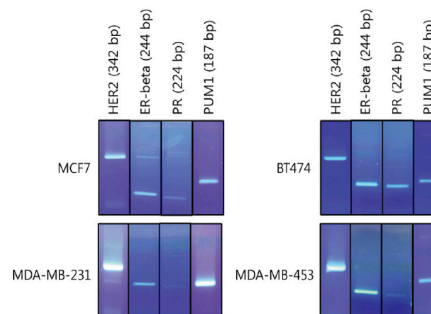


Figure 1. Agarose gel electrophoresis of singleplex RT-PCR products from cDNA of MCF7, BT-474, MDA-MB-231, and MDA-MB-453 breast cancer cell line.

Some nonspecific bands showed in Figure 1 could be a result of residual genomic DNA from the RNA extraction process because control reactions were not performed in this experiment.

Since the PCR conditions were optimized in Figure 1, multiplex RT-PCR was performed in four different breast cancer cell lines. Multiplex RT-PCR showed viable results for all cell lines as the relative expression levels for ER, PR, and HER2 were low for the ER, PR, and HER2-negative breast cancer cell lines and high for the ER, PR, and HER2-positive breast cancer cell lines (Figure 2). PUM1 also proved to be very compatible with ER, PR, and HER2 in the multiplex process as the multiplex results yielded consistent expression levels in breast cancer cell lines (Figure 2). These observations show that gel-based RT-PCR multiplex detection of ER, PR, and HER2 is a reliable way of detecting the expression of ER, PR, and HER2 in breast cancer cell lines and have the potential to be further applied to other genes involved in breast cancer.

CellExpress is a web-based tool that allows for analysis of gene expression levels in all of the cancer cell lines and clinical samples available online. The program takes queries based on gene, cell line, and normalization method and outputs all relevant data with a value corresponding to the relative expression of the gene and microRNA in the cell line in question.<sup>31</sup> This system is highly useful for cross analysis of gene expression in different cell lines, as it provides a universal ranking and value with the same normalization method.

Figure 3 shows the relative expression of the four studied genes in the MCF7, BT-474, MDA-MB-231, and MDAMB-453 cell lines. PUM1 has a uniform distribution of relative expression and low standard deviations as consistent with pre-

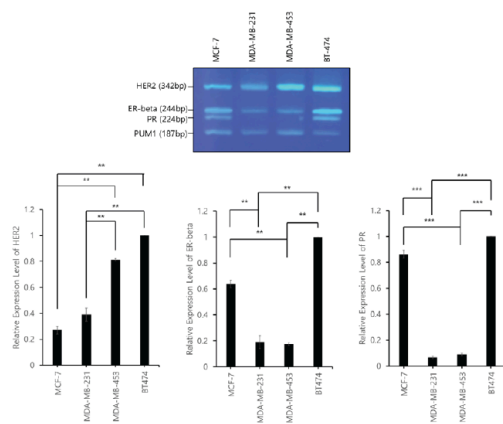


Figure 2. Quantification of HER2, ER $\beta$ , and PR expression level on cDNA from MCF7, BT-474, MDA-MB-231, and MDA-MB-453 using agarose gel electrophoresis of multiplex RT-PCR. (upper) Gel electrophoresis of HER2 (342bp), ER $\beta$  (244bp), PR (224bp), and PUM1 (187bp) (lower) Bar chart of band intensity calculated for HER2 expression level. The expression level of HER2, ER $\beta$ , and PR was normalized by PUM1 expression level (Mean + SD). Student's t test, \*\* P<0.01, \*\*\* P<0.001.

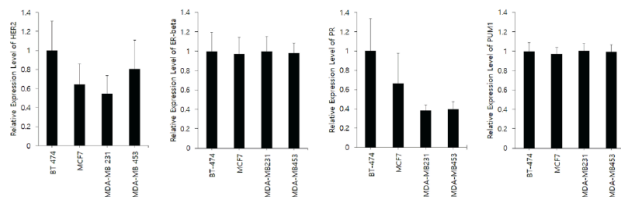


Figure 3. Relative expression for HER2, ER $\beta$ , PR, and PUM1 from MCF7(n=6), BT-474(n=6), MDA-MB-231(n=6), and MDA-MB-453(n=6) using cell line microarray data provided by CellExpress (Mean + SD).

vious studies, suggesting it is an appropriate normalizing gene for this study.<sup>30</sup>

All microarray data is consistent with Figure 2 except the relative expression of ER $\beta$ . The microarray data shows a much more even distribution of expression of ER $\beta$  compared with Figure 2, which shows distinct differences in expression between the four cell lines. This could be explained by the fact that ER $\beta$  has nine exons in total and the selected region for the microarray and the primer could have targeted different exons in the gene. Since there are several isoforms of ER $\beta$  the relative expression could differ depending on targeted exon.

Triple negative breast cancer is more likely to metastasize which further emphasizes the need for fast detection of receptor positive/negative cancer.<sup>32</sup> To visualize the effects of triple negative breast cancer on patients, 14 studies and 9134 samples were compiled to construct data (Figure 4) using a website called cBioPortal to analyze the difference in survival rate between patients with gene deletion in HER2, ER, and/or PR and patients without the deletion.<sup>33</sup> There was a markedly lower rate of survival in patients with gene deletion with a p-value of 1.237e-3. A previous study on a Brazilian cohort confirms that Triple Negative Breast Cancer (TNBC) displays a more aggressive behavior, recurs more frequently, and has a worse survival rate.<sup>34</sup> These patients have to receive different treatment (i.e. chemotherapy) and make it crucial to detect the expression of these receptors in the early stages of cancer.<sup>32</sup>

## Discussion

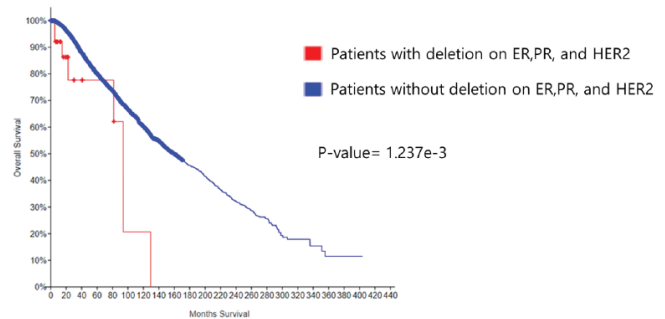


Figure 4. Quantification of HER2, ER $\beta$ , and PR expression level on cDNA from MCF7, BT-474, MDA-MB-231, and MDA-MB-453 using agarose gel electrophoresis of multiplex RT-PCR. (upper) Gel electrophoresis of HER2 (342bp), ER $\beta$  (244bp), PR (224bp), and PUM1 (187bp) (lower) Bar chart of band intensity calculated for HER2 expression level. The expression level of HER2, ER $\beta$ , and PR was normalized by PUM1 expression level (Mean + SD). Student's t test, \*\* P<0.01, \*\*\* P<0.001.

FISH and IHC are widely accepted as the best methods for ER, PR, and HER2 detection, a critical factor in the treatment of invasive breast cancer patients.<sup>18,22</sup> However, these methods both have limitations and are not perfect at detecting ER, PR, and HER2.<sup>35</sup> RT-qPCR detection of ER, PR, and HER2 has many advantages over these two methods, including cost timeliness, accuracy, and sensitivity.<sup>36</sup> The results in this study show that the gelbased RT-PCR assessments were accurate in detecting the amplification of ER, PR, and HER2 in different breast cancer cell lines (Figure 2). The results from this study are consistent with various microarray data (Figure 3). Which further confirms the accuracy of this method. Therefore, ER, PR, and HER2 detection via gelbased RT-PCR can remediate the disadvantages of methods like IHC and FISH in the future for rapid and accurate detection of ER, PR, and HER2 in a large number of samples. Since ER, PR, and HER2 expression levels are quantitatively measured by gelbased multiplex RT-PCR, measuring the expression level of novel genes relate to breast cancer progression by gelbased multiplex can be developed in the future.

A limitation of this study is that the qRT-PCR was tested on breast cancer cell lines instead of tissue samples from actual patients. Cancer cell lines were initially derived from tumors and cultured in two dimensional conditions. Cell cultures are widely used as models to study molecular markers of cancer.<sup>37</sup> However, data obtained from the cancer cell lines could be different from the data obtained from actual patient tissue samples as tissue samples are often heterogeneous, containing tumor cells as well as normal cells such as red blood cells.<sup>38</sup> Previous research found a strong correlation of the expression levels of ER ( $r=0.85$ ) and PR ( $r=0.9$ ) between IHC and RT-qPCR methods in patient tissue samples.<sup>39</sup> This result suggests that qRT-PCR is a promising complementary method to IHC for determining hormone receptors and protein markers used in breast cancer diagnosis.<sup>39</sup>

All primer pairs have an unknown amplification efficiency so they may differ in their ability to anneal and promote amplifi

cation of their target DNA region.<sup>40</sup> The primers used in this study were not tested to prove their equal efficiency to anneal the target gene to promote DNA amplification so the expression level of one marker gene relative to another in each cell lines could be inaccurate. Therefore, the annealing ability of primers should be analyzed to further address this limitation.

Development of a multiplex RT-PCR assay for four different genes required careful selection of primers and manipulation of PCR conditions because multiple primers could dimerize or suppress other primers. In each gene there are several isoforms that consist of different combinations of exons.<sup>41-43</sup> Thus, primers are chosen from a specific gene region that is conserved in most isoforms to eliminate biases related to uneven isoform representation. Ensembl, a web-based genome browser, was employed to visualize the exon structure and sequence of the four genes and exon regions.<sup>44</sup> Furthermore, we ensured the melting temperature of the primers were similar and differentiated the length of PCR products to ensure distinct detection during gel electrophoresis. Primers were tested individually to ensure optimal PCR conditions as well as in different combinations of over 500 PCR reactions to maximize the multi-PCR products' quality.

## CONCLUSION

The result of this study will help for rapid detection of the expression level of ER, PR, and HER2, especially in laboratories that cannot afford a real-time PCR machine. Unlike FISH and IHC assays, our assay is much simpler and more convenient. The multiplex analysis greatly reduces time-consuming procedures and eliminates additional manipulations that FISH and IHC assays require.

## METHODS

### *Breast Cancer Cell Lines*

All cell lines were obtained from the Korean Cell Line Bank (Seoul, Korea). All cell lines were maintained in RPMI-1640 medium (Gibco) supplemented with 10% fetal bovine serum (Thermo Fisher) and 1% penicillin and streptomycin in a 5% CO<sub>2</sub> atmosphere at 37°C. All cells were kept in culture for four or fewer passages and cell phenotypes were verified in every experiment. Four different known breast cancer cell lines were used in this study as templates for the HER2 detection: MCF7, MDAMB231, BT474, and MDAMB453. These cell lines display different types of cell markers being HER2-, triple negative, triple positive, and HER2+ respectively (Table 1).

### *Primer Set Design*

Primers were designed for ER, PR, HER2, and PUM1 with GenomCompiler program and they were synthesized by Bioneer (Table 2). The amplified DNA products were designed to be different lengths to be differentiated during agarose gel electrophoresis with ER (244 bp), PR (224 bp), HER2 (342 bp), and PUM1 (187bp). The annealing temperature was set for 60 °C for downstream applications.

### *RT-PCR Reaction*

RNA was extracted from breast cancer cell lines by RNA-spin™ Total RNA Extraction Kit (Intron) following the manufacturer's instructions. cDNA was synthesized from the extracted RNA using TOPscript™ Reverse Transcriptase (Enzynomics) following the manufacturer's instructions. For the PCR reaction, the different primers were tested individually using 20 µL reaction containing 2µL forward/ reverse primers (10 pmol), 2µL reaction buffer, 2µL dNTP, 1.125µL Taq polymerase (Bioneer), 0.5 µL cDNA, and RNase Free dH<sub>2</sub>O up to 20 µL. PCR was done with an annealing temperature of 60°C and an extension time of 40 seconds in 72°C for 40 cycles. For the multiplex reactions, nTaq-multi HOT (Enzynomics) was used with 20 µL reaction containing 2µL forward/reverse primers, 0.2µL nTaq- multiHOT polymerase, 0.5 µL cDNA, and RNase Free dH<sub>2</sub>O up to 20 µL.

### *Agarose Gel Electrophoresis*

2-5% agarose gel and TBE buffer were used in this study. RedSafe™ Nucleic Acid Staining Solution (Intron), an alternative to traditional ethidium bromide (EtBr), was used to stain nucleic acid. Amplified DNA was detected by direct examination of the gel in ultraviolet (UV) light.

### *Agarose Gel Quantification Analysis*

LI-COR Image Studio software version 2.1.10 and gel images were saved as a work area. All gel intensity quantification analyses were performed on images saved in TIFF format.

All experiments in this study, including running the agarose gel electrophoresis, were performed in University of Suwon, Korea.

## ACKNOWLEDGEMENTS

I would like to thank Dr. Woo Rin Lee, my mentor from University of Suwon for his assistance and guidance in this project.

## REFERENCES

- Godone, R. L. N.; Leitão, G. M.; Araújo, N. B.; Castelletti, C. H. M.; Lima-Filho, J. L.; Martins, D. B. G. Clinical and molecular aspects of breast cancer: Targets and therapies. *Biomed. Pharmacother.* 2018, 106, 1434.
- Dai, X.; Cheng, H.; Bai, Z.; Li, J. Breast Cancer Cell Line Classification and Its Relevance with Breast Tumor Subtyping. *J. Cancer* 2017, 8 (16), 3131-3141.
- Ullrich, J. W.; Miller, C. P. Estrogen receptor modulator review. *Expert Opin. Ther. Pat.* 2006, 16 (5), 559-572.
- Farzaneh, S.; Zarghi, A. Estrogen Receptor Ligands: A Review (2013-2015). *Sci. Pharm.* 2016, 84 (3), 409-427.
- Parise, C. A.; Caggiano, V. Breast Cancer Survival Defined by the ER/PR/HER2 Subtypes and a Surrogate Classification according to Tumor Grade and Immunohistochemical Biomarkers. *J. Cancer Epidemiol.* 2014, 2014, 469251.
- Berru, D. A.; Cirrincione, C.; Henderson, I. C.; Citron, M. L.; Budman, D. R.; Goldstein, L. J.; Martino, S.; Perez, E. A.; Muss, H. B.; Norton, L., et al. Estrogen-receptor status and outcomes of modern chemotherapy for patients with node-positive breast cancer. *JAMA* 2006, 295 (14), 1658-1667.



- (7) Shou, J.; Massarweh, S.; Osborne, C. K.; Wakeling, A. E.; Ali, S.; Weiss, H.; Schiff, R. Mechanisms of tamoxifen resistance: increased estrogen receptor-HER2/neu cross-talk in ER/Her2-positive breast cancer. *J. Natl. Cancer Inst.* 2004, 96 (12), 926-935.
- (8) Cahill, M. A. Progesterone receptor membrane component 1: an integrative review. *J. Steroid Biochem. Mol. Biol.* 2007, 105 (1-5), 16-36.
- (9) Mason, B. H.; Holdway, I. M.; Mullins, P. R.; Yee, L. H.; Kay, R. G. Progesterone and estrogen receptors as prognostic variables in breast cancer. *Cancer Res.* 1983, 43 (6), 2985-2990.
- (10) Bartlett, J. M. S.; Brookes, C. L.; Robson, T.; van de Velde, C. J. H.; Billingham, L. J.; Campbell, F. M.; Grant, M.; Hasenburger, A.; Hille, E. M.; Kay, C.; et al. Estrogen receptor and progesterone receptor as predictive biomarkers or response to endocrine therapy: a prospectively powered pathway study in the Tamoxifen and Exemestane Adjuvant Multination trial. *J. Clin. Oncol.* 2011, 29 (12), 1531-1538.
- (11) Carney, W. P.; Letizel, K.; Ali, S.; Neumann, R.; Lipton, A. HER-2/ neu diagnostics in breast cancer. *Breast Cancer Res.* 2007, 9 (3), 207.
- (12) Zhang, J.; Liu, Y. HER2 over-expression and response to different chemotherapy regimens in breast cancer. *J. Zhejiang Univ. Sci. B.* 2008, 9 (1), 5-9.
- (13) Loibl, S.; Gianni, L. HER2-positive breast cancer. *Lancet.* 2017, 389 (10087), 2415-2429.
- (14) Bartlett, J. M.; Going, J. J.; Mallon, E. A.; Watters, A. D.; Reeves, J. R.; Stanton, P.; Richmond, J.; Donald, B.; Ferrier, R.; Cooke, T. G. Evaluating HER2 amplification and overexpression in breast cancer. *J. Pathol.* 2001, 195 (4), 422-428.
- (15) Pritchard, K. I.; Shepherd, L. E.; O'Malley, F. P.; Andrulis, I. L.; Tu, D.; Bramwell, V. H.; Levine, M. N. HER2 and Responsiveness of Breast Cancer to Adjuvant Chemotherapy. *N. Engl. J. Med.* 2006, 354, 2103-2111.
- (16) Piccart-Gebhart, M. J.; Proctor, M.; Leyland-Jones, B.; Goldhirsch, A.; Untch, M.; Smith, I.; Gianni, L.; Baselga, J.; Bell, R.; Jackisch, C.; et al. Trastuzumab after Adjuvant Chemotherapy in HER2-Positive Breast Cancer. *N. Engl. J. Med.* 2005, 353, 1659-1672.
- (17) Von Minckwitz, G.; Proctor, M.; de Azambuja, E.; Zardavas, D.; Benyunes, M.; Viale, G.; Suter, T.; Rahmani, A.; Rouchet, N.; Clark, E.; et al. Adjuvant Pertuzumab and Trastuzumab in Early HER2-Positive Breast Cancer. *N. Engl. J. Med.* 2017, 377 (2), 122-131.
- (18) Subik, K.; Lee, J. F.; Baxter, L.; Strzpel, T.; Costello, D.; Crowley, P.; Xing, L.; Hung, M. C.; Bonfiglio, T.; Hicks, D. G.; Tang, P. The Expression Patterns of ER, PR, HER2, CK5/6, EGFR, Ki-67 and AR by Immunohistochemical Analysis in Breast Cancer Cell Lines. *Breast Cancer (Auckl.)* 2010, 4, 35-41.
- (19) Wu, N. C.; Wong, W.; Ho, K. E.; Chu, V. C.; Rizo, A.; Davenport, S. Kelly, D.; Makar, R.; Jassem, J.; Duchnowska, R.; et al. Comparison of central laboratory assessments of ER, PR, HER2, and Ki67 by IHC/FISH and the corresponding mRNAs (ESR1, PGR, ERBB2, and MKI67) by RT-qPCR on an automated, broadly deployed diagnostic platform. *Breast Cancer Res. Treat.* 2018, 172, (2), 327-338.
- (20) Mrozowski, A.; Olszewski, W. P.; Piascik, A. HER2 status in breast cancer determined by IHC and FISH: comparison of the results. *Pol. J. Pathol.* 2004, 55 (4), 165-171.
- (21) Zafrani, B.; Aubriot, M. H.; Mouret, E.; De Crémoux, P.; De Rycke, Y.; Nicolas, A.; Boudou, E.; Vincent-Salomon, A.; Magdelénat, H.; Sastre-Garau, X. High sensitivity and specificity of immunohistochemistry for the detection of hormone receptors in breast carcinoma: comparison with biochemical determination in a prospective study of 793 cases. *Histopathology* 2000, 37 (6), 536-545.
- (22) Pauletti, G.; Godolphin, W.; Press, M. F.; Slamon, D. J. Detection and quantitation of HER-2/neu gene amplification in human breast cancer archival material using fluorescence in situ hybridization. *Oncogene.* 1996, 13(1), 63-72.
- (23) Kallioniemi, O. P.; Kallioniemi, A.; Kurisu, W.; Thor, A.; Chen, L. C.; Smith, H. S.; Waldman, F. M.; Pinkel, D.; Gray, J. W. ERBB2 amplification in breast cancer analyzed by fluorescence in situ hybridization. *Proc. Natl. Acad. Sci. U. S. A.* 1992, 89 (12), 5321-5325.
- (24) Elnifro, E. M.; Ashshi, A. M.; Cooper, R. J.; Klapper, P. E. Multiplex PCR: optimization and application in diagnostic virology. *Clin. Microbiol. Rev.* 2000, 13 (4), 559-570.
- (25) Liu, L.; Widén, F.; Baule, C.; Belák, S. A one-step, gel-based RT-PCR assay with comparable performance to real-time RT-PCR for detection of classical swine fever virus. *J. Virol. Methods* 2007, 139 (2), 203-207.
- (26) El Hadi, H.; Abdellaoui-Maane, I.; Kottwitz, D.; El Amrani, M.; Bouchoutrouh, N.; Qmichou, Z.; Karkouri, M.; ElAttar, H.; Errihani, H.; Fernandez, P. L.; et al. Development and evaluation of a novel RT-qPCR based test for the quantification of HER2 gene expression in breast cancer. *Gene* 2017, 605 (20), 114-122.
- (27) Yamasaki, H.; Allan, J. C.; Sato, M. O.; Nakao, M.; Sako, Y.; Nakaya, K.; Qiu, D.; Mamuti, W.; Craig, P. S.; Ito, A. DNA differential diagnosis of taeniasis and cysticercosis by multiplex PCR. *J. Clin. Microbiol.* 2004, 42 (2), 548-553.
- (28) Hockman, D.; Dong, M.; Zheng, H.; Kumar, S.; Huff, M. D.; Grigorenko, E.; Beanan, M.; Duncan, R. Comparison of multiplex PCR hybridization-based and singleplex real-time PCR-based assays for detection of low prevalence pathogens in spiked samples. *J. Microbiol. Methods* 2017, 132, 76-82.
- (29) Del Valle, P. R.; Milani, C.; Brentani, M. M.; Katayama, M. L. H.; de Lyra, E. C.; Carraro, D. M.; Brentani, H.; Puga, R.; Lima, L. A.; Rozenchan, P. B.; et al. Transcriptional profile of fibroblasts obtained from the primary site, lymph node and bone marrow of breast cancer patients. *Genet. Mol. Biol.* 2014, 37 (3), 480-489.
- (30) Kiliç, Y.; Çelebiler, A. Ç.; Sakizli, M. Selecting housekeeping genes as references for the normalization of quantitative PCR data in breast cancer. *Clin. Transl. Oncol.* 2014, 16 (2), 184-190.
- (31) Lee, Y. F.; Lee, C. Y.; Lai, L. C.; Tsai, M. H.; Lu, T. P.; Chuang, E. Y. CellExpress: a comprehensive microarray-based cancer cell line and clinical sample gene expression analysis online system. *Database (Oxford)* 2018, bax101.
- (32) Dent, R.; Trudeau, M.; Pritchard, K. I.; Hanna, W. M.; Kahn, H. K.; Sawka, C. A.; Lickley, L. A.; Rawlinson, E.; Sun, P.; Narod, S. A. Triple-negative breast cancer: clinical features and patterns of recurrence. *Clin. Cancer Res.* 2007, 13 (15 Pt 1), 4429-4434.
- (33) Gao, J.; Askoy, B. A.; Dogrusoz, U.; Dresdner, G.; Gross, B.; Sumer, S. O.; Sun, Y.; Jacobsen, A.; Sinha, R.; Larsson, E.; et al. Integrative analysis of complex cancer genomics and clinical profiles using the cBioPortal. *Sci. Signal.* 2013, 6 (269), p11.
- (34) Foulkes, W. D.; Smith, I. E.; Reis-Filho, J. S. Triple-negative breast cancer. *N. Engl. J. Med.* 2010, 363 (20), 1938-1948.
- (35) Tawfik, O. W.; Kimler, B. F.; Davis, M.; Donahue, J. K.; Persons, D. L.; Fan, F.; Hagemister, S.; Thomas, P.; Connor, C.; Jewell, W.; Fabian, C. J. Comparison of immunohistochemistry by automated cellular imaging system (ACIS) versus fluorescence in-situ hybridization in the evaluation of HER-2/neu expression in primary breast carcinoma. *Histopathology* 2006, 48 (3), 258-267.
- (36) Balamurugan, V.; Sen, A.; Venkatesan, G.; Yadav, V.; Bhanot, V.; Bhanuprakash, V.; Singh, R. K. A rapid and sensitive one step-SYBR green based semi quantitative real time RT-PCR for the detection of peste des petits ruminants virus in the clinical samples. *Virol. Sin.* 2012, 27 (1), 1-9.
- (37) Holliday, D. L.; Speirs, V. Choosing the right cell line for breast cancer research. *Breast Cancer Res.* 2011, 13 (4), 215.
- (38) Kostic, A.; Lynch, C. D.; Sheetz, M. P. Differential matrix rigidity response in breast cancer cell lines correlates with the tissue tropism. *PLoS One* 2009, 4 (7), e6361.
- (39) Christopherson, C.; Chang, M.; Eberhard, D. A.; Sninsky, J. J.; Anderson, S. M.; Wang, A. M.; Kwok, S.; Calhoun, B. Comparison of immunohistochemistry (IHC) and quantitative RT-PCR: ER, PR, and HER2 receptor status. *J. Clin. Oncol.* 2012, 30 (27), 47.
- (40) Tichopad, A.; Dzidic, A.; Pfaffl, M. W. Improving quantitative real-time RT-PCR reproducibility by boosting primer-linked amplification efficiency. *Biotechnol. Lett.* 2002, 24, 2053-2056.
- (41) Vranic, S.; Gatalica, Z.; Deng, H.; Frkovic-Grazio, S.; Lee, L. M. J.; Gurjeva, O.; Wang, Z. Y. ER- $\alpha$ 36, a novel isoform of ER- $\alpha$ 66, is commonly over-expressed in apocrine and adenoid cystic carcinomas of the breast. *J. Clin. Pathol.* 2011, 64 (1), 54-57. (32) Dent, R.; Trudeau, M.; Pritchard, K. I.; Hanna, W. M.; Kahn, H. K.; Sawka, C. A.; Lickley, L. A.; Rawlinson, E.; Sun, P.; Narod, S. A. Triple-negative breast cancer: clinical features and patterns of recurrence. *Clin. Cancer Res.* 2007, 13 (15 Pt 1), 4429-4434.



- (42) Menon, R.; Panwar, B.; Eksi, R.; Kleey, C.; Guan, Y.; Omenn, G. S. Computational Inferences of the Functions of Alternative/Noncanonical Splice Isoforms Specific to HER2+/ER-/PR- Breast Cancers, a Chromosome 17 C-HPP Study. *J. Proteome Res.* 2015, 14 (9), 3219-3529.
- (43) McCormack, O.; Harrison, M.; Kerin, M. J.; McCann, A. Role of the progesterone receptor (PR) and the PR isoforms in breast cancer. *Crit. Rev. Oncog.* 2007, 13 (4), 283-301.
- (44) Cuhhingam, F.; Achuthan, P.; Akannni, W.; Allen, J.; Amode, M. R.; Armean, I. M.; Bennett, R.; Bhai, J.; Billis, K.; Boddu, S.; et al. *Nucleic Acids Res.* 2019, 47, D745-D751.

## AUTHORS

Stephanie Yoon is a senior at Hong Kong International-School. She has been a varsity rugby player throughout high school. For the past three years, she has been leading her school's Math and Science Center providing STEM resources to students. Her research experiences have led her to consider bioengineering as a major in college.

## Effects of Milk, Cheese, and Strawberry Counteracting Tooth Discoloration Induced by Coffee or Red Wine

Selina Yuri Kim

Daegu International School, 22 Palgong-ro 50-gil, Dong-gu, Daegu, South Korea

**ABSTRACT:** This study investigated the kinds of foods that counteract teeth discoloration caused by consumption of coffee and red wine. A protein contained in dairy products is known for possessing enamel demineralization properties, and strawberries have been associated with teeth whitening functions. In this study, dairy, and strawberries were examined to determine if they contain properties that can substantially counteract tooth enamel discoloration caused by the consumption of coffee and red wine. When considering discoloration caused by coffee, milk, and strawberries were examined; when considering discoloration caused by red wine, cheese and strawberries were examined. Sixty cow teeth were assigned to ten combination groups and the  $\Delta E^*$  (total color change in Commission Internationale de L'Eclairage (CIE)) was calculated for the color change of teeth after immersion in respective solutions. Dairy products such as milk and cheese reduced discoloration induced by coffee and red wine while strawberry did not. The concentration of beverages was critical to teeth discoloration. Based on our results, we recommend that people consume dairy products such as milk or cheese when they drink coffee or wine. We also recommend people drink light coffee (Americano) or light wine in order to keep teeth whiter and brighter.

**KEYWORDS:** Dental Hygiene, Tooth discoloration; Cow teeth; Coffee; Wine; Dairy products; Strawberries.

### INTRODUCTION

One part of the face people care about most is their teeth. Some of the most common causes of tooth discoloration come from beverages including coffee and wine. These beverages are consumed with high frequency by people with varying lifestyles due to the positive effects that are felt after consumption. The caffeine in coffee increases psychomotor function to stay awake and provides physiological effects by increasing energy.<sup>1</sup> Wine gives relaxation and pleasure to people as well as reduces the risk of cancer, diabetes, gallstones, and cardiovascular disease.<sup>2</sup> However, our teeth become discolored by such beverages, thus, we need to find out the foods which are effective for the prevention of teeth discoloration when taken together with wine and coffee. This paper will look at the kinds of foods that counteract teeth discoloration and make recommendations based on the findings to revise one's diet. The specific research question is as follows: Which foods can prevent teeth discoloration when they are taken together with the stain-inducing beverages?

Coffee and wine are frequently consumed by people, but these drinks are shown to cause tooth discoloration. Coffee contains brown or black colors, and red wine contains red, purple and brown colors.<sup>3</sup> These beverages contain chromogenic polyphenols capable of chemical interaction, and the color of stained teeth is thought to be derived from polyphenolic compounds which provide the color in food.<sup>4</sup> The substances in coffee and wine that are responsible for causing dental stains are known as tannins and are composed of polyphenols such

as catechins and leucoanthocyanins. Nathoo<sup>5</sup> explained that these materials generate color due to the presence of conjugated double bonds and are thought to interact with tooth surfaces via an ion exchange mechanism and categorized this discoloration as an N1 type mechanism. The tannins in the pigmented foods react with chromogen which is responsible for colors and result in discoloration by precipitating with chromogenic substances on the enamel of the tooth that is naturally porous. Additionally, the tannins in coffee and wine which are acidic, lower the pH inside a person's mouth and eventually causes discoloration, which is facilitated by a low pH level; acidity causes erosion of tooth surfaces.<sup>6</sup> Moreover, acidity in wine is so strong that it creates rough spots and grooves that enable chemicals that cause staining to penetrate deeper into the tooth.<sup>7</sup> Therefore, frequent intake of wine can lead to the erosion of dental hard tissues and thus, increase the likelihood of tooth discoloration in the presence of pigmented foods and beverages by allowing the penetration of these pigments into the tooth.<sup>6,8</sup>

People commonly drink coffee together with milk and pair wine with cheese. The milk protein, casein is known to prevent enamel demineralization;<sup>9</sup> more specifically, it stabilizes high levels of amorphous calcium phosphate on tooth surfaces, and thus, prevents demineralization.<sup>10</sup> Therefore, it is pertinent to study whether milk and cheese can counteract teeth discoloration induced by coffee and red wine through protecting enamel surfaces of teeth.

Strawberries are also well known for their function to whiten teeth. Strawberries contain a substance known as malic acid, which is effective at dissolving any superficial staining such as chromogenic substances on teeth.<sup>11</sup> Therefore, the tooth-whitening activity of malic acid that is present in straw berries might help diminish discoloration by eliminating some of the stains on the surface of teeth. However, the pigments and dyes in strawberries may deepen discoloration, especially the red dye in strawberries. In addition, the acid of this food may facilitate the discoloration of teeth through the erosion of enamel.<sup>6</sup> Therefore, we need to examine whether strawberries minimize or deepen discoloration of teeth. We also need to investigate a way of combining these dairy products and strawberries with stain-inducing beverages and to determine how they may influence teeth discoloration differently.

In studies of discoloration and whitening of teeth, many researchers use cow teeth of which the surface closely resembles that of human teeth. These studies examined the staining of enamel with red and white wine;<sup>7</sup> the effect of children's favorite beverages on enamel;<sup>12</sup> the effects of a bleaching agent with calcium;<sup>13</sup> the effect of fluoridated carbamide peroxid on enamel surface change and whitening<sup>14</sup> and the effect of carbonated water on enamel erosion and plaque adhesion.<sup>15</sup> Therefore, cow teeth can be used for the experimentation of discoloration and whitening of human teeth.

## RESULTS

### Discussion

In order to discover different types of food that would best prevent tooth discoloration, the current experiment was conducted with two cases of stain-inducing beverages: coffee and red wine. For coffee, milk, and strawberry were set as the counteracting beverage and food. For red wine, cheese, and strawberry were the counteracting beverage and food. Those foods were combined with possible causations for counteracting discoloration; for coffee groups, coffee and milk at the same time ('coffee + milk') or milk before coffee ('milk → coffee'), and coffee and strawberry (Str.) at the same time or strawberry before coffee; for red wine groups, the same combination as the coffee groups incorporating cheese instead of milk. A control group was set for coffee groups and another for red wine groups respectively; 'coffee only' group and 'wine only' group. Thus, five particular groups were set up for the coffee groups and five groups for wine groups, for a total of 10 groups. The change of color was measured after immersing the teeth in different combinations of solution, where the  $\Delta E^*$  means the increase of color change from the pretest scores.

#### Coffee Groups

The results of coffee groups are presented in Table 1 and Figure 1.

Considering the data resulting from the teeth immersed in each solution for three hours, the teeth groups that were transferred from strawberry to coffee solution (mean 18.58) and the teeth groups that were immersed in the mixture of coffee with strawberry (mean 15.98) resulted in higher color change compared to the control coffee only group (mean 10.87). On the other hand, the teeth groups that milk were set as the counteracting beverage, both the group of transferring from milk to coffee solution (mean 8.50) and the group of mixture of coffee with milk (mean 5.29), resulted in lower color change than the coffee only group. Therefore, in the case of coffee groups, the solutions that contained milk, counteracted discoloration of teeth while the solutions that contained strawberries accelerated discoloration. In addition, the mixture groups (coffee + milk, coffee + strawberry) were lower in their color changes than their respective transferring groups (milk → coffee, strawberry → coffee).

**Table 1.** The color change of coffee groups ( $\Delta E^*$ ).

Solution	N	$E^*_0$ (pretest) Mean (SD)	$\Delta E^*_1$ (1 hour) Mean (SD)	$\Delta E^*_2$ (2 hours) Mean (SD)	$\Delta E^*_3$ (3 hours) Mean (SD)
Coffee only	6	63.62 (2.49)	3.45 (1.33)	5.98 (1.42)	10.87 (1.29)
Coffee + Milk	6	69.13 (3.48)	2.89 (0.86)	3.99 (1.77)	5.29 (1.79)
Milk → Coffee	6	67.44 (4.93)	4.55 (2.51)	5.74 (1.16)	8.50 (2.34)
Coffee + Str.	6	74.51 (4.56)	6.09 (2.45)	10.48 (4.09)	15.98 (5.27)
Str. → Coffee	6	67.26 (3.98)	6.49 (2.00)	12.41 (2.08)	18.58 (1.80)

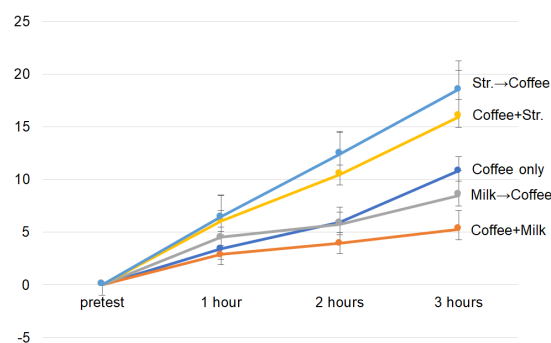


**Figure 1.** The color change of coffee group ( $\Delta E^*$ ).

#### Red Wine Groups

The results of red wine groups are presented in Table 2 and Figure 2. In the case of wine groups, the teeth that were transferred from strawberry to wine solution (mean 20.59) presented higher color change than the control wine only group (mean 17.27). However, contrasted with the coffee groups, the teeth that were immersed in the mixture of wine with strawberry (mean 10.88) resulted in a smaller mean change than the tooth saturated in the wine only solution. The teeth groups transferring from cheese to wine (mean 15.52) and the group in the mixture of wine with cheese (mean 5.62) also had a lower change in color than the control (wine only) group. This

further shows that the solutions containing cheese (cheese → wine, wine + cheese) and the mixture of wine with strawberry reduced teeth discoloration. In addition, the mixture groups (wine + cheese, wine + strawberry) experienced less color change than their respective transferring groups (cheese → wine, strawberry → wine).

**Table 2.** The color change of wine group ( $\Delta E^*$ ).

Solution	N	E <sup>a</sup> <sub>0</sub> (pretest) Mean (SD)	$\Delta E^*_1$ (1 hour) Mean (SD)	$\Delta E^*_2$ (2 hours) Mean (SD)	$\Delta E^*_3$ (3 hours) Mean (SD)
Wine only	6	68.74 (6.17)	7.87 (2.40)	13.44 (2.99)	17.27 (3.96)
Wine + Cheese	6	68.49 (5.25)	3.26 (1.11)	4.07 (1.59)	5.62 (1.85)
Cheese → Wine	6	65.06 (3.35)	8.87 (2.49)	10.93 (1.93)	15.52 (2.62)
Wine + Str.	6	65.00 (4.28)	4.15 (1.69)	7.26 (2.25)	10.88 (2.70)
Str. → Wine	6	68.17 (3.45)	9.82 (5.71)	15.77 (4.53)	20.59 (3.77)

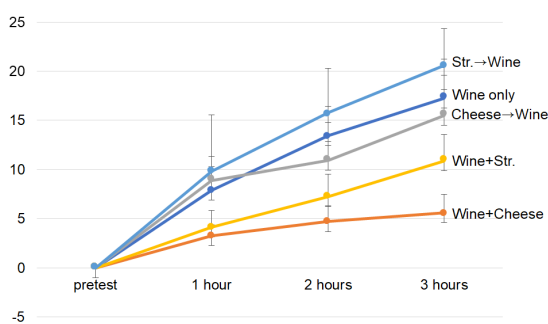


**Figure 2.** The color change of wine group ( $\Delta E^*$ ).

## CONCLUSION

Two issues regarding prevention of tooth discoloration are discussed: the effects of dairy products, and concentration of stain-inducing beverages including the issue of both acidity and colorants.

Dairy products such as milk and cheese seem to counteract tooth discoloration induced by coffee and wine. When we refer to the results with less color change among the teeth groups immersed in the mixture of coffee with milk and with cheese, compared with teeth groups in the coffee only or wine only solutions, it is assumed that dairy products such as milk and cheese contain properties that may help reduce discoloration of teeth which were exposed to coffee or wine. Dairy products seem to be able to diminish discoloration as a protein in dairy products protects tooth enamel by stabilizing calcium phosphate on tooth surface.<sup>9,10</sup>

Strawberries did not contribute to diminishing the discoloration of teeth even though they are well-known for their whitening effect by dissolving any superficial staining such as chromogenic substances on the teeth.<sup>11</sup> Rather strawberries facilitated tooth discoloration. This discoloration may be attributed to the colorants in strawberries and their acidity. In this study, cow teeth were immersed in the mixture of coffee with strawberry or in the mixture of wine with strawberry

for three hours. The negative effects of discoloration might be amplified through erosion on the surface of the tooth due to acid, therefore letting the pigments infiltrate deeper into the structure.<sup>6</sup> Therefore, considering the results, the custom of adding milk in different kinds of coffee and having cheese together when drinking wine may be beneficial since dairy products may counteract against discoloring the teeth from the colorants in coffee. However, the opposite might be true for strawberries.

Additionally, the concentration of a stain-inducing beverage might be an element that affects tooth discoloration. Comparing the color changes of the mixture groups with the transferring groups, the color of teeth immersed in the mixture groups of 'coffee + milk', 'coffee + strawberry', 'wine + cheese', and 'wine + strawberry' changed consistently less than the respective transferring groups ('milk → coffee', 'strawberry → coffee', 'cheese → wine', and 'strawberry → wine'). These results seem to come from the low concentration of colorants; the colorants in coffee and wine are diluted in the mixture groups, and thus the amounts of polyphenolic compounds that are responsible for the coloring of teeth were reduced.<sup>4</sup>

From the experiment with red wine, we can assume that the concentration of wine is critical to teeth discoloration. The color change of the mixture group of 'wine + strawberry' was less than the transferring group 'cheese → wine' and the wine only group although strawberry contains stain-inducing colorants. It is assumed from this result that the acidity of wine was diluted and further reduced the degree of tooth discoloration when we refer the previous research asserting that the low pH level leads to erosion of dental hard tissues.<sup>6,7,16</sup> More specifically, a low pH causes dissolution of calcified tooth structure, a decrease in enamel hardness and an increase in enamel porosity, and as a result, allows penetration of the pigments of beverages or food into the tooth. Therefore, lowering the concentration of stain-inducing beverages which are acidic is important in order to prevent tooth discoloration.

In conclusion, dairy products such as milk or cheese can minimize the discoloration of teeth induced by coffee or red wine. Another important finding is that the concentration of beverages is critical to teeth discoloration. Therefore, we recommend that people consume dairy products such as milk or cheese when they drink coffee or wine. It will be better if they drink light coffee (or light wine in order to keep teeth minimize the effects of discoloration).

## METHODS

### Materials

As the physical and chemical characteristics of cow teeth much resemble that of human teeth,<sup>13</sup> 60 cow teeth were used in this study. The extracted cow teeth were obtained from a



butcher and were cleaned and kept in a 0.9% NaCl saline solution. Before the experiment, the parts of cow teeth that were cracked were covered with nail polish in order to prevent the solutions from leaking through. The cow teeth were assigned to 10 groups, with six in each group, in order of the size of the cow teeth, as the thickness of teeth enamel is a critical element to the degree of discoloration.

Materials included 10 capsules of ground coffee bean (Nespresso Ristretto), a bottle of red wine (JINRO house wine of 16.67% alcohol by volume (ABV)), whole milk, cream cheese (Philadelphia), frozen strawberry, 0.9% NaCl saline solution, and a bottle of nail polish. In detail, 40mL of coffee (espresso) was extracted from each capsule of 5.5g; cream cheese was mixed with mineral water in a 1:1 ratio to form a liquid state; and frozen strawberry was ground without any additional water or sweetener. The tool used for measuring color was Minolta CR 400.

#### *Pilot Study*

A pilot study was conducted in order to find out how much time was needed for the cow teeth to be discolored and for the researcher to become familiar with the procedure of the experiment and the use of the Minolta CR 400. A tooth was immersed in coffee and another tooth in the mixture of coffee and milk at a ratio of 1:1 for 1 hour. The  $L^*$ ,  $a^*$ ,  $b^*$  values were measured every 10 minutes. As a result, measuring every hour for three times was determined to be sufficient.

#### *Experimentation for the coffee groups*

The cow teeth were immersed in the extracted espresso coffee for the 'coffee only' group and in the coffee and milk mixture - at a ratio of 1:1 - for an hour respectively. For the transferring from milk to coffee ('milk → coffee') group, the cow teeth were immersed in milk for five minutes, rinsed with 0.9% NaCl saline solution, and then immersed in coffee for 20 minutes repeatedly until the time immersed in the coffee solution reached one hour. This procedure was continued so that the teeth to be immersed in each solution for three hours, while measuring the colors each hour. For the experimentation of the 'coffee + strawberry' group and the 'strawberry → coffee' group, the same procedure was conducted as described above.

#### *Experimentation for the red wine groups*

Liquid cheese which was made of cream cheese mixed with mineral water was used for the cheese in the transferring from 'cheese → wine' group, and the liquid cheese was mixed with wine at a ratio of 1:1. Except for this cheese condition, all other procedures were the same as described for the coffee groups.

#### *Measurement and Analysis*

In this study, the colors of the cow teeth were measured with CIE (Commission Internationale de L'Eclairage, CIE) standard wherein the  $L^*$ ,  $a^*$ ,  $b^*$  refer to the variation in the white-black, red-green and yellow-blue chromaticity respectively.<sup>13</sup> The colors of teeth were assessed four times; pretest,

and one hour, two hours and three hours after immersion in the solutions utilizing the Minolta CR 400. Each cow tooth was measured three times for each assessment and the average of  $L^*$ ,  $a^*$  and  $b^*$  values was calculated for those color values. Then, the value of the total color change ( $\Delta E^*$ ) was calculated using the following formula:

$$\Delta E^* = \sqrt{((\Delta L^*)^2 + (\Delta a^*)^2 + (\Delta b^*)^2)}$$

#### **ACKNOWLEDGEMENTS**

I thank Professor Go from the Department of Chemistry, Soonchunhyang University, for mentoring and giving me advice when I had difficulties. I also thank my mother for preparing cow teeth, helping with the experimentation, and editing the manuscript.

#### **REFERENCES**

- (1) Wildman R. E. C.; Richard, S. B. Handbook of Nutraceuticals and Functional Food, 3rd ed.; CRC Press: Boca Raton, FL, 2019, 453-462.
- (2) Pramesti, A.; Jasrin, T. A.; Hidayat, O. T. Teeth Re-Whitening Juice on Coffee Stained Teeth. *Padjadjaran Journal of Dentistry*. 2013, 25(1), 15-20.
- (3) Kelleher, M. Dental Bleaching; Quintessence Publishing Co. Ltd: London, 2008.
- (4) Watts, A.; Addy, M. Tooth Discoloration and Staining: A Review of the Literature. *Br. Dent. J.* 2001, 190(6), 309-316. doi:10.1038/sj.bdj.4800959.
- (5) Nathoo, S. A. The Chemistry and Mechanisms of Extrinsic and Intrinsic Discoloration. *JADA*. 1997, 128(April), 6S-10S.
- (6) Azer, S. S.; Hague, A. L.; Johnston, W. M. Effect of pH on Tooth Discoloration from Colorant in Vitro. *J. Dent.* 2010, 38s, e106-e109. doi:10.1016/j.jdent.2010.07.014.
- (7) Dobrescu, C.; Wolff, M. S.; Estafan, D. Staining of the Bovine Enamel with Red and White Wine. Paper presented at International Association for Dental Research (IADR). 2009. Retrieved from: <https://iadr.abstractarchives.com/abstract/2009miami-115224/staining-of-the-bovine-enamel-with-redand-white-wine>.
- (8) Willershausen, B.; Callaway, A.; Azrak, B.; Kloss, C.; Schulz-Dobrick, B. Prolonged in Vitro Exposure to White Wines Enhances the Erosive Damage on Human Permanent Teeth Compared with Red Wines. *Nutrition Research*. 2009, 29, 558-567. doi:10.1016/j.nutres.2009.08.004.
- (9) Aimutis, W. R. Bioactive Properties of Milk Proteins with Particular Focus on Anticarcinogenesis. *J. Nutr.* 2004, 134(4), 989-995.
- (10) Ferrazzano, G. F.; Cantile, T.; Quarto, M.; Ingenito, A.; Chianese, L.; Addeo, F. Protective Effect of Yogurt Extract on Dental Enamel Demineralization in Vitro. *Aust. Dent. J.* 2008, 53(4), 314-319.
- (11) Karmawati, I. A.; Yulita, I.; Budiarti, R. The Effect of Strawberry on Color Changing of Tooth with Extrinsic Stain. Paper Presented at the 17th KPPINK Annual Meeting. 2016.
- (12) Baek, H. J.; Kang, K. H.; Kim, J. H. An Experimental Study on the Effect of Children's Range Beverage on Bovine Enamel. *Journal of the Korea Academia-Industrial Cooperation Society*. 2009, 10(9), 2523-2529. (in Korean)
- (13) Alexandrino, L.; Gomes, Y.; Alves, E.; Costi, H.; Rogez, H.; Silva, C. Effects of a Bleaching Agent with Calcium on Bovine Enamel. *Eur. J. Dent.* 2014, 8, 320-325.
- (14) Lee, H. J.; Kim, H. D.; Kim, M. Y.; Kwon, T. Y.; Kim, K. H. Effects of Fluoridated 10% Carbamide Peroxide on Enamel Surface Change and Whitening. *J. Dent. Hyg. Sci.* 2010, 10(2), 95-100. (in Korean)
- (15) Lim, D. S.; Ban, Y. H.; Min, Y. E.; Park, J. J.; Yu, Y. J.; In, S. R.; Ju, H. J.; Jung, S. Y.; Hwang, Y. S. The effect of Carbamide Water on Bovine Enamel Erosion and Plaque Adhesion. *J. Dent. Hyg. Sci.* 2015, 15(4), 437-444. (in Korean)
- (16) Al-Dlaigan YH; Shaw L.; Smith A. Dental Erosion in a Group of British 13-year-old School Children. Part : Influence of Dietary Intake. *Br. Dent. J.* 2001, 190, 258-261.

## AUTHORS

Selina Yuri Kim, the author of this research, is in her junior year of high school in South Korea. She has always had a passion for science (chemistry, biology and physics) and their applications to human life.



American Commission for Accreditation  
of Schools and Universities

## **STANDARDS**

- \* Governance
  - \* Education
  - \* Culture
  - \* Operations
  - \* Quality
- 

## ***Lifetime Qualities***

### **MORAL**

Caring, Modest,  
Ethical, Respectful

### **THINKER**

Knowledgeable, Inquirer,  
Curious

### **PRODUCTIVE**

Achiever,  
Excellence Seeker

### **INNOVATIVE**

Problem Solver, Explorer

### **VISIONARY**

Global Citizen, Inclusive

## **ACASU BENEFITS**

Enhances your institution's reputation and garners the esteem of Americans.

Assures students and their families that your institution meets American standards for high quality education.

Shows students and parents your institution's commitment to success and your ability to perform at high quality educational standards.

Shows your colleagues and the general public that your institution has a genuine interest in institutional improvement.

Sets your institution apart as a leader among others.

Provides you with a network of skilled professionals and resources to assist meeting your accreditation, enrollment, and college attainment goals.

Ensures that your standard operating procedures are compliant with U.S. international student regulations.



[ACASU.ORG](http://ACASU.ORG)



The International Journal of High School Research is published  
by Terra Science and Education